THE BIOCHEMICAL AND MOLECULAR BASIS OF HYPOXANTHINE-GUANINE PHOSPHORIBOSYLTRANSFERASE DEFICIENCY.

A THESIS PRESENTED FOR THE DEGREE OF
DOCTOR OF PHILOSOPHY
IN THE DEPARTMENT OF CHEMICAL PATHOLOGY
UNIVERSITY OF CAPE TOWN

JUNE, 1996

Anthony Marin Marinaki

ABSTRACT

Hypoxanthine-guanine phosphoribosyltransferase (HPRT) catalyses the first step in purine salvage. A complete deficiency of the enzyme results in the devastating neurological symptoms of the Lesch-Nyhan syndrome. The Lesch-Nyhan syndrome is characterised by purine overproduction leading to hyperuricemia and gout and a central nervous system disorder characterised by severe spasticity, choreoathetosis, mental retardation and compulsive self-mutilatory behaviour, A partial deficiency of the enzyme results in purine overproduction , gout and occasionally, mild neurological symptoms. Patients are spared the compulsive self-mutilation of the Lesch-Nyhan syndrome.

The major part of the thesis consists of the characterisation of the molecular defects in nine patients with the Lesch-Nyhan syndrome. The polymerase chain reaction was used to amplify reverse transcribed HPRT mRNA. The coding region of the amplified HPRT cDNA was either directly sequenced, or cloned and sequenced. All the mutations characterised were insertion or deletion events which resulted in premature termination of the predicted protein. Three patients were found to have a deletion of exon 7, two patients had single base insertions, while two patients appeared to have a complete deletion of the HPRT gene. An insertion in one patient was the result of a mutation within intron 6 which created a new splice donor site. The new splice donor site in concert with a cryptic splice acceptor resulted in the creation of a new exon. A deletion of exons 2, 3 and 4 in another patient was found to lead to the alternative splicing of exon 5. These unusual splice junction mutations provided *in vivo* support for the exon definition model of pre-mRNA splicing.

Four patients with partial HPRT deficiency were characterised at the biochemical and molecular levels. An Ala_{161} to Ser and a similar Ala_{161} to Gly substitution were identified in two patients with partial HPRT deficiency. These HPRT variants showed normal substrate affinities, but marked thermal instability. A substitution of Asp_{135} by Asn was defined in $HPRT_{Cape\ Town}$, a variant HPRT enzyme characterised by purine base inhibition.

The carboxylate residue is located at the center of the PRPP binding motif within the active site of the enzyme and is proposed to interact with the pyrophosphate moiety of PRPP during catalysis. No defect within the HPRT cDNA of a fourth patient with apparent partial HPRT deficiency could be detected.

The incorporation by cultured cells of [^{14}C] hypoxanthine relative to a [^{3}H] control substrate such as phenylalanine, is a rapid method for the diagnosis of complete HPRT deficiency. However, the major physiological variation in the incorporation of purine base substrates shown by cells in culture has led us to question the validity of double label methods in the diagnosis of partial HPRT deficiency. The incorporation by cultured lymphoblasts of the label pairs, [^{14}C] hypoxanthine and [^{3}H] phenylalanine, or [^{14}C] hypoxanthine and [^{3}H] adenine, were analysed in a nested analysis of variance. Large between experiment variation in the incorporation of the label pair [^{14}C] hypoxanthine and [^{3}H] phenylalanine masked differences between control and partially HPRT deficient cell lines. Due to large variation between individual cell lines within an experiment for the ratio [^{14}C] hypoxanthine/[^{3}H] adenine, it was necessary to pool data from repeated experiments in order to correctly identify cell lines as partially deficient in HPRT. The unexpected large variation in purine label incorporation by cultured lymphoblasts suggests that a diagnosis of partial HPRT deficiency should not be made on the basis of a single double label experiment.

The rate of PRPP accumulation in erythrocytes of patients with gout was measured under conditions of pathophysiologically low pH and non-physiologically high external inorganic phosphate. Preliminary evidence suggests that three of four patients identified with overproducing gout had increased rates of erythrocyte PRPP accumulation *in vitro*. An unexpected finding was a significant decrease in the rate of PRPP accumulation in erythrocytes of patients with gout due to urate underexcretion. These results suggest that a generalised defect in anion transport across membranes cannot be excluded.

ACKNOWLEDGEMENTS

I wish to acknowledge the guidance and vision of my supervisor, Professor Eric Harley. Helene Vreede and Mike Louw were generous in assisting with the collection of clinical material. Ingrid Baumgarten provided technical assistance by establishing the cell lines used in this study, while Brandon Weber provided technical assistance with the DNA sequencing of the HPRT variant F749. Tricia Owen, Brigitte Marinaki and Colleen O'Ryan provided critical comment on the manuscript. Lucille Human and Tricia Owen unselfishly carried the burden of my routine service commitment during the time I took to write this thesis. I am deeply indebted to John Duley and Anne Simmonds of the Purine Research Laboratory, Guy's Hospital, London for allowing me access to tissue culture material of ten HPRT deficient patients. The Medical Research Council, Cape Town, South Africa, provided financial support for this study. My wife, Brigitte, was unstinting in her support and encouragement, even when it looked as if this would never end.

ABBREVIATIONS

ad,	adenine
amidoPRT,	amidophosphoribosyltransferase
AMP,	adenosine-5'-monophosphate
ANOVA,	analysis of variance
APRT,	adenine phosphoribosyltransferase
bp,	base pair
cDNA,	copy DNA
cpm,	counts per minute
E. coli,	*Esherichia coli*
dATP,	deoxyadenosine-5'-triphosphate
dCTP,	deoxycytosine-5'-triphosphate
dGTP,	deoxyguanosine-5'-triphosphate
DEPC,	diethylpyrocarbonate
dITP,	deoxyinosine-5'-triphosphate
DMEM,	Dulbecco's Modified Eagles medium
dNTP,	deoxynucleotide triphosphates
2,3-DPG,	2,3-bisphosphoglycerate
dpm,	disintegrations per minute
dTTP,	thymidine-5'-triphosphate
Fe_{ur},	fractional excretion of uric acid
g,	gravity
GMP,	guanosine-5'-monophosphate
HPRT,	hypoxanthine-guanine phosphoribosyltransferase
hx,	hypoxanthine
IMP,	inosine-5'-monophosphate
IPTG,	isopropyl-1-thio-ß-galactoside
kb,	kilobase
mRNA,	messenger RNA

nt,	nucleotide
OPRT,	orotate phosphoribosyltransferase
PCR,	polymerase chain reaction.
Pi,	inorganic phosphate
PNP,	purine nucleoside phosphorylase
PPi,	inorganic pyrophosphate
PRPP,	5-phosphoribosyl-α-1-pyrophosphate
RBC,	red blood cells
snRNP,	small nuclear ribonucleoprotein
TCA,	trichloroacetic acid
UV,	ultra violet light
Xgal,	5-bromo-4-chloro-3-indolyl-ß-D-galactoside
XMP,	xanthosine monophosphate
ZTP,	5-amino-4-imidazole-carboxamide ribotide triphosphate

TABLE OF CONTENTS

INDEX OF FIGURES

SECTION 1.

SECTION 2.

SECTION 3.

SECTION 4.

SECTION 5.

SECTION 6.

INDEX OF TABLES.

SECTION 6.

1. INTRODUCTION.

1.1 Overview of the Thesis.

The thesis is divided into three broad sections. The first deals with the molecular genetics of hypoxanthine-guanine phosphoribosyltransferase (HPRT) deficiency in nine patients with the Lesch-Nyhan syndrome. The biochemistry and the molecular genetics of four partially deficient HPRT variant enzymes in patients with gout comprises the second portion of the thesis. In the third section, the biochemical basis of primary overproducing gout is investigated.

1.2 Overview of Purine Metabolism.

1.2.1 *De Novo* Purine Synthesis.

The pathways of purine *de novo* synthesis, salvage, interconversion and degradation have been comprehensively reviewed by Pallela and Fox (1989) and are shown in Figure 1.1. The compound 5-phosphoribosyl-α-1-pyrophosphate (PRPP) plays a central role in purine metabolism. PRPP condenses with L-glutamine to form ß-phosphoribosylamine in the first committed step of *de novo* purine synthesis and PRPP is also the phosphoribosyl donor in the purine base salvage reactions catalysed by hypoxanthine-guanine phosphoribosyltransferase and adenine phospho-ribosyltransferase (APRT). In subsequent reactions of the *de novo* pathway, the purine ring is built in a stepwise fashion with contributions of a formyl unit from N^{10}-formyl tetrahydrofolic acid (Benkovic, 1984), an amide group from glutamine, contributions from bicarbonate and aspartate, and the further donation of a one-carbon unit from N^{10}-formyl tetrahydrofolic acid. Finally, the purine ring is closed by the exclusion of a water molecule and inosine monophosphate (IMP) is formed. IMP can be converted to either adenosine monophosphate (AMP) or guanosine monophosphate (GMP) in two-step energy requiring reactions.

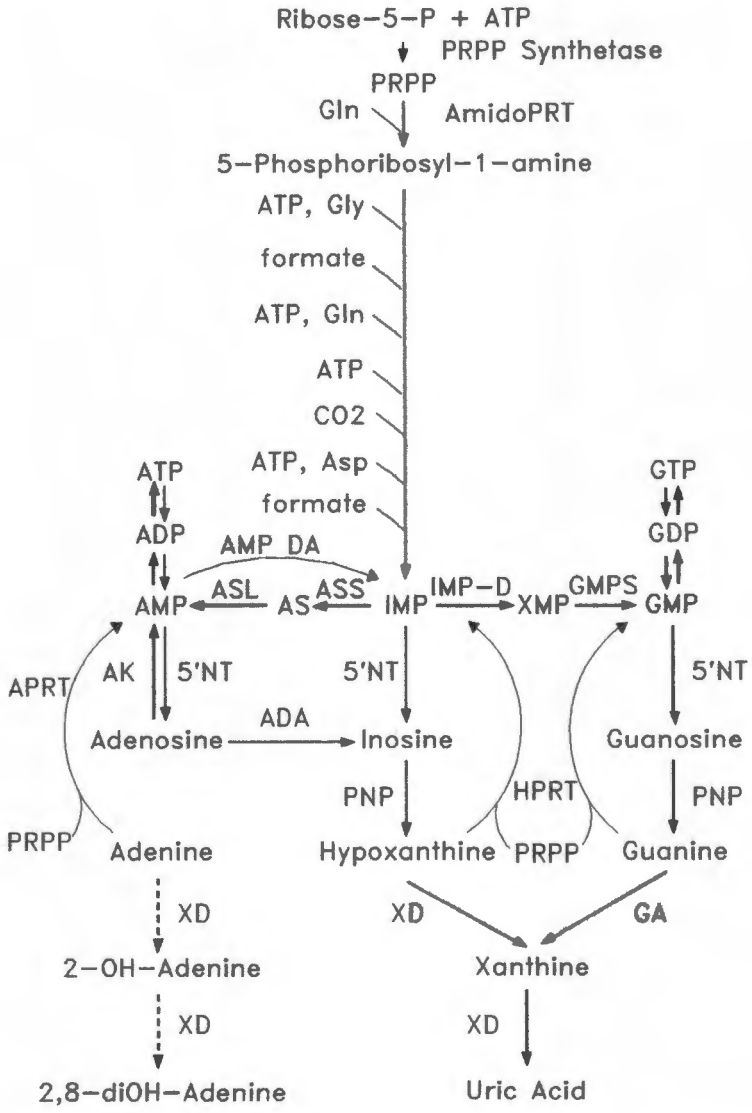

Figure 1.1: An overview of purine metabolism. Only the first committed step of *de novo* purine synthesis catalysed by amidophosphoribosyltransferase (amidoPRT) is shown. Abbreviations for the enzymes, adenylosuccinate synthetase (ASS), adenylosuccinate lyase (ASL), adenylic acid deaminase (AMP DA), IMP dehydrogenase (IMP-D), GMP synthetase (GMPS), adenosine kinase (AK), 5'-nucleotidase (5'NT), purine nucleoside phosphorylase (PNP), adenosine deaminase (ADA), adenine phosphoribosyltransferase (APRT), hypoxanthine-guanine phosphoribosyltransferase (HPRT), guanase (GA) and xanthine dehydrogenase (XD) are indicated at the point of the reactions they catalyse. Substrates: adenylosuccinate (AS), 2-hydroxy-adenine (2-OH-adenine), 2,8-dihydroxy-adenine (2,8-diOH-adenine).

1.2.2 Purine Catabolism.

Mononucleotides are converted to nucleosides by 5'-nucleotidases located on cell membranes and in the cytosol. Normal intracellular purine catabolism proceeds via various cytosolic 5'-nucleotidases, each with preferred activity towards a certain class of nucleoside monophosphates (Bontemps, 1988). Purine nucleoside phosphorylase (PNP) is able to cleave, in a reversible reaction, the purine nucleosides (guanosine, inosine and to a lesser extent xanthosine) to the purine bases (guanine, hypoxanthine and xanthine respectively) and ribose-1-phosphate. Adenosine is converted to inosine by adenosine deaminase. Any hypoxanthine which escapes salvage is converted to xanthine and then uric acid by xanthine oxidase.

1.2.3 Purine Salvage Pathway.

The phosphoribosyltransferase pathways are the most active in the salvage of preformed purine bases. The purine bases hypoxanthine, guanine and much less efficiently, xanthine, are salvaged by HPRT to form IMP, GMP and xanthosine monophosphate (XMP) respectively, while APRT salvages adenine. Under normal conditions, the two-step nucleoside phosphorylase-nucleoside kinase salvage pathway does not appear to be very active in most tissues.

1.3 The Biochemistry of HPRT.

Hypoxanthine-guanine phosphoribosyltransferase (HPRT EC 2.4.2.8, McKusick 25890), more commonly abbreviated to HPRT, catalyses the magnesium dependent transfer of a phosphoribosyl moiety from PRPP to the N9 nitrogen of the purine bases hypoxanthine or guanine, to form IMP or GMP respectively. In humans, up to 90% of purines are salvaged by HPRT (Stout and Caskey, 1989) resulting in a saving, compared to *de novo* purine synthesis, of 4 ATP molecules for each purine base salvaged.

1.3.1 Kinetics of HPRT.

Henderson et al (1968) performed kinetic studies on HPRT using dialysed haemolysates. Initial velocity experiments produced parallel double reciprocal plots when substrate concentrations of hypoxanthine and PRPP were mutually varied, which provided evidence for a ping pong mechanism in which the two substrates are not present on the enzyme simultaneously. They speculated that the reason for parallel double reciprocal plots in their initial rate experiments was a low (<0.1) K_i to K_m ratio for PRPP, which implies that any deviation from parallel lines in double reciprocal plots would be virtually impossible to detect. However, product inhibition patterns by inorganic pyrophosphate (PPi) as well as the observed PPi stimulation of IMP-hypoxanthine exchange suggested an ordered bi-bi reaction mechanism in which PRPP binds first and IMP leaves last, rather than a ping pong mechanism.

Krenitsky et al (1969) purified HPRT fifty-fold from human erythrocytes and suggested that PRPP in the form of a di-magnesium salt rather than a mono-magnesium salt was the preferred substrate of the enzyme. The kinetic studies of Krenitsky and Papaioannou (1969) on purified HPRT showed features of both ping pong and ordered reaction mechanisms, depending on the magnesium concentration. They showed that the K_i to K_m ratio for PRPP was greater than 0.1 and that initial velocity curves at low magnesium concentrations were non-parallel. Product inhibition by PPi was markedly influenced by the concentration of magnesium. PPi was an ineffective inhibitor at high concentrations of magnesium (5 mM) but at low magnesium concentrations (0.05 mM), PPi showed marked inhibition. As a result, they argued that data based on the use of PPi in inhibition studies such as those of Henderson et al (1969) were unsuitable for mechanistic interpretation. After preincubation of HPRT with PRPP, the addition of hypoxanthine resulted in an initial burst of IMP synthesis and this was taken as evidence for the existence of an enzyme-ribosylphosphate intermediate. They also showed that some nucleotide-base exchange could occur in the absence of PPi, and that PPi stimulation was non-hyperbolic, evidence against an ordered reaction mechanism. Inhibition by mononucleotides was

competitive with respect to Mg_2PRPP and non-competitive with respect to hypoxanthine and provided evidence in agreement with Henderson et al (1968) that Mg_2PRPP was the first substrate to add to the enzyme and IMP the last product to leave. Krenitsky and Papaioannou (1969) however postulated alternate reaction sequences, depending on magnesium salt concentration. At high magnesium concentrations, the predominant reaction sequence involves an enzyme-phosphoribosyl intermediate compatible with a ping pong reaction mechanism. At low magnesium concentrations, they suggested that the mono-magnesium salt of PRPP participates in an ordered reaction, but the di-magnesium salt of PRPP entered a ping pong reaction.

Giacomello and Salerno, (1978) have provided the most definitive study of the kinetics of human HPRT to date. They studied the reaction catalysed by HPRT in the reverse direction. They proposed a sequential mechanism where the monomagnesium complexes of IMP and PPi bind to the enzyme in a rapid equilibrium random fashion, while the products of the reverse reaction, PRPP and hypoxanthine, then dissociate in an ordered sequence with first the purine base and then the magnesium complex of PRPP being released. MgPPi and MgIMP are competitive with respect to Mg_2PRPP and non-competitive with respect to hypoxanthine. Their results thus strongly supported an ordered bi rapid equilibrium random bi mechanism in good agreement with Henderson et al (1968). In summary, available evidence suggests that the substrates hypoxanthine and PRPP bind to human HPRT in an ordered sequence, with PRPP binding first. The products of the reaction, PPi and IMP are released from the enzyme in a random manner.

It is possible that HPRT in other organisms may be characterised by different kinetic mechanisms, for example, Yaun et al (1992) have proposed an ordered bi-bi mechanism for schistosomal HPRT.

Human erythrocyte HPRT has a reported true K_m value for hypoxanthine and PRPP of 9.9 μM and 240 μM respectively (Henderson et al, 1968; Krenitsky and Papaioannou, 1969). A true K_m value of 4 μM has been reported for guanine (Henderson et al, 1968). It should

be noted that the true K_m for the two substrate reaction catalysed by HPRT is calculated from data generated by mutually varying the concentrations of both substrates, hypoxanthine and PRPP. The apparent K_m is an estimate of the true K_m and is more easily determined from substrate velocity curves, where one substrate is kept constant at a single saturating concentration, while the concentration of the other substrate is varied.

1.3.2 Enzyme Structure.

Native human HPRT is a multimeric enzyme and exists predominantly as a tetramer of identical subunits (Holden and Kelley, 1978; Smithers and O'Sullivan, 1984). Under certain non-physiological conditions, the enzyme can exist as catalytically active dimers (Johnson et al, 1979). Wilson et al (1982b) have determined the complete amino acid sequence of the enzyme purified from human erythrocytes. After cleavage of the N-terminal methionine, the N-terminal alanine is acetylated, a feature characteristic of many soluble cytoplasmic enzymes. Each subunit is thus 217 amino acids long with a molecular weight of 24 470.

In 1994, Eads et al solved the three-dimensional structure of recombinant human HPRT with bound GMP using X-ray diffraction data to 2.5 Å resolution. The enzyme monomer is composed of ten ß strands and six α helices. The enzyme contains a core region (amino acid residues 37-189, the amino acid sequence is numbered with the N-terminal alanine as residue 1) with a twisted parallel ß sheet consisting of five ß strands surrounded by four α helices. The core region resembles a dinucleotide binding fold (Argos et al, 1983) and is equivalent to the core region observed by Scapin et al (1994) in the crystal structure of the related enzyme orotate phosphoribosyltransferase (OPRT). A long disordered loop of residues (103-117) is referred to as the flexible loop by the authors and is believed to move during catalysis. The sequences flanking the core region form a separate substructure which differs between HPRT and OPRT and appears to confer substrate

specificity. Above the core is a lobe that contains residues Glu-13 to Pro-37 and Asp-184 to Ala-217.

The interface between monomers in dimer formation involves interactions between 27 residues on each subunit, contributed from strand B3, helix A3 and residues 196-200 and 24-26.

Eads et al (1994) described interaction between the conserved PRPP binding motif (amino acid residues 129-140) identified by Wilson et al (1983d) and Hershey and Taylor (1986) and bound GMP. The motif starts with hydrophobic residues which have no direct interactions with the active site. The side chains of Glu-133 and Asp-134 are located on the floor of the active site cleft below the ribose group. The ß strand makes a sharp turn at Asp-134 to lead into a loop composed of the residues Asp-137 to Thr-141 which are involved in binding the 5'-phosphate group of GMP.

1.3.3 Posttranslational Modification of HPRT.

Johnson et al (1982) identified three isoenzymes in erythrocytes, the relative quantities of which change as the cell ages. Modification of HPRT appears to be initiated in the reticulocyte and continues throughout the life span of the erythrocyte. Johnson et al pointed out that various combinations of modified and unmodified subunits in the native multimeric enzyme could account for the electrophoretic heterogeneity seen in preparations of erythrocyte HPRT. In contrast, only one electrophoretic form of the enzyme was present in lymphoblasts. At least three charge variant forms of HPRT purified from human brain have also been distinguished by Smithers and O'Sullivan (1984). These findings suggest that HPRT is subject to at least one posttranslational modification. One such modification defined in erythrocyte HPRT appears to be the time dependent deamination of asparagine at position 106 (Wilson et al, 1982a).

1.3.4 Tissue Distribution.

HPRT is expressed in all tissue at relatively low levels, with the exception of the brain and testes. Testes had the highest specific activity of all tissues studied by Adams and Harkness (1976), with values almost a third higher than HPRT activity in cerebral cortex grey matter. Although high compared to most other tissue, HPRT activity in the basal ganglia was lower than in cerebral cortex grey matter, a result in conflict with an earlier study (Rosenbloom, 1967). It seems likely that high levels of HPRT activity in a tissue are inversely correlated with a lower capacity to synthesize purines *de novo* (Stout and Caskey, 1989).

1.4 The HPRT Gene.

Jolly et al (1983) cloned and sequenced HPRT cDNA. The cDNA is just under 1350 nucleotides long with a single open reading frame of 654 base pair (bp). The cDNA predicts a polypeptide of 218 amino acids (including the N-terminal methionine) with an amino acid sequence identical to that found by Wilson et al (1982b).

The human HPRT locus is located on the X-chromosome at Xq26-q27 (Pai et al, 1980). Edwards et al (1990) sequenced 57 kilobases (kb) of the human HPRT locus, including 1676 bp upstream of the start codon and 15238 bp downstream of the termination codon. The gene is organised into 9 exons and 8 introns (Patel et al, 1986) and is shown in Figure 1.2 Four HPRT-like non-functional pseudogenes have been localised to chromosomes 3, 5 and 11 (Patel et al, 1984).

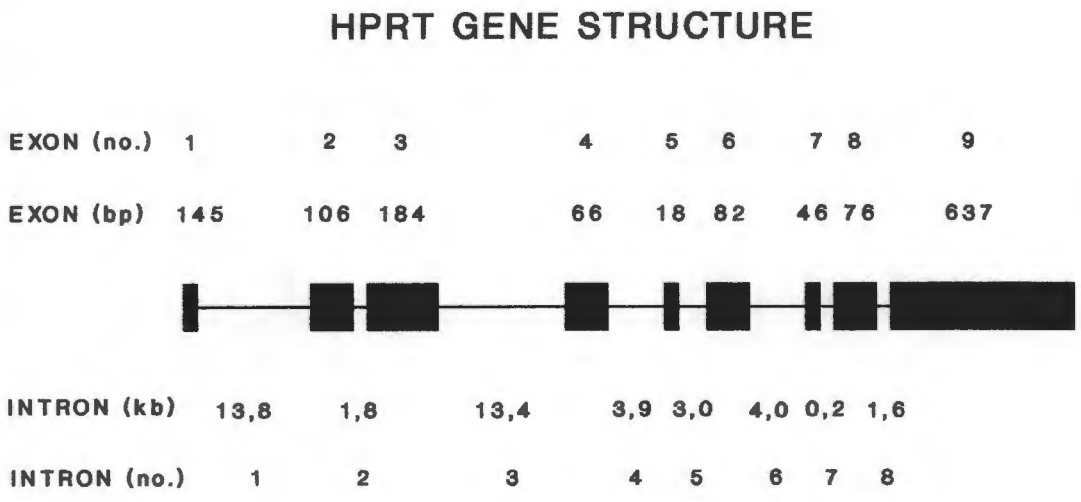

Figure 1.2: Structure of the HPRT gene. The nine exons are shown as rectangles with sizes in base pair (bp) shown above the cartoon and introns are shown as lines connecting the exons. The sizes of the 8 interconnecting introns in kilobases (kb) are shown below the cartoon.

1.4.1 Regulation of HPRT Gene Expression.

The 5'-noncoding region of the HPRT gene is GC rich and lacks a TATA box and a CAAT sequence, two elements which play a regulatory role in transcription of most eukaryotic mRNAs. The 5'-flanking region does, however, contain three copies of the sequence 5'-CCGCCC-3', which is characteristic of the promoters of many housekeeping genes, as well as many viral promoters (Patel et al, 1986). There are 46 CpG sequences within 400 bases upstream of the translation start site and these CpG clusters are under methylated when the gene is active, and extensively methylated when the gene is inactive. This correlates with transcriptional silencing on the inactive X chromosome in female mammals (Wolf and Migeon, 1985). Hornstra and Yang (1994) analysed the methylation

of individual cytosines in the 5'-CpG island of human HPRT on the active and inactive X chromosomes. The inactive allele is methylated at nearly all CpG nucleotides, except in a 68 bp region containing 4 adjacent GC boxes which are unmethylated or partially methylated. This is in contrast with the gene for human phosphoglycerate kinase which shows complete methylation of all CpG sites in the 5' CpG island.

A *cis* acting element from nucleotide (nt) -219 to nt -122 relative to the initiating codon is necessary for maximal expression of the gene and functions in both normal and reverse orientations, while a negative regulatory cis acting element is present in the region nt -570 to nt -388 (Rincon-Limas et al, 1991). This suppresser element is also orientation independent, but appears to be distance dependent. It is interesting that not all the regulatory elements are located 5' to the coding region. An element in intron 2 was found to be required for effective expression of HPRT minigene constructs in embryonic stem cells and an element in intron 1 acts as an enhancer of HPRT expression (Reid et al, 1990).

2. DEVELOPMENT OF MOLECULAR METHODS.

2.1. Introduction.

Total RNA was extracted from cultured fibroblasts or Epstein Barr virus transformed lymphoblasts and reverse transcribed using AMV reverse transcriptase in a reaction primed by an oligo dT_{15} primer. The polymerase chain reaction (PCR) was used to amplify the coding region of HPRT cDNA using HPRT specific oligonucleotide primers. PCR products were directly sequenced or, when this did not give easily readable sequences, the PCR products were cloned and sequenced.

2.1.1 The Polymerase Chain Reaction.

The polymerase chain reaction, first devised by Mullis and Faloona and described in detail in 1987, has simplified the detection and characterisation of mutations. Synthetic oligonucleotide sequence specific primers are annealed to heat denatured singled stranded target DNA in a buffer containing all four deoxynucleotide triphosphates (dNTPs). Mullis and Faloona (1987) used the thermolabile Klenow fragment of *Esherichia coli* (*E coli*) DNA polymerase I to extend the annealed primers. The newly synthesised DNA duplex was then denatured by heating, the reaction mixture cooled to allow the primers to anneal, more Klenow added to extend the annealed primer, recreating a double stranded DNA molecule. Each cycle of denaturing, annealing and extension results in a doubling of the number of double stranded DNA molecules present and a geometric accumulation of a primer defined segment of the target DNA. In 1988, Saiki et al substituted a thermostable DNA polymerase, Taq DNA polymerase, isolated from a thermophilic bacterium, *Thermus aquaticus* for Klenow. The use of a thermostable DNA polymerase enabled annealing and extension of the primer to occur at higher temperatures, increasing the specificity of the reaction and obviating the need to add more polymerase after each denaturing step.

2.1.2. Screening for Unknown Mutations.

Two PCR based approaches were considered for determining the molecular defect responsible for HPRT enzyme deficiency: exon by exon screening and cDNA screening.

Exon by Exon Screening.

Each exon is amplified by a unique set of primers located in the 5' and 3' introns. The marked heterogeneity of mutations reported at the HPRT gene locus would necessitate the synthesis of nine primer pairs to screen each of the nine HPRT exons. Splice junction mutations would be detected and defined as a change in the sequence of the splice junction. Mutations within an intron, outside of the sequence defined by the primer pair would not, however, be detected. Structural deletions of all or part of the gene would not be detected directly, being seen rather as a failure to amplify one or more exons.

A major advantage of exon by exon screening is that genomic DNA can be readily isolated from peripheral leukocytes and a source of preserved mRNA is not necessary.

Screening at the cDNA level.

Total RNA is extracted from nucleated cells, mRNA is reverse transcribed to cDNA using a reverse transcriptase and an oligo dT_{15} primer and the coding region of the cDNA amplified using HPRT gene specific primers. The reverse transcribed mRNA represents a "summary" of the gene. The size of the amplified cDNA can sometimes serve as an indicator to the nature of the mutation. Mutations affecting splice donor and acceptor sites are detected as smaller or larger than normal PCR products caused by exon skipping or an insertion of an intron derived sequence respectively. These mutations however, would still need to be defined at the gene level. A PCR product of the predicted size suggests a small deletion or insertion event, or a point mutation. Mutations affecting the primer binding domains or mutations deleting the whole gene (null mutations) would be seen as a failure to amplify HPRT cDNA

A major disadvantage of screening cDNA is that a source of mRNA needs to be available. However, HPRT is ubiquitously expressed (Section 1.2.4.) and the availability of tissue culture material from all patients in this study, the greater sensitivity of cDNA screening compared to exon by exon screening in detecting a variety of mutational types, as well as the greater cost of synthesising nine primer pairs for exon by exon screening, suggested that the most efficient approach to screening for mutations at the HPRT gene locus was by cDNA screening.

2.2 Materials.

AMV reverse transcriptase, oligo dT_{15} primer, deoxynucleotide triphosphates, proteinase K, restriction endonucleases and pUC 18 were purchased from Boehringer Mannheim GmbH, Germany. RNAsin, a ribonuclease inhibitor was obtained from Promega, Madison, Wisconsin, USA. Taq DNA polymerase was purchased from BRL, Gaitherburg, Maryland, USA, Stratagene, La Jolla, California, USA or Boehringer Mannheim GmbH, Germany. Vent DNA polymerase was obtained from New England Biolabs, Beverly, Massachussets, USA. DH5α *E. coli* cells were from GIBCO BRL, Gaitherburg, Maryland, USA. [^{35}S] dATP was purchased from the Radiochemical Centre, Amersham, UK.

Ultrafree-MC 30,000 and 100,000 NMWL filter units were obtained from Millipore Corporation, Bedford, Massachussets, USA. All other chemicals were of reagent or molecular biology grade.

2.2.1. PCR and Sequencing Primers.

DNA oligonucleotide primers were synthesised on an automated DNA synthesiser by the Departments of Biochemistry or Medical Biochemistry, University of Cape Town, Cape Town, South Africa.

The primers were designed using the computer software programme Oligo 3.4 (National Biosciences Inc, Plymouth MN, USA) and numbered according to the sequence shown in Figure 2.1 with the A of the ATG start codon numbered as base 1. A schematic representation of the position of the primers within the HPRT cDNA and the HPRT gene are shown in Figure 2.2, while the T_m and sequence for each primer are shown in Tables 2.1, 2.2 and 2.3.

The T_m in °C for each PCR and sequencing primer was calculated according to the formula:

$$T_m = 4(G+C) + 2(A+T)$$

where (G+C) is the number of guanines and cytosines in the primer sequence and (A+T) is the number of adenines and thymines in the sequence.

			-90	-80	-70
			TCTTG	CTGCGCCTCC	GCCTCCTCCT
-60	-50	-40	-30	-20	-10
CTGCTCCGCC	ACCGGCTTCC	TCCTCCTGAG	CAGTCAGCCC	GCGCGCCGGC	CGGCTCCGTT
1	11	21	31	41	51
ATGGCGACCC	**GCAGCCCTGG**	**CGTCGTGATT**	**AGTGATGATG**	**AACCAGGTTA**	**TGACCTTGAT**
61	71	81	91	101	111
TTATTTTGCA	**TACCTAATCA**	**TTATGCTGAG**	**GATTTGGAAA**	**GGGTGTTTAT**	**TCCTCATGGA**
121	131	141	151	161	171
CTAATTATGG	**ACAGGACTGA**	**ACGTCTTGCT**	**CGAGATGTGA**	**TGAAGGAGAT**	**GGGAGGCCAT**
181	191	201	211	221	231
CACATTGTAG	**CCCTCTGTGT**	**GCTCAAGGGG**	**GGCTATAAAT**	**TCTTTGCTGA**	**CCTGCTGGAT**
241	251	261	271	281	291
TACATCAAAG	**CACTGAATAG**	**AAATAGTGAT**	**AGATCCATTC**	**CTATGACTGT**	**AGATTTTATC**
301	311	321	331	341	351
AGACTGAAGA	**GCTATTGTAA**	**TGACCAGTCA**	**ACAGGGGACA**	**TAAAAGTAAT**	**TGGTGGAGAT**
361	371	381	391	401	411
GATCTCTCAA	**CTTTAACTGG**	**AAAGAATGTC**	**TTGATTGTGG**	**AAGATATAAT**	**TGACACTGGC**
421	431	441	451	461	471
AAAACAATGC	**AGACTTTGCT**	**TTCCTTGGTC**	**AGGCAGTATA**	**ATCCAAAGAT**	**GGTCAAGGTC**
481	491	501	511	521	531
GCAAGCTTGC	**TGGTGAAAAG**	**GACCCCACGA**	**AGTGTTGGAT**	**ATAAGCCAGA**	**CTTTGTTGGA**
541	551	561	571	581	591
TTTGAAATTC	**CAGACAAGTT**	**TGTTGTAGGA**	**TATGCCCTTG**	**ACTATAATGA**	**ATACTTCAGG**
601	611	621	631	641	651
GATTTGAATC	**ATGTTTGTGT**	**CATTAGTGAA**	**ACTGGAAAAG**	**CAAAATACAA**	**AGCCTAA**GAT
661	671	681	691	701	711
GAGAGTTCAA	GTTGAGTTTG	GAAACATCTG	GAGTCCTATT	GACATCGCCA	GTAAAATTAT
721	731	741	751	761	771
CAATGTTCTA	GTTCTGTGGC	CATCTGCTTA	GTAGAGCTTT	TTGCATGTAT	CTTCTAAGAA
781	791	801	811	821	831
TTTTATCTGT	TTTGTACTTT	AGAAATGTCA	GTTGCTGCAT	TCCTAAACTG	TTTATTTGCA
841	851	861	871	881	891
CTATGAGCCT	ATAGACTATC	AGTTCCCTTT	GGGCGGATTG	TTGTTTAACT	TGTAAATGAA
901	911	921	931	941	951
AAAATTCTCT	TAAACCACAG	CACTATTGAG	TGAAACATTG	AACTCATATC	TGTAAGAAAT
961	971	981	991	1001	1011
AAAGAGAAGA	TATATTAGTT	TTTTAATTGG	TATTTTAATT	TTTATATATG	CAGGAAAGAA
1021	1031	1041	1051	1061	1071
TAGAAGTGAT	TGAATATTGT	TAATTATACC	ACCGTGTGTT	AGAAAAGTAA	GAAGCAGTCA
1081	1091	1101	1111	1121	1131
ATTTTCACAT	CAAAGACAGC	ATCTAAGAAG	TTTTGTTCTG	TCCTGGAATT	ATTTTAGTAG
1141	1151	1161	1171	1181	1191
TGTTTCAGTA	ATGTTGACTG	TATTTTCCAA	CTTGTTCAAA	TTATTACCAG	TGAATCTTTG
1201	1211	1221	1231	1241	
TCAGCAGTTC	CCTTTTAAAT	GCAAATCAAT	AAATTCCCAA	AAATTT	

Figure 2.1: Nucleotide sequence of HPRT cDNA. The nucleotide sequence of the HPRT cDNA is according to Jolly et al (1983). The coding region is in bold print, with the A of the ATG start codon numbered as base 1.

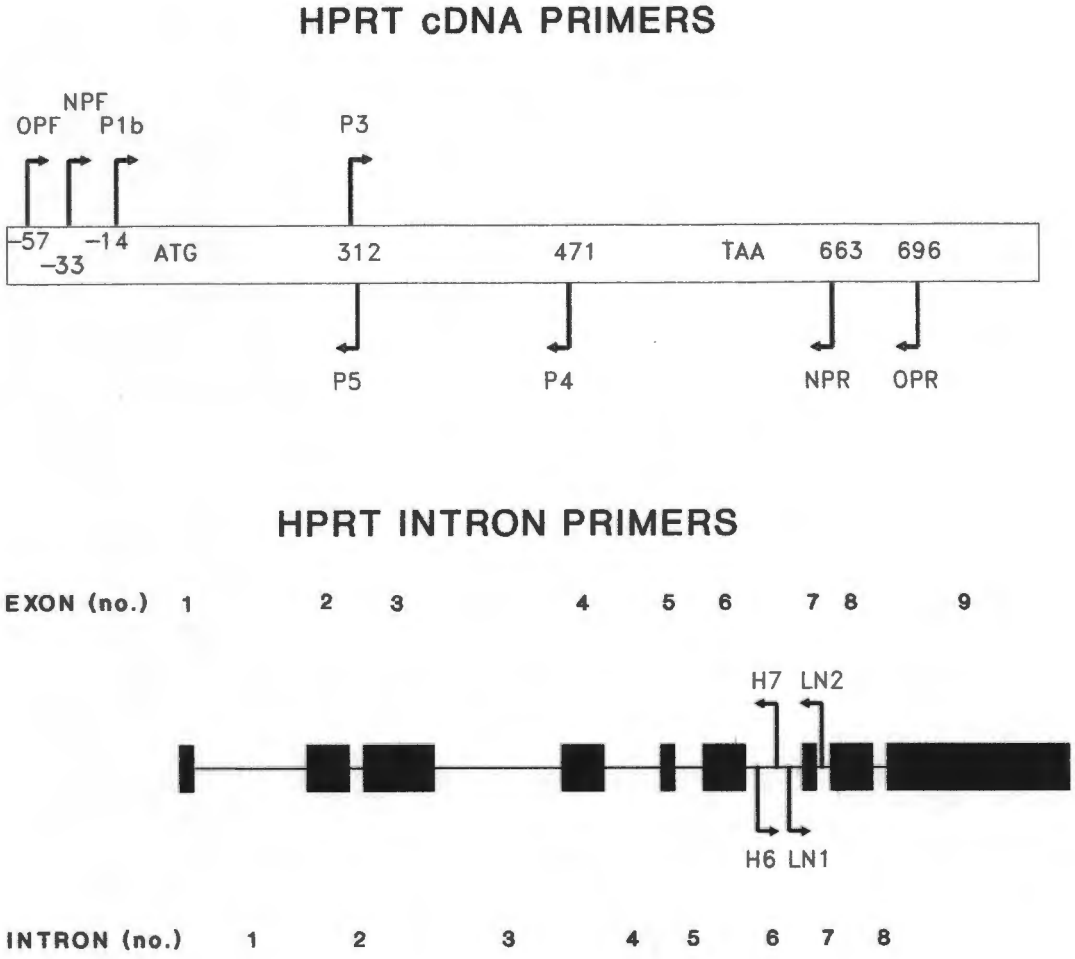

Figure 2.2: Position of PCR and sequencing primers within the HPRT cDNA and gene. The cDNA is represented as a rectangle in the upper panel, with the coding region defined by the start codon ATG and ending at the stop codon TAA. The forward or reverse direction of the primers is indicated schematically by the direction of the arrow, while the nucleotide position of the 3'-terminal base of each primer is indicated by the number within the rectangle. The lower panel shows the position of primers in the HPRT gene which were used to amplify a section of intron 6 (primers H6 and H7) and across exon 7 (primers LN1 and LN2).

Table 2.1: cDNA PCR primers.

PRIMER	POSITION	T_m	SEQUENCE
P1a	F -12	74°C	5'-aatctGCAGTCAGCCCGCGCGCCGG-3 cDNA PCR primer. Incorporates a *Pst*1 site at the non-complementary 5' end
P1b	F -14	66°C	5'-aatctGCAGTCAGCCCGCGCGCC-3' cDNA PCR primer. Differs from P1a by lack of the GG at the 3' end
P2	R +663	62 °C	5'-tGcgaaTTCCAAACTCAACTTGAACTC-3' cDNA PCR primer. Incorporates an *Eco*R1 site at the non-complementary 5' end.
OPF	F -57	66°C	5'-CCTCCGCCTCCTCCTCTGC-3' cDNA outer forward PCR primer.
OPR	R +696	76°C	5'-TTGATAATTTTTACTGGCGATGTC AATAG-3' cDNA outer reverse PCR primer.
NPF	F -33	68°C	5'-CCACCGGCTTCCTCCTCCTG-3' cDNA nested forward PCR primer.
NPR	R +663	64°C	5'-tGcgGaTcCCAAACTCAACTTGAACTC-3' cDNA nested reverse primer, same as P2 except for a *Bam*H1 site at the 3' end.

Forward primers are designated F and reverse primers R. The 3' terminal base of each primer used for cDNA amplification and sequencing is numbered according to the HPRT cDNA sequence published by Jolly et al, 1983, with the A of the initiation codon ATG numbered as base 1. Restriction endonuclease sites incorporated into the 5'-end of primers P1a, P1b, and P2 are underlined. Non-complementary bases at the 5'-end of primers P1a, P1b and P2 are shown as lower case letters and were not used in calculating the T_m using the formula shown in the text.

Table 2.2: cDNA sequencing primers.

PRIMER	POSITION	T_m	SEQUENCE
P3	F +312	42°C	5'-TCAGACTGAAGAGC-3'
P4	R +471	48°C	5'-CTTGCGACCTTGACC-3'
P5	R +300	42°C	5'-AGCTCTTCAGTCTG-3'

Forward primers are designated F and reverse primers R. The 3' terminal base of each primer used for cDNA sequencing is numbered according to the HPRT cDNA sequence published by Jolly et al, 1983, with the A of the initiation codon ATG numbered as base 1. The T_m of each primer was calculated according to the formula shown in the text.

Table 2.3: Primers for the amplification and sequencing of genomic DNA.

PRIMER	POSITION	T_m	SEQUENCE
H6	F 36154	78°C	5'-TTGCTTATTTTTCTACATGCTCTTTAGGG-3' Forward primer for amplification of a segment of intron 6.
H7	R 36385	66°C	5'-AAGCAGCACTGACGTGGGGTTC-3' Reverse primer for amplification of a segment of intron 6.
LN1	F 39634	70°C	5'-GTAGTGTCAACTCATTGCTGCCC-3' Forward primer located in intron 6 for amplification of exon 7.
LN2	R 40187	68°C	5'-TCTGTTCAAATTATGAGGTGCTGG-3' Reverse primer located in intron 7 for amplification of exon 7.

The 3' terminal base of each primer is numbered according to the numbering and sequence of the HPRT gene published by Edwards et al, 1990. Forward primers are designated F and reverse primers R. The T_m of each primer was calculated according to the formula shown in the text.

2.3. Methods.

2.3.1. DNA Extraction.

High molecular weight genomic DNA was extracted from tissue culture material using a standard proteinase K-SDS method as described in Ausubel et al, 1994.

2.3.2. RNA Extraction.

Total RNA was extracted from cultured fibroblasts or lymphoblasts using the single step acid guanidinium thiocyanate - phenol - chloroform method modified from Chomzynski and Sacchi, 1987. All aqueous reagents which did not contain guanidinium thiocyanate were treated with diethylpyrocarbonate (DEPC) to destroy ribonuclease activity (Ausubel et al, 1994).

Cells in an intact fibroblast monolayer or in a saline washed cell pellet were lysed in 1 ml of a denaturing solution containing 4 M guanidinium thiocyanate, 25 mM sodium citrate, pH 7, 0.5% N-lauroyl sarcosine and 0.1 M 2-mercaptoethanol. The lysate was passed through a 21 gauge needle several times to shear high molecular weight DNA and transferred to a polypropylene centrifuge tube. An equal volume (1 ml) of water saturated phenol and 0.2 ml of chloroform:isoamyl alcohol (49:1) were then added. The suspension was then shaken vigorously for 10 s and cooled on ice for 15 min. The organic phase containing DNA and protein was then separated from the RNA containing aqueous phase by centrifugation at 10000g for 15 min at 4°C. RNA was recovered from the aqueous phase by the addition of 2 volumes of 100% ethanol followed by precipitation at -80°C for 30 min. The precipitate was pelleted by centrifugation at 10000g for 20 min, washed with 75% ethanol made up with DEPC treated water and dried under vacuum. The dry pellet was then resuspended in 200 µl DEPC treated water, 400 µl 100% ethanol was added and the RNA stored at -80°C. The RNA was recovered for cDNA synthesis by centrifugation after the addition 0.1 the original volume (20 µl) DEPC treated 3 M sodium acetate

pH 5.2, washed in 1 ml 75% ethanol, the pellet dried under vacuum and resuspended in 200 µl DEPC treated water. The absorbance of a 10 µl aliquot in 490 µl water was measured at 260 nm and 280 nm. The 260 nm/280 nm ratio was used to detect the presence of contaminating proteins. A conversion factor of 1 absorbance unit = 40 µg RNA/ml was used to quantify the amount of RNA present.

The quality of the RNA isolate was checked by electrophoresis on 1% formaldehyde-agarose gels using standard techniques (Ausubel et al, 1994).

2.3.3. First Strand cDNA Synthesis.

First strand cDNA was synthesised by a method modified from Ausubel et al, 1994. A typical reaction volume of 100 µl contained the following: 10 µg of total RNA annealed to 5 µg oligo dT_{15} primer or a HPRT cDNA specific primer (P2), 80 U AMV reverse transcriptase, 50 mmol/l Tris-HCL pH 8.3, 60 mmol/l KCL, 3 mmol/l $MgCL_2$, 10 µg bovine serum albumin, 5 U ribonuclease inhibitor, 5 mmol/l dithiothreitol and 500 µmol/l of each of the four dNTPs. The reaction mixture was incubated at 42°C for 60 min, and stored at -20°C.

2.3.4. Polymerase Chain Reaction.

The standard PCR 100 µl reaction volume contained the following: 50 pmole of each PCR primer, 200 µM of each of dATP, dGTP, dCTP and dTTP, in a buffer containing 10 mM Tris-HCL pH 8.3, 50 mM KCL, 0.01% gelatine and an appropriate amount of $MgCL_2$ in the range 1.5 mM to 5.0 mM, as established for each primer pair by a $MgCL_2$ titration. The equivalent of 1 µg of total reverse transcribed RNA or 1 µg of genomic DNA was used for each reaction. cDNA synthesis or DNA extraction blanks were amplified for each patient to control for contamination during template preparation.

A PCR blank containing all the components of the reaction, except the template, was used as a control for contamination of the amplification reaction components. The reaction was overlaid with 70 µl mineral oil to prevent evaporation during 30 to 40 cycles of amplification.

Primers.

Primers were diluted to a concentration of 50 pmol/µl in TE buffer, divided into aliquots and stored at -20°C.

Deoxynucleotide triphosphates.

Each dNTP was prepared in sterile distilled water to a concentration of 20 mM and the pH adjusted to 8. Equal volumes of the four dNTPs combined to yield a final concentration of 5 mM for each dNTP. The combined dNTPs were then divided into aliquots and stored at -80°C.

10X PCR Buffers.

Two buffers at a 10x concentration were used: a 10X Tris/KCL/gelatine buffer was prepared from autoclaved stock solutions and contained 100 mM Tris-HCL pH 8.3, 500 mM KCL, 0.1% gelatine and a variable amount of $MgCL_2$ in the range 15 to 50 mM. A second 10X buffer contained 1% Triton X-100 in 700 mM Tris-HCL pH 8.8 with 15 to 50 mM $MgCL_2$. The buffers were filter sterilised, divided into aliquots and stored at -20°C. A proprietary 10X detergent based buffer containing 15 mM $MgCL_2$ supplied by some Taq polymerase vendors was also used.

Thermostable DNA polymerase.

Taq DNA polymerase from a variety of vendors was used at 2.5 U per standard 100 µl reaction volume. Vent DNA polymerase was used at 2 U per 100 µl reaction volume in a buffer supplied by the manufacturer.

Thermocyclers and Temperature Profile.

Initially, an in house thermocycler, designed and manufactured by L. Purves and J. Thornthwaight of the Department of Chemical Pathology, University of Cape Town, was used. The instrument consisted of a carbon block with an array of holes drilled into the top to accommodate the PCR reaction vessels. The block was heated by the resistance of the carbon to the passage of an electrical current and cooled by allowing water to flow through a channel drilled through the center of the block. The machine was later replaced by two commercial thermocyclers: a Techne PHC-2 and a Techne Gene-E (Techne, Cambridge, UK).

A typical temperature profile for the amplification of cDNA using primers P1a and P2 consisted of:

denaturation:	94°C	45 s to 1 min	
annealing:	57°C	45 s to 1 min	
extension:	72°C	2 min	13 cycles
		3 min	13 cycles
		4 min	13 cycles
		10 min	1 cycle

A temperature 5 to 10°C below the lowest T_m of the primer pair being used in amplification was used as the annealing temperature. Stepped extension times were used to allow for degradation of Taq polymerase during thermocycling. Generally, a 1 to 2 min extension time was allowed per 1000 bases of template to be amplified.

Nested PCR.

Primers OP1 and OP2 were used to amplify cDNA in 40 cycles of amplification. One microliter of the PCR reaction served as template for a further 30 cycles of amplification using nested primers NP1 and NP2. One microliter of a cDNA synthesis blank was carried through both amplification systems to control for contamination.

2.3.5. Agarose Gel Electrophoresis and Visualisation of PCR Products.

PCR products were separated by agarose gel electrophoresis in 1X TAE buffer and visualised on a long wavelength UV light box after ethidium bromide staining. The concentration of agarose was varied between 1.5% and 2% for standard agarose, depending on the size of the PCR products to be separated. Low melting point agarose or MetaPhor agarose (FMC BioProducts, Rocklands, ME, USA) was used at a concentration of 2% to 3%, as appropriate for the size of the amplified product.

Molecular Weight Markers for Gel Electrophoresis.

Lambda DNA was digested to completion (overnight at 37°C) with *Hind*111 or *Dra*1, in a buffer supplied by the restriction endonuclease manufacturer. *Hind*111 digestion yielded fragment sizes of 23130, 9415, 6557, 4361, 2322, 2027, 564 and 125 bp. Digestion with *Dra*1 produced fragment sizes of 8596, 8370, 7834, 6816, 6038, 3599, 2303, 2152, 1075, 696, 533, 228, 174 and 90 bp. A commercial DNA marker, Bio Marker Low, with DNA fragment sizes 1000, 700, 500, 400, 300, 200, 100 and 50 bp, was purchased from Bio Ventures Incorporated, Murfreesboro, Tennessee, USA.

2.3.6. Purification of PCR Products.

2.3.6.1. Filtration Methods.

Millipore Ultrafree-MC 30,000 and 100,000 NMWL filter units were used to separate high molecular weight PCR products from low molecular weight primers and primer dimers. Five 100 µl PCR reactions were extracted with an equal volume of TE buffered phenol:chloroform:isamyl alcohol (25:24:1). DNA in the aqueous phase was precipitated by the addition of 0.2 volumes 10 M ammonium acetate and 2 volumes of 100% ethanol. After incubation for 20 min at -80°C, the precipitate was recovered by centrifugation, washed with 70% ethanol and then dried under vacuum. The pellet was resuspended in

300 µl TE buffer and loaded into the cartridge of the filter unit and spun for 2 min at 7500g in a variable speed fixed angle microfuge. The filtrate was discarded and the high molecular weight DNA retained by the membrane was then washed twice more with 300 µl of TE. The DNA was recovered from the membrane by rinsing with 20 µl TE buffer.

2.3.6.2. Gel Purification Methods.

Five 100 µl PCR reactions were combined, the mineral oil overlay removed by extraction with an equal volume of chloroform and the DNA in the aqueous phase ethanol precipitated. The DNA pellet was resuspended in 20 µl TE buffer and loaded into a single lane of an agarose gel. After electrophoresis, the gel was stained with ethidium bromide and the position of the DNA band to be isolated, visualised under UV light. Care was taken to avoid damaging DNA during UV visualisation by using a hand held, long wavelength, low intensity UV lamp.

Electrophoresis onto DEAE Cellulose.

Strips of DEAE cellulose were placed in two slits cut on either side of the DNA band. The DNA band was electrophoresed onto one strip of DEAE cellulose, while non-specific high molecular weight smearing, if present, was blocked by the other strip. DNA bound to the cellulose strip was then washed free of inhibitors present in the agarose using a high salt buffer and eluted in a low salt buffer as described in Ausubel et al, 1994.

Electro-elution from agarose gel slices.

Excised DNA containing agarose gel slices were tied into dialysis tubing containing 400 µl TAE buffer. The dialysis tubing was placed into the buffer tank of an electrophoresis apparatus and the DNA electrophoresed out of the gel slice at 100 volts for 10 min. The DNA containing buffer was then transferred to a microfuge tube, extracted with an equal

volume of phenol:chloroform:isoamyl alcohol and the DNA recovered by ethanol precipitation.

Extraction of DNA from Agarose Gel Slices Using Commercially Available Kits.

Two commercially available kits, Promega Magic or Wizard Prep (Promega, Madison, Wisconsin, USA) and Qiaex gel extraction kit (Qiagen, Hilden, Germany), both based on the binding of DNA in solubilised agarose gel slices to a proprietary DNA binding matrix, were also used.

2.3.7. Re-amplification of PCR Products.

Gel purified PCR fragments were serially diluted (1:100, 1:1000 and 1:10000) and 1 µl of the dilution was amplified for 30 cycles.. Care was taken to avoid contamination with other PCR products by washing the buffer tank of the electrophoresis apparatus prior to electrophoresis. Only one PCR product was loaded per gel to avoid cross contamination between PCR products.

2.3.8. Cloning PCR products.

Competent DH5α cells were prepared to a competency of 10^6 to 10^7 by a rubidium chloride/calcium chloride method as described in Ausubel et al (1994). PCR products were gel purified to remove unincorporated primers, primer dimers and non-specific amplification products prior to cloning into the plasmid pUC 18. Generally, 50 ng of plasmid was ligated to a 10 fold molar excess of PCR product

2.3.8.1. Klenow-Kinase-Ligase Method (Sorens, 1991).

This method was used to clone PCR products generated by primers with restriction endonuclease sites at the 5'-ends (primer sets P1a/P2, and P1b/P2). Briefly, the PCR products were blunt ended with the Klenow fragment of *E. coli* DNA polymerase 1 to remove the single 3' terminal A added by the terminal transferase activity of Taq polymerase (Clarke, 1988), phosphorylated at the 5'-end using T4 polynucleotide kinase, which allowed T4 DNA ligase to concatenate the PCR products. The concatenated PCR products were then digested with *Pst*1 and *Eco*R1. The sticky ended PCR products were gel purified and ligated into *Pst*1/*Eco*R1 digested pUC 18, using standard protocols, as described in Ausubel et al (1994). A portion of the ligation was transformed into competent *E. coli* DH5(α) cells and plated onto LB plates coated with 5-bromo-4-chloro-3-indolyl-ß-D-galactoside (Xgal) and isopropyl-1-thio-ß-galactoside (IPTG) and containing 100 μg ampicillin. Recombinants (clones unable to metabolise Xgal due to insertional inactivation of the α-peptide coding region of the enzyme ß-galactosidase after induction with IPTG) were selected, grown to saturation in 2X TY medium, and plasmid DNA prepared by a modified alkaline lysis miniprep method as described by Kraft et al, 1988. The presence of an insert was confirmed on a 0.8% agarose gel by either releasing the cloned fragment from the multiple cloning site by *Pst*1/*Eco*R1 digestion, or by comparing the mobility of the intact recombinant plasmid to that of a plasmid containing no insert.

2.3.8.2. Blunt Ended Cloning.

pUC 18 was linearised with *Sma*1 and dephosphorylated using shrimp alkaline phosphatase as described in Ausubel et al (1994). Purified PCR products amplified by Vent DNA polymerase were ligated directly into the vector. PCR products amplified with Taq DNA polymerase were blunt ended with Klenow prior to ligation.

2.3.8.3. *Sma*1 Cloning (Lui and Schwarz, 1992).

Blunt ended PCR products were ligated to *Sma*1 linearised pUC 18 vector in the presence of *Sma*1. Vector self-religation reconstitutes a *Sma*1 site, which was then re-digested by *Sma*1 thereby reducing the background of religated vector. The *Sma*1 site was destroyed in plasmids which ligated to a PCR product.

2.3.8.4. TA Cloning.

The single 3'-A added by Taq (Clark, 1988) is complementary to a single 3'-T present at each end of the linearised vector pGEM-T. This enables cloning of Taq generated PCR products without having to blunt end the PCR products. PCR products were cloned into pGEM-T (Promega, Madison, Wisconsin, USA) following the manufacturers recommended protocol.

2.3.9. DNA Sequencing.

DNA was sequenced using the Sanger dideoxy method (Sanger et al, 1977) with the Sequenase Version 2.0 kit purchased from United States Biochemical, Cleveland, Ohio, USA.

2.3.9.1. Direct Sequencing of Double Stranded PCR Products.

Four 100 µl PCR reaction volumes where combined and gel purified by one of the methods described. The basic Sequenase protocol (United States Biochemical Corporation, 1987) as suggested by the manufacturer, was modified according to Casanova et al (1990) and Bachman et al (1990). The protocol differed from the standard

Sequenase protocol by the method of annealing primer to template and the inclusion of detergents in all the sequencing steps. Tween 20 and NP 40 at 0.5% were included in all steps of the Sequenase protocol (Bachman et al, 1990). Primers were annealed to heat denatured template by snap cooling on ethanol/dry ice (Casanova et al, 1990). The 10 µl annealing reaction contained 3 to 5 µg of purified PCR product, 5 pmole of the sequencing primer, 2 µl sequencing buffer (USB) and 0.5% Tween 20 and MP40 detergent. After annealing, the following were added on ice: Tween 20 and MP40 to 0.5%, 2 µl dGTP labelling mix diluted 1:4 (USB), 1 µl 0.1 M dithiothreitol (USB) and 0.5 to 1 µl [^{35}S] dATP. The manganese containing Mn buffer (USB) was included when sequencing close to the primer. The labelling reaction was started with 2 µl diluted Sequenase enzyme (USB) and incubated for 3 min at 18°C. 3.5 µl of the labelling mix was transferred to tubes containing 2.5 µl of each of ddA, ddG, ddC, ddT termination mixes (USB) at 37°C. The extension/termination reaction was terminated after 5 min by the addition of 4 µl stop solution (USB).

2.3.9.2. Sequencing of Cloned PCR Products.

Recombinant plasmids were prepared for sequencing using a modified alkaline lysis miniprep method which incorporated a PEG 8000 precipitation step (Kraft et al, 1988). 3 to 5 µg of purified plasmid was alkaline denatured, and sequenced without detergents using the basic Sequenase protocol (United States Biochemical Corporation, 1987).

2.3.9.3. Denaturing Polyacrylamide Gel Electrophoresis.

Sequencing reactions were separated on 6% polyacrylamide gels (19:1 acrylamide to bis-acrylamide) containing 8 M urea as a denaturant, using 1X TBE as the electrophoresis buffer. Dried gels were autoradiographed against ß-Max film (Radiochemical Centre, Amersham, UK) for periods of 24 hr to 2 weeks.

2.4. Results and Discussion.

2.4.1. RNA extraction and cDNA Synthesis.

Total RNA extraction from confluent fibroblast monolayers cultured in 250 ml tissue culture flasks consistently yielded between 25 and 40 µg of RNA with a 260 nm / 280 nm ratio >1.9. Visualisation of the isolated RNA on formaldehyde agarose gels showed that the RNA was undegraded, with sharp 28s and 18s rRNA bands (data not shown). RNA stored as an ethanol precipitate was stable for at least a year when stored at -80°C.

First strand cDNA synthesis was primed using either an oligo dT_{15} primer, or a HPRT cDNA specific primer P2 and the results of cDNA amplification using these differently primed templates are described below. A 100 µl cDNA reaction volume proved useful in optimising PCR, but was subsequently reduced to 25 µl, with a proportional reduction in the amount of template reverse transcriptase and the other components of the reverse transcription reaction. First strand cDNA preparations were stable for at least a year at -20°C. Second strand cDNA synthesis was primed by primer P1a during the first round of the polymerase chain reaction.

2.4.2. HPRT cDNA Amplification.

Initial attempts at amplification of a 721 bp fragment encompassing the coding region of HPRT cDNA using primers P1a and P2 were unsuccessful at a range of $MgCL_2$ concentrations (1.5, 2, 3, 4, and 5 mM), with an annealing temperature of 57°C and a 1 min extension time at 72°C. Primer degradation was eliminated as possible cause of amplification failure by analysing primers P1a and P2 on a 20% acrylamide gel. The primers were undegraded with most of the primer concentrated in a single band.

Low molecular weight primer dimers were massively amplified during PCR. Adding Taq polymerase after a 3 min incubation at 94°C to start amplification (a hot start) did not significantly decrease the amount of primer dimers amplified, nor yield a detectable PCR product of the predicted size. Decreasing primer P1a concentration from 50 pmole/100 µl reaction to 1 pmole had no effect. In an attempt to destabilise primer dimer formation and improve the specificity of amplification, formamide was added to the PCR reaction at concentrations of 2.5%, 5% and 10% (Sarkar et al, 1990), but also had no effect on reducing primer dimer formation. Incrementally decreasing or increasing the annealing temperature of 57°C in the range 50 to 60°C was unsuccessful in generating a PCR product.

Altering the extension time profile at 72°C to 2 min extension for the first 13 cycles, followed by 3 min extension for 13 cycles, 4 min for 13 cycles and a final extension of 10 min for one cycle, while keeping denaturing and annealing temperatures constant at 94°C and 57°C respectively, resulted in the successful amplification of a PCR product of the predicted size.

It is interesting that amplification of HPRT cDNA was only possible when extension times were increased in a stepped system of 2, 3 and 4 minutes. P1a dimer formation is probably low at an annealing temperature of 57°C however, some primers will anneal to themselves. Once dimers are primed and amplified, they will amplify efficiently and increase geometrically with each PCR cycle. The amount of Taq polymerase becomes limiting as the amount of primer dimer template increases and is compounded by the cumulative loss of enzyme activity due to heat denaturation during 40 cycles of amplification. Increasing the extension time is then necessary to allow time for limiting Taq polymerase to bind to and extend specific HPRT cDNA products.

In retrospect, primer P1a is an example of how not to design a PCR primer. The GC rich nature of the 5'-noncoding end of the HPRT gene sequence is a constraint on choosing a primer sequence with a balanced GC-AT content. However, lack of experience when

designing this first PCR primer resulted in choosing a primer sequence with inter-primer self-complementarity at the 3'-end (Figure 2.3a). Ten out of twelve bases at the 3'-end of the primer were complementary, and all of these bases where G or C resulting in stable dimer priming and extension. In addition, the 3'-end of the primer was also complementary to a sequence within itself (Figure 2.3a), and intra-primer annealing and extension could result in some of P1a being effectively destroyed, especially at the low temperatures used during sequencing. The GC richness of the self-complementary regions and the resultant stability of the primer P1a - primer P1a complex resulted in primer dimers being efficiently amplified at the expense of specific HPRT cDNA sequences. Primer P2 is a "good" PCR primer, with a balanced GC-AT content and no significant propensity to dimer formation, either with itself, or with primer P1a.

Primer P1a also proved to be a "bad" sequencing primer due to dimer formation. A new primer, P1b was synthesised to overcome the problem of dimer formation. The 3'-end of the primer P1a sequence was shortened by the removal of the terminal GG eliminating complementarity at the 3'-terminal base (Figure 2.3b), and resulted in reduced dimer formation. However, between primer complementarity still remained a problem.

Figure 2.3: Predicted dimer formation and primer secondary structure of primers P1a and P1b. (a) Possible intra--primer priming conformation and dimer formation in primer P1a. (b) Reduced between primer complementarity of the modified primer, P1b.

The composition of the PCR buffer was also a factor contributing to the efficiency and success of amplification. Two PCR buffers were assessed (Figure 2.4). A detergent based buffer containing 0.1% Triton X-100 in 70 mM Tris-HCL pH 8.8 produced optimal amplification at 2 mM $MgCL_2$. However, amplification yields as estimated on ethidium bromide stained gels, were consistently lower and often, use of this buffer resulted in failure to amplify a cDNA PCR product. A detergent free buffer containing 50 mM KCl, 10 mM Tris-HCl pH 8.3 and 0.01% gelatine had a broader $MgCL_2$ requirement with optimal amplification at 2 mM and at 4 and 5 mM. Amplification yields at 4 to 5 mM $MgCL_2$ were generally higher than at 2 mM $MgCL_2$.

Although Eckert and Kunkel (1991) reported that Taq polymerase errors occur at a higher frequency when $MgCL_2$ concentration is in large excess to dNTP concentration, yields of PCR products were sufficiently greater at 5 mM $MgCL_2$ compared to 2 mM $MgCL_2$ to justify the use of the higher $MgCL_2$ concentration.

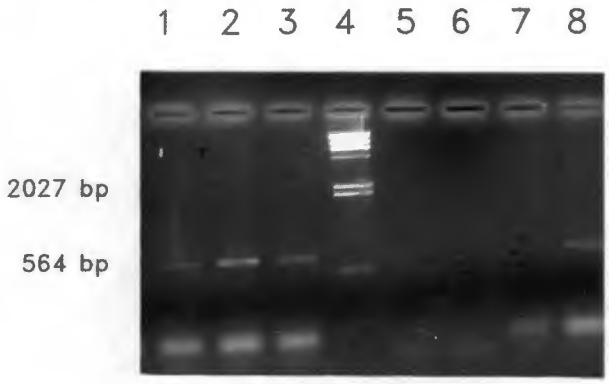

Figure 2.4: A comparison of detergent based and detergent free PCR buffers used in cDNA amplification. Primers P1a and P2 were used to amplify the equivalent of 1 µg of total RNA from the same 100 µl volume oligo dT_{15} primed reverse transcription reaction, using a KCl - Tris-HCl - gelatine buffer or a detergent - Tris-HCl buffer as described in the text. 15 µl of 100 µl each PCR reaction was loaded onto a 2% agarose gel and visualised under UV after ethidium bromide staining. Lanes 1 to 3: amplification in a detergent free buffer at $MgCL_2$ concentrations of 2, 4 and 6 mM. Lanes 5 to 8: amplification using a detergent containing buffer with $MgCl_2$ concentrations at 1.5, 2, 4, and 6 mM. Lane 4: molecular weight marker, lambda phage DNA digested with *Hind*III, the 564 bp and 2027 bp bands are indicated

The optimal amplification conditions for primer pair P1b-P2 were thus established as being a function of the thermocycling profile and the PCR buffer composition. A detergent free buffer containing 10 mM Tris-HCL pH 8.3, 50 mM KCL, 0.01% gelatine and 5 mM $MgCL_2$, with 200 µM of each dNTP and 50 pmoles of each of primers P1a and P2 in a 100 µl reaction volume was used. The thermocycler profile was:

denaturation:	94°C	1 min	
annealing:	57°C	1 min	
extension:	72°C	2 min	13 cycles
		3 min	13 cycles
		4 min	13 cycles
		10 min	1 cycle

Amplification of HPRT cDNA from control cell lines using 0.3 to 1 µg of reverse transcribed total RNA as template was routinely achieved.

2.4.2.1. Oligo dT vs Primer P2 Primed Reverse Transcribed Total RNA as PCR Template.

Amplification of oligo dT_{15} primed cDNA under the optimal conditions defined above, produced a single PCR product of the predicted size with minimal background smearing. Conversely, amplification of cDNA primed with PCR primer P2, although yielding a PCR product of expected size, also resulted in significant high and low molecular weight smearing (Figure 2.5). This background smearing is probably a consequence of mispriming at the low primer annealing temperature (0°C) and extension temperature (42°C) at which reverse transcription occurs. These miss-primed templates are linearly amplified through 40 PCR cycles. The use of oligo dT_{15} to prime cDNA synthesis and an internal, upstream sequence specific primer P2 in PCR, is a semi-nested primer system and results in increased specificity.

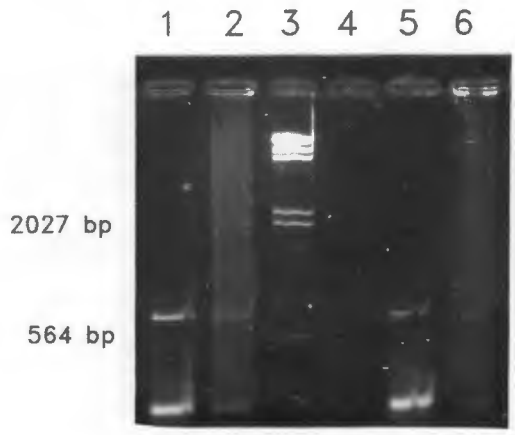

Figure 2.5: Amplification of oligo dT_{15} primed or P2 primed cDNA. Amplification of oligo dT_{15} primed and P2 primed cDNA. The equivalent of 1 µg of oligo dT_{15} or P2 primed reverse transcribed total RNA, isolated from a control cell line (lanes 1 and 2) and a patient cell line F45 (lanes 5 and 6), was amplified for 40 cycles using primer pair P1a and P2 under optimal PCR conditions as described in the text. 16 µl of the amplification reaction was separated on a 2% agarose gel. Lanes 1 and 5: oligo dT_{15} primed cDNA. Lanes 2 and 6: P2 primed cDNA. Lane 4 is a PCR blank which have been carried through both the RNA extraction protocol and cDNA synthesis. Lane 3: DNA molecular weight marker, *Hind*III digest of lambda DNA, the 546 bp and 2027 bp bands are indicated. The low molecular weight bands visible below the 564 bp band of the marker are primer dimers.

2.4.2.2. Re-amplification of PCR Products.

The cDNA templates were a limited resource, and in order to generate sufficient PCR product for direct sequencing, it was necessary to re-amplify PCR products. Direct re-amplification of 1 µl of unpurified PCR product resulted in primer dimers being efficiently re-amplified and the system became rapidly saturated with non-specific amplification products. Amplification of a gel purified PCR product was optimal at 1:1000 or 1:10000 dilution as judged by the presence of a single, bright band of the predicted size on

ethidium bromide stained agarose gels. The diluted purified PCR fragment provided an effectively unlimited template stock for re-amplification.

2.4.2.3. Nested Primer Amplification of HPRT cDNA.

A nested primer HPRT cDNA amplification system was developed for convenience and for added sensitivity. The first amplification reaction using OP1 and OP2 to amplify cDNA, serves as a "stock" of template for re-amplification using primers NP1 and NP2. Gel purification of PCR products with the associated risk of cross-contamination, is no longer necessary. The system is extremely sensitive and specific: any non-specific PCR products amplified during the first, outer round of amplification, would not be amplified during the second, nested, round of amplification. The leverage of an additional 30 cycles of amplification enables rare cDNA transcripts to be amplified with sometimes spectacular success (Figure 2.6). Primer pairs OP1/OP2 and NP1/NP2 produced optimal amplification at a $MgCL_2$ concentration of 1.5 mM.

To reduce the risks of contamination, the following precautions were taken:

1. All reagent stocks were aliquotted in a laminar flow cabinet and stored separately from cDNA templates and PCR products. Any contamination could then be eliminated by discarding the PCR "kit" in use without great expense.
2. PCR reactions were set up at a different bench to where PCR products were processed.
3. An RNA extraction blank was carried through cDNA synthesis and amplified in parallel with cDNA templates to control for contamination during template preparation.
4. A PCR reaction blank was included with each series of PCR reactions.
5. If two or more different templates were to be amplified simultaneously, an additional PCR reagent blank was used. The first blank was set up and closed before the template was brought to the bench and served as a true reagent blank.

The second PCR blank controlled for cross-contamination during PCR reaction preparation and was the last PCR reaction tube to be closed.

6. All PCR products in a series with a positive blank were discarded.

Rigorous adherence to these precautions resulted in only occasional PCR contamination during this study.

2.4.3. DNA Sequencing.

The sequencing primers were located so as to allow sequencing of both strands of the PCR product in overlapping segments (Figure 2.2). Compressions were resolved by running the sequencing gel at 90 watts so as to increase the temperature of the gel and aid denaturation of DNA secondary structure, or by using the dITP labelling mix supplied with the sequencing kit (USB), or by sequencing the complementary strand. Where necessary, sequences close to the PCR primers were obtained by sequencing cloned PCR products using vector sequencing primers.

2.4.3.1. Direct Sequencing of PCR Products.

Successful direct sequencing of PCR products depended on the preparation of 2 to 5 µg of pure, primer free, PCR product. The following methods of PCR fragment purification were assessed in terms of ease, efficiency of product recovery and the quality of the sequence generated.

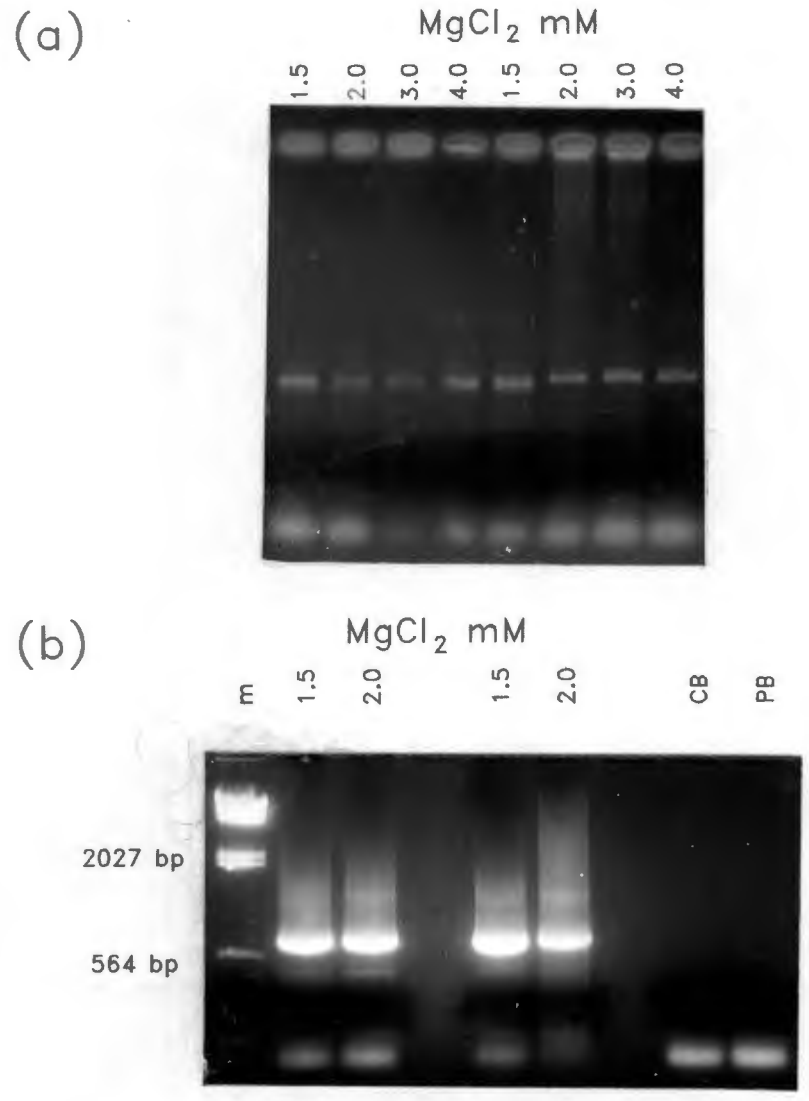

Figure 2.6: **Nested amplification of HPRT cDNA.** (a) HPRT cDNA from 2 normal fibroblast cell lines was amplified for 40 cycles with outer primers OP1 and OP2 with $MgCl_2$ concentration varied from 1.5 mM to 4 mM. (b) 1 µl of the outer primer PCR reactions at 1.5 mM and 2.0 mM $MgCl_2$ were amplified at the corresponding $MgCl_2$ concentrations with the nested primers NP1 and NP2 for an additional 30 cycles. A PCR blank ($MgCl_2$ at 1.5 mM) carried through from cDNA synthesis is shown in the lane CB and a PCR blank carried through both outer and nested PCR is shown in lane PB. Both PCR blanks confirm the absence of contaminating HPRT cDNA in the PCR system. Lane m is a DNA molecular weight marker (*Hind*III digest of lambda DNA), with the 564 bp and 2027 bp bands indicated. 15 µl of each 100 µl reaction volume was loaded onto a 1.5% agarose gel.

a) Direct Purification of PCR Products Using Millipore Ultrafree-MC filter Units.

The 30,000 NMWL filter unit retained primer dimers and PCR fragments prepared using this unit were unsuitable for sequencing. The 100,000 NMWL unit efficiently removed primer dimers, but at the cost of some loss of high molecular weight PCR product. As a result, it was necessary to autoradiograph sequencing gels for up to 2 weeks. The DNA sequences generated were, however, of excellent quality. This purification method was quick and easy, but the yield of purified PCR product was low. This method could not be used if any high molecular weight non-specific amplification products or background smearing in the PCR products were present, as these DNA species would be co-purified with the specific amplification product. The constraints of a single specific PCR product in the PCR reaction and the relatively high losses of PCR product during purification, meant that this method was not suitable for large scale direct sequencing of multiple templates.

b) Recovery of DNA from agarose gel slices after electrophoresis.

Agarose gel electrophoresis efficiently separates PCR products from non-specific amplification products or primer dimers in the PCR reaction. PCR fragments can then be recovered from agarose gel slices.

Electro-elution of PCR products from agarose gel slices proved to be unsuitable for purifying DNA for direct sequencing. DNA recovery was poor and the DNA co-purified with inhibitors present in the agarose gel slice.

Electrophoresis onto DEAE cellulose provided purified DNA variable in quality with fair yields. The method was time consuming and did not lend itself to the simultaneous preparation of multiple PCR fragments. An unavoidable consequence of accurately placing the DEAE cellulose strips and checking whether transfer was complete, was the exposure of the DNA in the agarose gels to damaging amounts of ultra violet light. As a result, the quality of DNA sequences varied, depending on how long the DNA had been

exposed to UV light. Readable sequences were obtained after 2 weeks exposure to autoradiographic film.

Commercial gel purification kits, such as the Magic/Wizard Prep and Qiaex kits, are based on the recovery of DNA from solubilised agarose gel slices using a proprietary DNA binding matrix. Recovery of DNA was better than 80% and readable sequences of high quality were attainable after a 24 hour exposure of the gel to autoradiographic film. Most of the direct sequencing in this study used PCR product template prepared with these kits.

The Promega Magic and Wizard Prep kits are cartridge based and were quick and easy to use. Solubilised agarose gel contaminants were removed by washing with 80% isopropanol, which is not as volatile as ethanol and can be difficult to remove completely, before DNA elution from the binding matrix. This was an occasional cause of failure to obtain a readable sequence. A disadvantage of the kit is that DNA is recovered in a 50 µl volume and further concentration was occasionally necessary before the DNA could be used for direct sequencing.

The Qiaex kit methodology is tube based and not as convenient to use. The wash steps are, however, with ethanol based buffers which are easier to evaporate prior to DNA elution. DNA could be eluted from the silica binding matrix in buffer volumes as small as 20 µl, which was a major advantage over the Magic/Wizard Prep kit, as no further concentration of DNA prior to direct sequencing was usually necessary.

2.4.3.2 Sequencing of Cloned PCR Products.

To Clone or Not to Clone...

Taq DNA polymerase lacks a 3'-5' exonuclease proof reading activity and is as a result, error prone. An error rate of $2x10^{-4}$ was reported by Saiki et al (1988), while an error rate of $2.6x10^{-5}$ is reported by one Taq polymerase manufacturer (Boehringer Mannheim).

Eckert and Kunkel (1991) reported an error rate of 10^{-4} to 10^{-5}, depending on dNTP and $MgCL_2$ concentration, and the pH of the PCR buffer. When PCR products are sequenced directly, these random errors are averaged out and the consensus sequence is read. When PCR generated DNA molecules are cloned, a single PCR amplified molecule is sequenced. Any errors due to lack of fidelity of Taq polymerase will then be seen as a change in the DNA sequence of that particular cloned PCR fragment and two clones would need to be sequenced and compared to the reference sequence in order to distinguish between Taq errors and true mutations. If the sequences of two clones differs, those sequences differences are a result of Taq errors. If two or more clones have the same sequence change, the sequence change is accepted as a genuine mutation. In autosomal recessive conditions, mutations in compound heterozygotes may be difficult to detect by sequencing of cloned PCR products. Two alleles, both different from the normal sequence would be present. Mutations on each allele would have to be found in more than one clone to confirm that the change is not the consequence of a Taq error. Fortunately, HPRT is X-linked with only one allele in affected males.

There are a number of advantages to cloning and then sequencing PCR products:

1. Milligram quantities of cloned PCR product can be generated in an overnight culture. For large PCR fragments requiring multiple sequencing reactions, this is particularly useful.
2. PCR products of similar size are sometimes difficult to separate during gel purifying for direct sequencing. Cloning PCR fragments allows easy sequence differentiation between similarly sized PCR products.
3. Sequences within a few bases of the primer may be difficult to read. Sequencing of cloned PCR products using vector sequencing primers enables sequencing of the entire PCR product.
4. Some PCR primers are "bad" sequencing primers as is the case with primer P1a, and to a lesser extent, P1b. Both are GC rich primers with a high degree of self-complementarity. Sequencing cloned PCR products with a vector sequencing primer avoids this problem.

Single stranded conformational polymorphism (Orita et al, 1989), heteroduplex analysis and chemical cleavage of mismatched heteroduplexes (Cotton et al, 1988) have been used as preliminary mutation screening methods to detect the presence of mutations in amplified DNA segments prior to DNA sequencing. These methods are particularly useful where a mutation in more than one candidate gene may be responsible for a specific biochemical defect. The clinical and biochemical profile of HPRT deficiency is however, sufficiently clear to justify sequencing HPRT cDNA without a preliminary mutational screen.

A combination of direct PCR sequencing and sequencing of cloned PCR products was used in this study to define the mutations responsible for HPRT deficiency.

3. MOLECULAR BASIS OF THE LESCH-NYHAN SYNDROME.

3.1 Introduction.

The Lesch-Nyhan syndrome (Lesch and Nyhan 1964) is a clinical condition consequent to a complete HPRT deficiency. The syndrome is characterised by purine overproduction leading to hyperuricemia and a central nervous system disorder, which includes severe spasticity, choreoathetosis, mental retardation and compulsive self-mutilatory behaviour.

3.1.1 Pathogenesis of HPRT Deficiency.

3.1.1.1 Biochemical basis of Purine Overproduction.

Fibroblasts cultured from Lesch-Nyhan patients have increased rates of *de novo* purine synthesis and an increased intracellular pool of PRPP (Rosenbloom et al, 1968). It is generally accepted that the rate limiting step of *de novo* purine biosynthesis is catalysed by amidophosphoribosyltransferase (amidoPRT), the enzyme that catalyses the formation of ß-phosphoribosylamine from glutamine and PRPP (Pallela and Fox, 1989). The enzyme is cumulatively inhibited by mono-, di- and triphosphate adenine and guanine nucleotides. Inhibition is relieved by binding of PRPP. Intracellular levels of PRPP are governed by the rate of PRPP synthesis by PRPP synthetase and by the rate of PRPP utilisation. HPRT deficiency results in decreased utilisation of PRPP and a rise in intracellular PRPP levels which drives *de novo* synthesis by relieving inhibition on amidoPRT. In addition, the K_m for amidoPRT (0.1-0.5 mM) is several-fold above the physiological concentration of PRPP (in the micromolar range). An increase in PRPP concentration will thus directly lead to an increase in the activity of amidoPRT (Holmes, 1978). Increased PRPP availability, rather than a deficiency in the nucleotide pool is mainly responsible for increased *de novo* synthesis in HPRT deficient cells (Becker et al, 1987, 1989).

3.1.1.2 Purine Nucleotide Pools in HPRT Deficiency.

There is a three to fourfold elevation in hypoxanthine and xanthine in plasma and a four to tenfold increase in the excretion of total purines in patients with the Lesch-Nyhan syndrome (Harkness et al, 1988; Mateos and Puig, 1993). This loss of purines appears to be adequately compensated in most tissues by an increase in *de novo* purine nucleotide synthesis and no major changes in the intracellular nucleotide pool profile have been observed in cultured human fibroblasts (Becker, 1987) and a rat neuroma cell line (Zoref-Shani et al, 1993). Erythrocytes lack the capability to synthesize purines *de novo* and disturbances in intracellular nucleotide pools are detectable. ATP and GTP nucleotide pools may be depleted in erythrocytes of some Lesch-Nyhan patients with the effect on GTP pools being more marked (Simmonds et al, 1988; Harkness and McCreanor, 1991). NAD levels are increased two to three fold (as a result of increased PRPP levels) and may be a reliable marker of severe HPRT deficiency (Simmonds, 1988; Simmonds, 1994). ZTP (5-amino-4-imidazole-carboxamide ribotide triphosphate) and other Z-nucleotides may be detectable in erythrocytes of patients with the Lesch-Nyhan syndrome (Simmonds, 1988), however this is not a specific consequence of HPRT deficiency since Z-nucleotides are also found in purine nucleoside phosphorylase deficiency and in some patients with PRPP synthetase superactivity (Sidi and Mitchell, 1985).

APRT activity has been reported to be increased in erythrocytes of Lesch-Nyhan patients due to stabilisation of APRT by increased PRPP pools (Kelley et al, 1969; Seegmiller et al, 1967).

3.1.1.3 Pathogenesis of Neurological Symptoms and Self-Mutilation.

The accumulation of hypoxanthine, xanthine and to a lesser extent uric acid, reported in the CNS of patients with the Lesch-Nyhan syndrome (Harkness et al, 1988) are unlikely to be a direct cause of the neurological symptoms in these patients. Similar levels of

oxypurine metabolites are found in neurologically normal patients with partial HPRT deficiency (Harkness et al, 1988; Puig and Mateos, 1993).

Amino acid pools in the brains of Lesch-Nyhan patients are generally markedly decreased. However, levels of glutamine and urea are increased (Rassin et al, 1982, Harkness et al, 1988). However, blood and urine amino acid levels are normal (Harkness et al, 1988), which would appear to exclude severe nutritional deprivation as a cause of the brain amino acid pool changes.

The brains of Lesch-Nyhan patients are morphologically normal (Stout and Caskey, 1989). One of the earliest neurological signs of the Lesch-Nyhan syndrome are movement disorders, which points to involvement of the basal ganglia of the brain, the major site of dopaminergic neurones and an area of the brain with high levels of HPRT activity. Lloyd et al (1981) reported a general deficit in dopamine-neurone function (low dopamine and homovanillic acid levels and low activities of dopa decarboxylase and tyrosine hydroxylase activities) in the brains of Lesch-Nyhan patients. Their results indicated a functional loss of between 65% and 90% of nigrostriatal and mesolimbic dopamine terminals. Recently, Ernst et al (1996) demonstrated abnormally few dopaminergic nerve terminals and cell bodies using positron-emission tomography to measure the accumulation of flourodopa F 18 tracer in the brains of Lesch-Nyhan patients. The dopaminergic deficits were pervasive and appeared to be developmental in origin. Since guanine nucleotides participate in the regulation of dopamine receptor binding, it is possible that decreased GTP pools which may result from HPRT deficiency in tissues with a low capacity for purine *de novo* synthesis, could affect dopaminergic function (Stout and Caskey, 1989, Puig and Mateos, 1993). Watts (1985) has explored the link between possible GTP depletion due to HPRT deficiency and disturbances in pterin metabolism. GTP-cyclohydrolase catalyses the rate limiting step of pterin *de novo* synthesis and a decrease in the GTP pool could affect the production of tetrahydrobiopterin, leading to impaired synthesis of norepinephrine, dopamine and serotonin. This would in turn lead to disturbed neurotransmission in the basal ganglia and may contribute to the pathogenesis of the neurological symptoms of the Lesch-Nyhan syndrome.

Reduced GTP levels have also been reported to occur in erythrocytes of patients with PRPP synthetase superactivity and purine nucleoside phosphorylase deficiency (Sidi and Mitchell, 1985; Simmonds et al, 1988). The presence of neurological symptoms in these patients (Simmonds et al, 1988) supports a link between GTP depletion due to HPRT deficiency and dopaminergic function. Moreover, the observed GTP depletion in erythrocytes correlates closely with the severity of the CNS involvement.

There is some evidence from animal models to support the involvement of dopaminergic neurones in the pathogenesis of the Lesch-Nyhan syndrome. The administration of a dopamine agonist to rats rendered hypersensitive to dopamine by unilateral intracerebral injection of 6-hydroxydopamine into the nigrostriatal region, caused an incessant biting of limbs and tail (Ungerstedt, 1971).

Transgenic HPRT deficient mice show no overt neurobehavioral abnormalities and HPRT deficiency has no notable affect on the content of brain purines (Jinnah et al, 1993). Purine synthesis *de novo* was however increased four to fivefold. The mice are not entirely neurologically normal and dopamine levels have been reported to be reduced by up to 50% (Finger et al, 1988; Jinnah et al 1992). The mouse model may be less dependant on HPRT for purine salvage, which may make it a poor model for the human condition. The reported ratio of HPRT/APRT enzyme activities is 1.86 in whole brain extracts of neonatal rats, and 11.66 to 51.38 in human brain obtained on autopsy (Brosh et al, 1990). The relative importance of APRT activity in mice suggests that doubly (APRT and HPRT) deficient mice may be a better animal model of the Lesch-Nyhan syndrome. Wu and Melton (1993) used an adenine analogue 9-ethyladenine to block APRT activity in 9 to 12 month old HPRT deficient mice. Treated mice showed a high frequency of self-injurious behaviour which resulted principally from excessive stereotypic grooming, rather than from the appearance of a new pattern of self-mutilatory behaviour. Genetically APRT and HPRT deficient mice may thus be an appropriate animal model for the study of the Lesch-Nyhan syndrome. The link between HPRT deficiency and the neurochemical changes apparent in the brains of Lesch-Nyhan patients still needs to be defined.

3.1.2 Genetic Basis of the Lesch-Nyhan Syndrome.

HPRT is an X-linked gene, hence hemizygous males with the Lesch-Nyhan syndrome may inherit a mutant allele though the maternal lineage, or the defective gene may result from a *de novo* germ line mutation. About one third of cases are the consequence of new mutations. The Lesch-Nyhan syndrome is rare in females and is usually the result of non-random X chromosome inactivation of the normal chromosome in a carrier female (Ogasawara et al, 1989; Aral et al, 1996).

Mutations at the HPRT locus show marked genetic heterogeneity *in vivo* (Wilson et al, 1986a; Davidson et al 1989a; Davidson et al, 1991; Tarle et al, 1991; Sege-Peterson et al, 1992; Sculley et al, 1992; Cariello and Skopek, 1993) and provide an opportunity to gain insight into the molecular basis of inborn errors of metabolism.

In this thesis, nine Lesch-Nyhan patients were investigated at the molecular level to determine the nature of the molecular defects in the HPRT gene.

3.2 Materials and Methods.

3.2.1 Origin of Patients.

Patients (P) are coded in the text by cell line reference numbers (Cell Bank, Department of Chemical Pathology, University of Cape Town, South Africa). Cell line numbers prefixed by "L" are Epstein Barr virus transformed lymphoblast cultures and cell line numbers prefixed by "F" are fibroblast cultures derived from forearm skin biopsies.

Patient JM (F526)

This male patient presented at Red Cross Children's Hospital, Cape Town, South Africa, at the age of 1 month with severe vomiting and diarrhoea leading to shock, renal failure, and hypotonia, progressing to spastic quadriplegia with marked irritability. At 18 months, the patient presented with macroscopic haematuria and a worsening of the neurological symptoms. Urinary calculi, composed of uric acid, were passed. Plasma urate was markedly elevated at 0.97 mmol/l.

HPRT enzyme activity assayed in haemolysates prepared from P526 using the method of Steyn and Harley (1984) described in Section 4.2.3.2., showed less than 0.1% residual activity compared to a control haemolysate. Doubling the amount of haemolysate in the assay to 200 µg protein and increasing the incubation time to 1 hour did not lead to a detectable increase in HPRT activity. The ratio of [^{14}C] hypoxanthine to [^{3}H] phenylalanine incorporation by fibroblasts cultured in a Hanks balanced salt based labelling medium (See Section 4.2.3.5.) was less than 0.01% of control values (Section 4.3.2. and Table 4.2), confirming a virtually complete deficiency of the enzyme in the patient.

The following HPRT deficient cell lines derived from Lesch-Nyhan patients were kindly supplied by John Duley and Anne Simmonds of the Purine Research Laboratory, Guy's Hospital, London.

Cell Line	Patient	Origin
F748	MJ	Italy
F749	PP	UK
F750	MP	UK
F751	AB	UK
F764	DT	UK
F765	JR	UK
F766	LW	UK
F768	LH	Brazil

3.2.2 Materials.

Dulbecco's Modified Eagle Medium was purchased from Gibco BRL, Gaithersburg, Maryland, USA or from Highveld Biological, Kelvin, South Africa. Foetal calf serum was purchased from Highveld Biological, Kelvin South Africa. Sterile plastic pipettes, centrifuge tubes, flasks and petri dishes were of tissue culture grade.

[8-^{14}C] Hypoxanthine and L-[2,3,4,5,6-^{3}H] phenylalanine were purchased from Amersham International plc, UK. Hionic-Fluor was from Packard, Downers Grove, Illinois, USA.

3.2.3 Methods.

3.2.3.1 Tissue Culture Methods.

Fibroblast cultures were established from forearm skin biopsies using standard methods. Cultures were grown in 250 ml tissue culture flasks in an atmosphere of 10% CO_2 at 37°C and fed twice weekly with Dulbecco's Modified Eagles medium (DMEM) supplemented with 10% foetal calf serum. No antibiotics were used in the medium as this reduced the risks of undetected *Mycoplasma* infection. The cultures were screened at intervals for *Mycoplasma* infection using bisbenzamide fluorochrome stain (Hoechst No. 33258), (Chen, 1977).

3.2.3.2 Fibroblast Double Label Experiments.

A confluent fibroblast monolayer in a 250 ml flask was trypsinised and seeded in triplicate into a six well tissue culture plate to give a level of confluency of approximately 80%. The plates were incubated overnight in DMEM supplemented with 10% foetal calf serum to allow the cells to recover. The medium was then replaced by 1 ml labelling medium containing 1 µCi [^{3}H] phenylalanine and 0.3 µCi [^{14}C] hypoxanthine in DMEM with no foetal calf serum. After a 3 hr incubation at 37°C in an atmosphere of 10% CO_2, the cells were treated with 1 ml ice cold 5% trichloroacetic acid (TCA) and the precipitate washed three times with 2 ml ice cold 5% TCA to remove unincorporated radiolabelled substrate. The washed precipitate was dissolved in 1 ml 0.1 M NaOH and neutralised by the addition of 100 µl 6.6% acetic acid. The dissolved precipitate was added to 10 ml Hionic-Fluor and counted in a Beckman LS6001C scintillation counter using windows of 0 to 200 keV for [^{3}H] and 400 to 1000 keV for the [^{14}C] label.

3.2.3.3 Molecular Methods

The molecular methods have been described in detail in Section 2. Initially, HPRT cDNA prepared from F526 was amplified using primers P1a and P2. In subsequent experiments, nested primers were used in the amplification of HPRT cDNA from all the Lesch-Nyhan patients investigated. Amplified PCR products were blunt end cloned into pUC 18 using the *Sma*1 method or sequenced directly as indicated in the results. The coding region of at least two independent clones was completely sequenced.

HPRT genomic DNA was amplified as indicated in the results using the primers and PCR conditions described in Section 2.3.4.

3.3 Results.

3.3.1 Double Label Studies.

A marked decrease in the incorporation of [^{14}C] hypoxanthine relative to normal [^{3}H] phenylalanine incorporation was observed in all the cell lines derived from the Lesch-Nyhan patients (Table 3.1). The results are consistent with the virtually complete absence of HPRT activity in these patients.

Table 3.1: Incorporation of [^{14}C] hypoxanthine relative to [^{3}H] phenylalanine by 8 Lesch-Nyhan and 3 control cell lines.

Cell Line	[^{14}C] Hx (cpm)	[^{3}H] Phe (cpm)	Ratio [^{14}C]/[^{3}H]
F747*	915	1026	0.89
F734*	743	1115	0.67
F735*	1537	1737	0.89
F748	73	1276	0.06
F749	82	1016	0.08
F750	84	1443	0.06
F751	105	1455	0.07
F764	70	1424	0.05
F765	91	1697	0.05
F766	40	727	0.06
F768	49	1150	0.04

* control cell lines.
Values are the means of triplicate determinations.
Abbreviations: hx, hypoxanthine

3.3.2 Results of the Molecular Investigations.

Amplification of 1 µg of reverse transcribed total RNA extracted from F526 using primers P1a and P2, yielded PCR products of a smaller size and with a lesser band intensity than PCR products from a control preparation amplified under identical conditions (Figure 3.1). However, low amplification yields due to with primer dimer formation necessitated the design of the nested primer system described in Section 2.3.4.

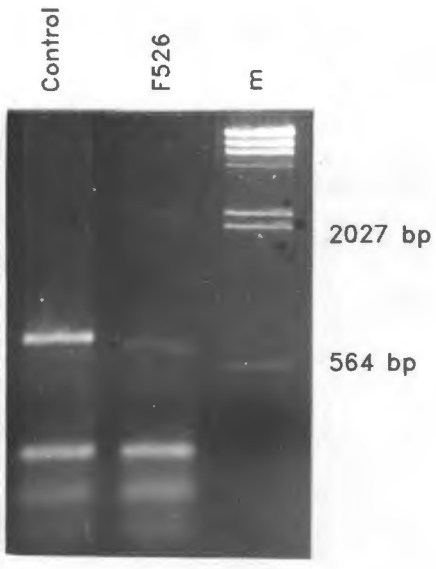

Figure 3.1: Amplification of HPRT cDNA using primers P1a and P2 from F526 and a control cell line. The DNA molecular weight marker in lane m is lambda DNA digested with *Hind*III. The 564 bp and 2027 bp bands are indicated. The low molecular weight bands visible below the 564 bp band of the marker are primer dimers.

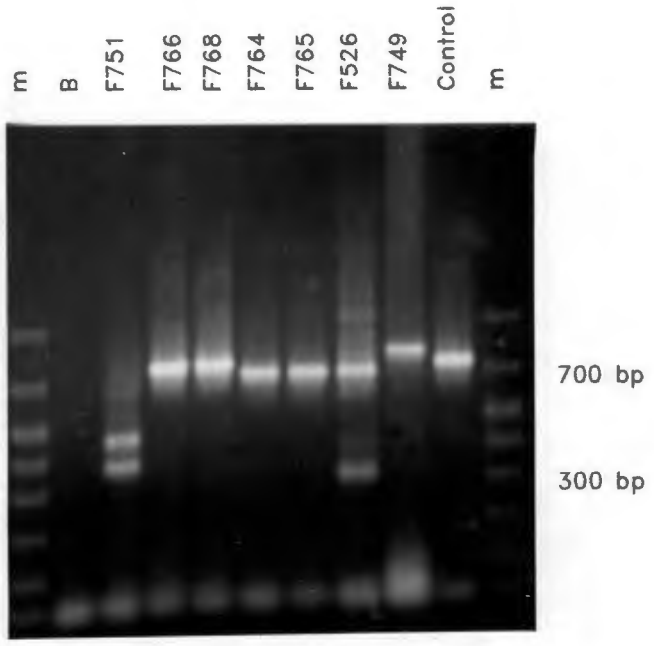

Figure 3.2: Nested primer amplification of HPRT cDNA from 7 Lesch-Nyhan cell lines. HPRT cDNA was amplified with the outer primers OP1 and OP2. 1 µl of the outer primer PCR reaction was then amplified using the nested primers NP1 and NP2. Lanes m; DNA molecular weight marker (Bio Marker Low) with DNA fragment sizes 1000, 700, 500, 400, 300, 200, 100 and 50 bp. Lane B; an amplification blank carried through both the outer and nested amplification systems. PCR products were resolved on a 2% MetaPhor agarose gel.

The results of the nested primer amplification are shown above in Figure 3.2. Abnormally sized PCR products were amplified with the nested primers NPF and NPR from five cell lines, F526, F749, F751, F764 and F765. HPRT cDNA amplified from F766 and F768 were consistent with a predicted size of 741 bp and of equivalent size to the PCR products amplified from a control. HPRT cDNA could not be amplified from two cell lines, F748 and F750.

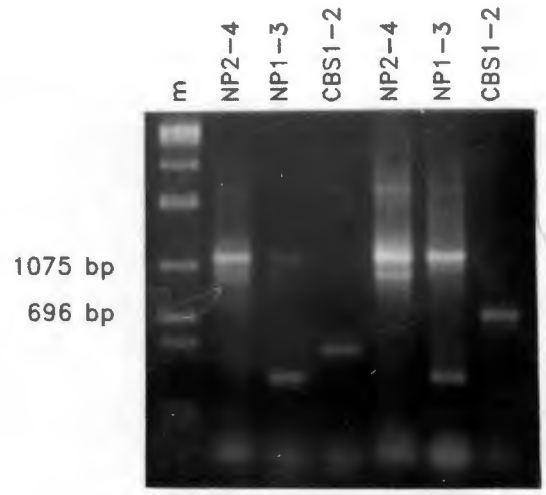

Figure 3.3: Amplification of a control cDNA (cystathionine-ß-synthase) from cDNA preparations of F748 and F750 using a nested primer system. Cystathionine-ß-synthase cDNA was amplified in two segments. Outer primers CBS1 and CBS2 were used in the initial 40 cycle amplification reaction (Lane CBS1-2), only low molecular weight non-specific amplification products are visible. In order to amplify the 5' end of the cDNA, 1 µl of the outer primer PCR reaction was amplified with nested primers NP1 and NP3 (lane NP1-3) and yielded a PCR product of approximately the predicted size of 1289 bp. An overlapping segment of the 3' end of the cDNA was amplified using primers NP2 and NP4 (Lanes NP2-4) and yielded a PCR product of approximately the predicted size of 1075 bp. Lane m; DNA molecular weight marker, lambda DNA digested with *Dra*I, the 696 bp and 1075 bp bands are indicated. Position of PCR primer pairs: CBS1 nt -109 to -93 (forward) and CBS2 nt 1741 to 1766 (reverse); NP1 nt -58 to -33 (forward) and NP3 nt 1212 to 1231 (reverse); NP2 nt 665 to 684 (forward) and NP4 nt 1714 to 1739 (reverse). Numbering is according to the sequence and convention of Kraus et al (1993), with the A of the ATG start codon numbered as base 1.

3.3.2.1 Null Mutations.

HPRT cDNA could not be amplified from three independent RNA and cDNA preparations of F748 and F750. A control mRNA (cystathionine-ß-synthase EC 4.2.1.22) could however be amplified from the same preparations (Figure 3.3), suggesting that the failure to amplify an HPRT mRNA did not lie in the experimental system, but was a true reflection of the defect responsible for the Lesch-Nyhan syndrome in these two patients.

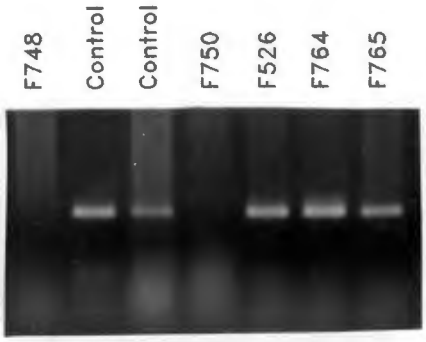

Figure 3.4: Genomic amplification of a segment of HPRT intron 6 from genomic DNA of F748, two control cell lines, F749 and the exon 7 deletion mutants F526, F764 and F765.

In order to determine whether the absence of an amplifiable HPRT cDNA was a consequence of a deletion of all or part of the HPRT gene, a 281 bp segment of intron 6 (nt 36127 to nt 36407) of the HPRT gene was amplified from genomic DNA preparations using primers P6 and P7. A segment of intron 6 could be amplified from controls, but not from F748 and F750 (Figure 3.4). These results suggest that a large structural deletion of all or part of the HPRT gene, affecting one or both of the 5' and 3' PCR primer binding sequences, is responsible for the absence of an amplifiable HPRT mRNA in F748 and F750.

3.3.2.2 Single Base Insertion Events.

Amplification of HPRT mRNA from F766 and F768 yielded PCR products which migrated in the same position as PCR products amplified from a control cell line (Figure 3.2). DNA sequencing of cloned PCR products showed different single base insertions in both patients. In the cell line F766, a single T was inserted within a run of four T 's. between nucleotides 294-T to 297-T within exon 3 (Figure 3.5a).

(a)

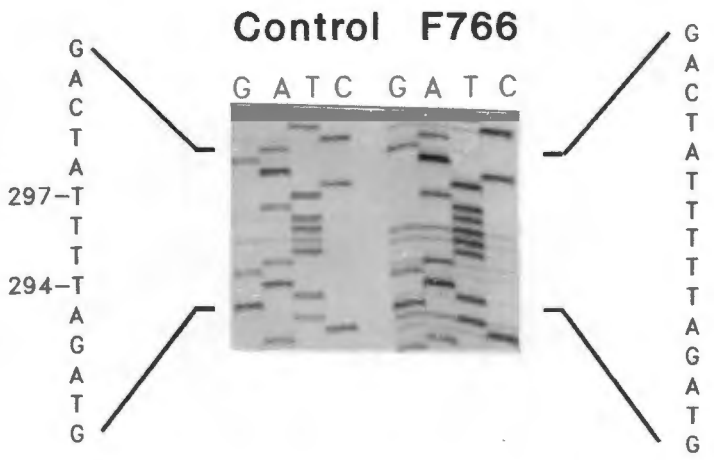

(b)

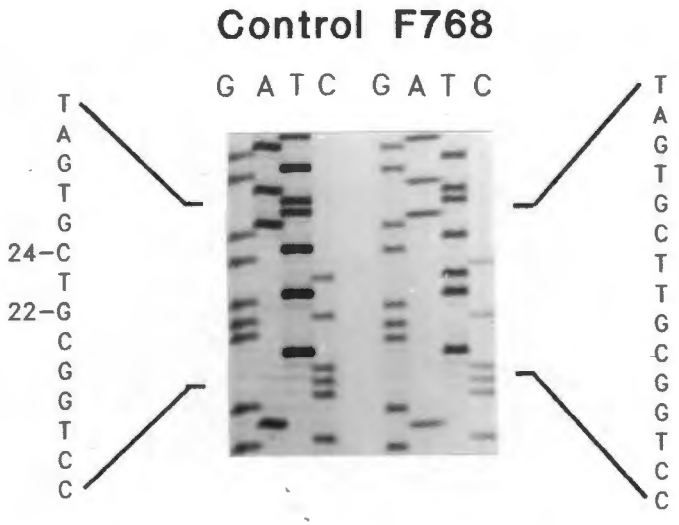

Figure 3.5: Single base insertions identified in the coding region of HPRT cDNA amplified from F766 and F768. (a) F766: insertion of a T between 294-T and 297-T. (b) F768: insertion of a T between 22-G and 24-C. The HPRT cDNA sequence is numbered with the A of the ATG start codon numbered as nucleotide 1.

In the cell line F768, a single T was inserted within the sequence 21-CGTCG-25 in exon 1, creating the sequence 21-CGTTCG (Figure 3.5b).

3.3.2.3 Large Insertion or Deletion Events.

Similarly sized PCR products, which were smaller than control PCR products, were amplified from three Lesch-Nyhan patient cell lines F526, F764 and F765. DNA sequencing of cloned PCR products showed an exact 47 bp deletion of exon 7 in all three patients (Figure 3.6). The lower molecular weight band present in F526 (Figure 3.2) was reproducibly amplified from three independent cDNA preparations. This low molecular weight PCR product was cloned and sequenced, but proved to be a non-HPRT specific amplification product with no sequence homology to either the HPRT cDNA or gene.

In order to determine whether the deletion of exon 7 in F526, F764 and F765 was due to a splice junction mutation or due to a deletion within the HPRT gene, primers LN1 and LN2 located within intron 6 and intron 7 respectively were synthesised. The predicted 599 bp segment included the whole of exon 7 and the flanking intron sequences. Amplification with the LN1 and LN2 primer pair proved difficult to optimise. PCR product yields from 5 control templates were variable, ranging from complete failure to amplify the target fragment to easily visualised PCR products. Varying the annealing temperature of the PCR reaction between 50°C and 60°C, well below the predicted primer T_m of 68°C and 70°C, did not improve PCR product yields. Yields of PCR products were greatest at a $MgCl_2$ concentration of 1.5 mM. Varying the $MgCl_2$ concentration within the PCR reaction in the range 1.5 to 5 mM did not result in an increase in the efficiency of the amplification reaction. The reasons for the poor amplification efficiency of the LN1-LN2 primer pair are not clear. There is no obvious intra- or inter- primer complementarity which can potentially reduce PCR efficiency. It is unlikely that the problem lay in the degradation of the DNA preparations, as a segment of intron 6 could be easily amplified using primers H6 and H7 from all the DNA preparations (Figure 3.4).

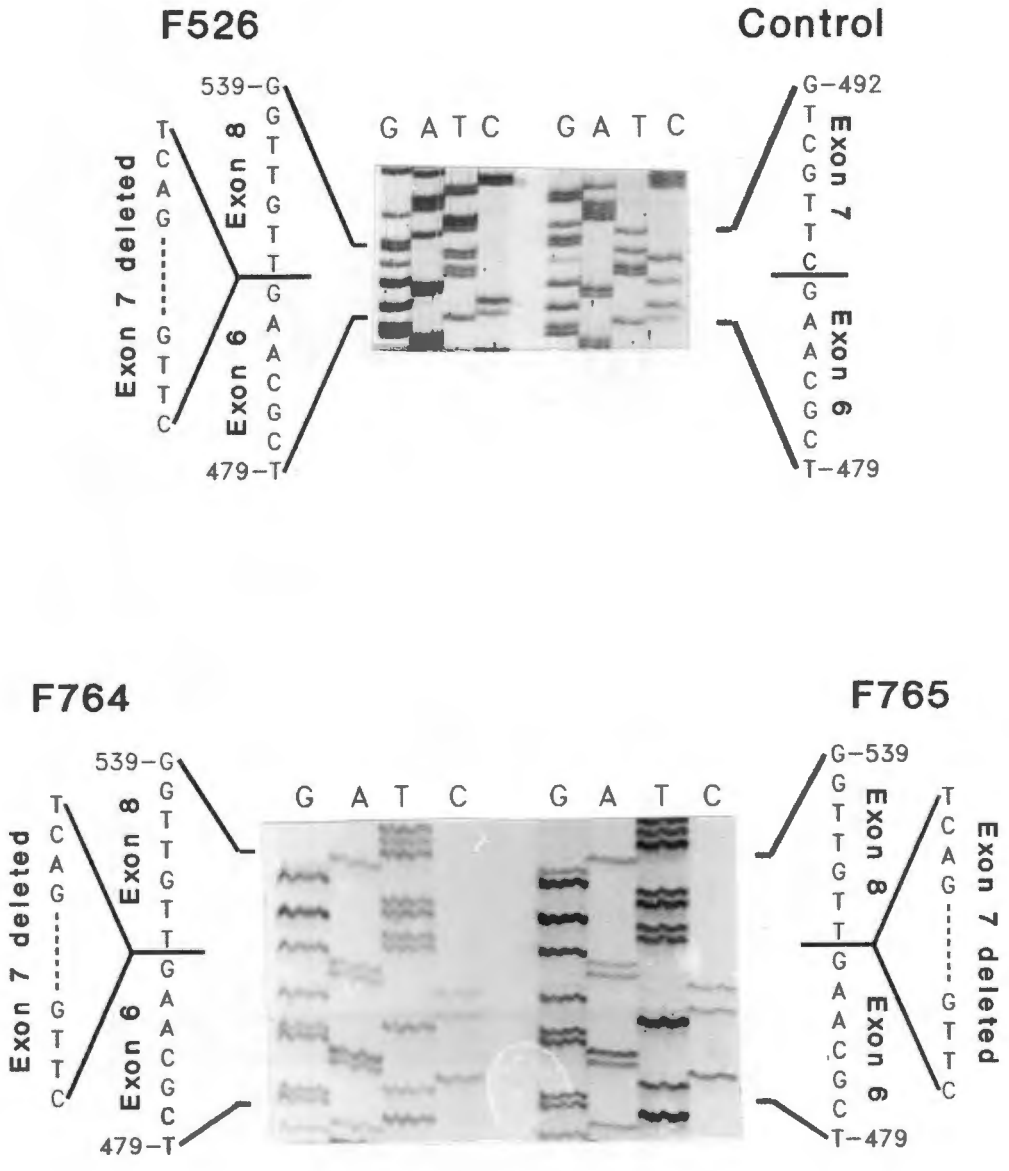

Figure 3.6: The 47 base pair cDNA deletion of exon 7 in F526, F764 and F765. The HPRT cDNA sequence is numbered with the A of the ATG start codon numbered as nucleotide 1.

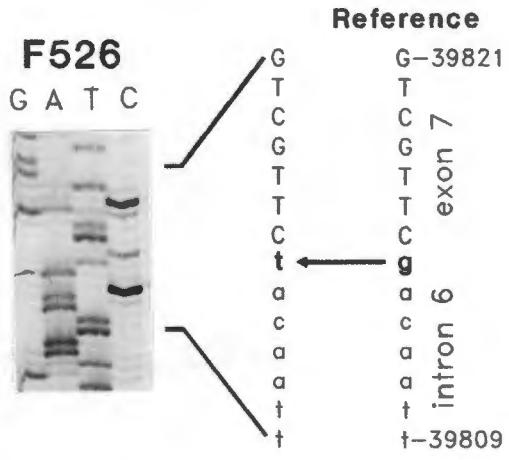

Figure 3.7: Splice junction mutation in F526. A 39815-G to T transversion in the invariant AG of the intron 6 splice acceptor results in a cDNA deletion of exon 7. Nucleotides within intron 6 are shown in lower case. The HPRT gene reference sequence and numbering is according to Edwards et al (1990).

Nevertheless, PCR products of approximately the predicted size could be amplified from genomic DNA preparations of F526. The PCR products were cloned and the intron/exon boundary of exon 7 sequenced using primer LN1. A 39815-G to T transversion in the invariant AG of the intron 6 splice acceptor was found (Figure 3.7).

Exon 7 could not be amplified from genomic DNA preparations of F764 and F765. These results suggest that the deletion of exon 7 in HPRT cDNA of these two HPRT variants is most likely to be the result of a deletion spanning exon 7 within the HPRT gene. However, in view of the difficulties experienced in amplification of exon 7 with the primer pair LN1 and LN2, this interpretation of the results is speculative and these two patients require further investigation in order to define the defects at the gene level.

A single, larger than expected PCR product was amplified from F749. Direct sequencing of the amplified cDNA showed a 60 bp insertion between the boundaries of exon 6 and 7 (Figure 3.8). A search of the HPRT gene sequence showed that the inserted sequence was derived from intron 6 with the 5'-end of the insert located at nt 36223 (1204 bp from the 3' boundary of exon 6) and the 3'-end of the insert at nt 36282 (3533 bp from the 5' boundary of exon 7).

In order to examine the flanking sequences of the insert in more detail, genomic DNA prepared from F749 was amplified using primers P6 and P7. These primers are located on either side of the intron 6 derived insertion and yielded a PCR product of approximately the predicted 281 bp size in both the patient and a control. Direct sequencing of PCR products revealed a 36221-T to A transversion in the genomic 5'-flanking sequence of the 60 base insertion (Figure 3.9).

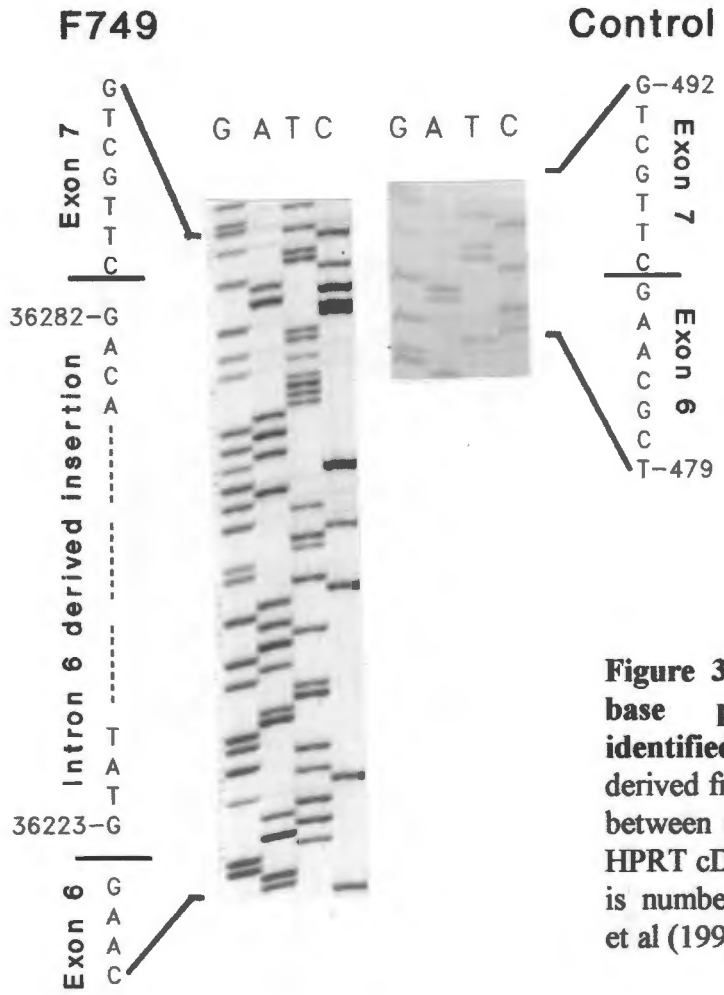

Figure 3.8: Sequence of the 60 base pair cDNA insertion identified in F749. The insertion is derived from intron 6 and is inserted between exon 6 and exon 7 of the HPRT cDNA. The inserted sequence is numbered according to Edwards et al (1990).

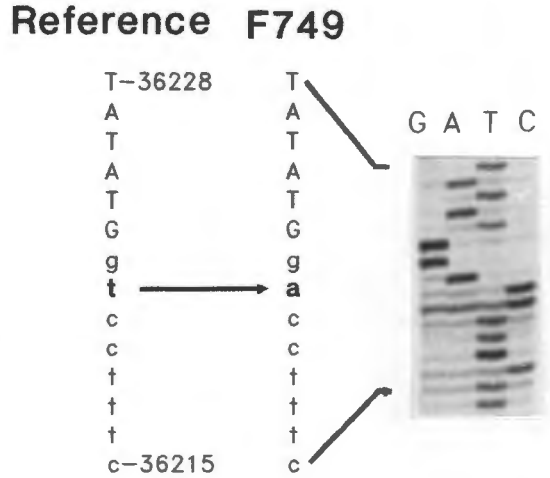

Figure 3.9: A 36221-T to A transversion in intron 6 of the HPRT gene of F749 creates a 3' splice site. Nucleotides flanking the insertion are shown in lower case.

Amplification of HPRT cDNA from F751 yielded two low molecular weight bands (Figure 3.3). Initial attempts at directly sequencing the lower molecular weight PCR product was complicated by the difficulty in separating the two bands completely on standard agarose gels. Direct sequencing of the low molecular weight PCR product showed a deletion of exons 2, 3, 4, and 5. However, it was possible to read a superimposed shadow sequence which appeared to be HPRT cDNA derived (data not shown).

For this reason, both PCR products were separately excised, cloned and sequenced. The lower molecular weight band, or Type A cDNA transcript, showed a 375 bp deletion of exons 2, 3, 4 and 5 (Figure 3.10). The higher molecular weight band (Type B transcript) showed a 357 bp deletion of exons 2, 3, and 4 (Figure 3.10). The two HPRT cDNA transcripts identified in F751 thus share a deletion of exons 2, 3 and 4, but differ in the presence or absence of exon 5. A total of 10 clones, 6 of the low molecular weight PCR products and 4 derived from the higher molecular weight species, were sequenced. All the clones proved to be either Type A or Type B transcripts.

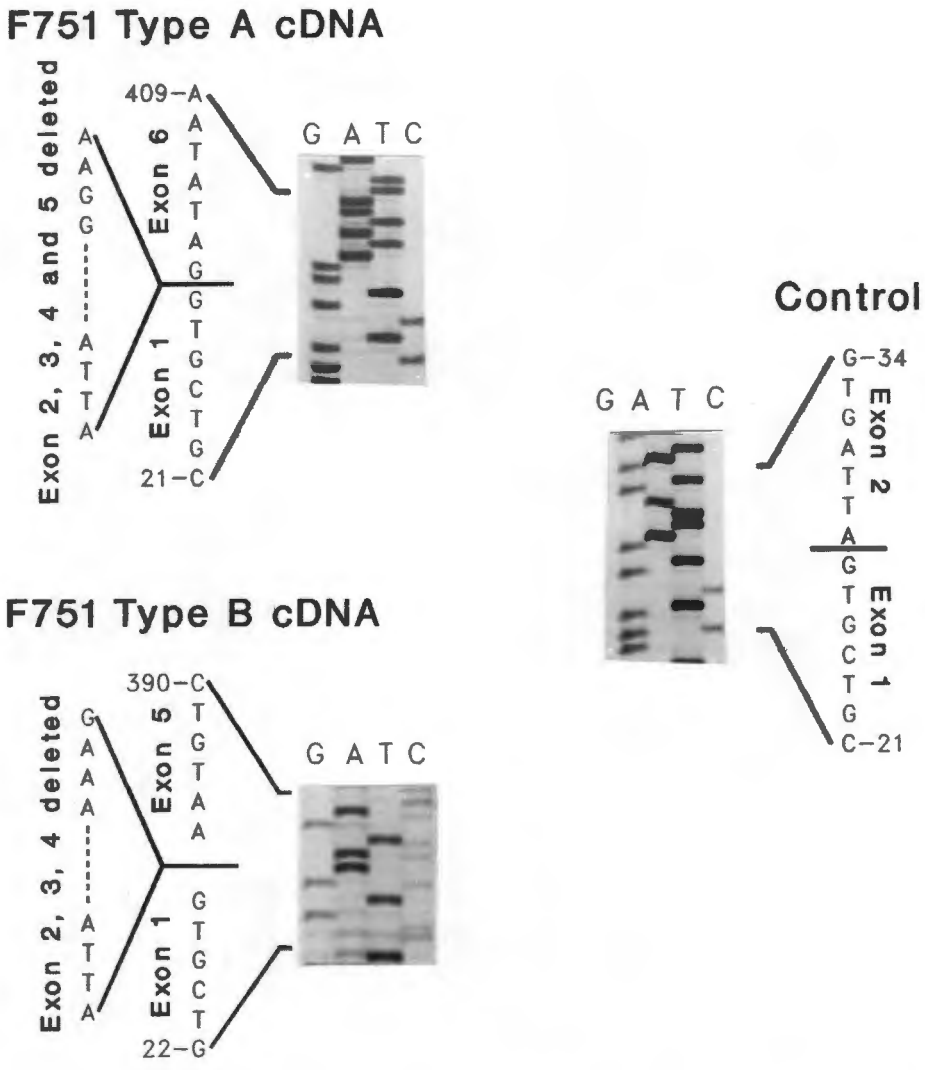

Figure 3.10: The two HPRT cDNA transcripts isolated from F751 share a deletion of exons 2, 3 and 4, but differ in the presence or absence of exon 5. Type A transcripts are characterised by a deletion of exons 2, 3, 4 and 5. Type B transcripts are characterised by a deletion of exons 2, 3 and 4. The HPRT cDNA sequence is numbered with the A of the ATG start codon numbered as nucleotide 1.

3.4 Discussion.

A review of mutations reported in Lesch-Nyhan patients (Table 3.2) shows remarkable genetic heterogeneity which is in accordance with Haldane's principle (Haldane, 1935). Haldane predicted that lethal X-linked mutations that confer no advantage to heterozygotes, would frequently arise as spontaneous new mutations. Complete selection against 50% of a carrier female's male offspring would result in a rapid loss of the deleterious mutation from the population and as a result, about one third of mutations at an X-linked locus are likely to have arisen *de novo*.

The neurological features of the Lesch-Nyhan syndrome are a consequence of severely impaired HPRT activity of usually less than 1% of control values. It is not surprising that nearly 50% of the reported mutations in the Lesch-Nyhan syndrome are insertion or deletion events (based on a survey of *in vivo* HPRT mutations shown in Tables 3.2 and 4.4). The effect of a DNA insertion or deletion on protein structure is not restricted to a single amino acid and in two thirds of cases, would result in an alteration of the reading frame. Termination codons account for 3 of 64 codons and a termination codon would be expected to occur in a random sequence once every 21 codons. A cDNA insertion or deletion event is thus likely to result in incorrectly coded amino acids as well as premature termination of the amino acid sequence. This would lead to total disruption of protein structure and function. Even without sequencing, the size of the HPRT cDNA amplified from the nine patients investigated gives an indication of the nature of the mutation. Three classes of mutations were distinguished:

1. Null mutations: no amplifiable HPRT mRNA.
2. Single base substitutions and small deletion/insertion events: mutations which do not significantly alter the size of the amplified cDNA.
3. Large deletion/insertion events: mutations resulting in a detectable change in the size of the amplified HPRT cDNA.

Table 3.2: Survey of *in vivo* mutations in HPRT which result in an altered protein size.

Variant	cDNA Change	Predicted Change in Protein	Comment	Reference
Female	no cDNA	no translation	entire gene deleted, non-random X-inactivation	Ogaswara et al, 1989
RJK 853 (McA)	no cDNA	no translation	entire gene deleted, no mRNA, no CRM	Yang et al, 1984; Wilson et al, 1986a
P748 (MJ)	no amplifiable cDNA	no translation	deletion not defined	this study
P750 (MP)	no amplifiable cDNA	no translation	deletion not defined	this study
$HPRT_{Illinois}$ (RKJ 951, RT)	13 bp deletion nt -12 to 1	cannot predict	partially deficient, A of ATG start codon deleted, normal mRNA levels, 0.8% CRM	Wilson et al, 1986a; Gibbs et al, 1989; Davidson et al, 1994
1151	G 3 to A	cannot predict	start codon altered	Tarle et al, 1991
P768 (LH)	insertion single T between nt 22 and 24	10 amino acids		this study
RJK 1760 (CB)	deletion exon 2 (nt 23 to 134)	10 amino acids		Gibbs et al, 1990
GM1662, 25 (DM)	duplication of exons 2 and 3	315 amino acids	no CRM partial activity, 1.6%	Yang et al, 1988 Sege-Peterson et al, 1992
P751 (AB)	deletion exons 2, 3, and 4 or deletion of exons 2, 3, 4, and 5	93 and 99 amino acids	deletion of exons 2, 3, and 4. Exon 5 alternatively spliced	this study
$HPRT_{Chicago}$ (DM)	insertion single T (run of 2 Ts, nt 56 and 57)	19 amino acids	normal mRNA, no CRM	Wilson et al, 1986; Davidson et al, 1989a
1423	deletion ATT nt 80 to 82	217 amino acids Tyr 28 deleted		Tarle et al, 1991
RJK 1939 (BB)	deletion single T (either nt 125 or 126)	51 amino acids		Gibbs et al, 1990
TH $HPRT_{Shelford}$ 754-4 AS MS	C 151 to T	Arg 51 to Stop 50 amino acids	same mutation in 5 different patients	Fujimori et al, 1990; Davidson et al, 1991; Tarle et al, 1991; Sege-Peterson et al, 1992
RJK 2108 (RK)	deletion nt 155 to 195	71 amino acids		Gibbs et al, 1990
$HPRT_{Coorparoo}$ (JG)	insertion T 171	25 amino acids	no mRNA, no CRM	Keough et al, 1988; Gordon et al, 1991

Variant	cDNA Change	Predicted Change in Protein	Comment	Reference
RJK 866 (CW) 1650	insertion of a G in run of 6 G between nt 207 and 212	72 amino acids	same mutation in 2 different patients	Gibbs et al, 1989; Tarle et al, 1991
Family 10 $HPRT_{Codicote}$	insertion T288 (run of 2 T nt 288 and 289)	106 amino acids	same mutation in 2 different patients	Gibbs et al, 1986; Davidson et al, 1991
RJK 1322 (RC) Patient 3 $HPRT_{Cheltenham}$	deletion GT 289, 290	105 amino acids	same mutation in 3 different patients	Gibbs et al, 1989; Watts et al, 1982; Davidson et al, 1991
P766 (LW)	insertion of a T in a run of 4 T between nt 194 and 297	106 amino acids		this study
RJK 1747 (JM)	deletion GT 317, 318	105 amino acids		Gibbs et al, 1990
Case 4	deletion 5 bp 5'-end of exon 4 (nt 319-322)	112, 196 and 215 amino acids	splice junction altered, multiple mRNA transcripts	Yamada et al, 1992
1052 1757/1758 (sibs) $HPRT_{Bamberidge}$ RT	deletion exon 4 (nt 319-384)	196 amino acids	same mutation in different patients	Tarle et al ,1991 Davidson et al, 1991 Sege-Peterson et al, 1992
RJK 1930	C 325 to T	Gln 109 to Stop		Gibbs et al, 1991
PW	C 368 to G	Ser 123 to Stop	Lesch-Nyhan	Sege-Peterson et al, 1992
TL	insertions between exon 5 and 6	additional amino acids added	A 32863 to G creates 5' splice site, multiple transcripts, partial activity, 50% activity	Sege-Peterson et al, 1992
RJK 2019	deletion single T, either nt 391 or 392	130 amino acids		Gibbs et al, 1990
$HPRT_{Chemside}$ (RW)	deletion exon 6 (nt 402 to 484)	146 amino acids	splice junction mutation, no RNA 0.5% CRM	Keough et al, 1988; Gordon et al, 1991
RJK 984	deletion exons 6, 7, 8 and 9		7989 bp genomic deletion from nt 34612 to 42600	Fuscoe and Nelsen, 1994
MiG	deletion nt 403 to 452	Asp 135 to Val 150 deleted, premature termination	abnormal splicing, multiple transcripts, cryptic splice site in exon 6 utilised partial, 9% activity	Sege-Peterson et al, 1992

Variant	cDNA Change	Predicted Change in Protein	Comment	Reference
RW	Insertion GCA at nt 429	219 amino acids insertion of Ala after Met 143	partial activity 7.5%	Sege-Peterson et al, 1992
1656	insertion single T in run of T's nt 435-437	153 amino acids		Tarle et al, 1991
$HPRT_{Paris}$	T 459 to G	Tyr 153 to Stop	Female Lesch-Nyhan, non-random X-inactivation	Aral et al, 1996
P749 (PP)	insertion 60 nt between exon 6 and exon 7	177 amino acids	T 36221 to A in intron 6 creates 3' splice site for a new "exon"	this study
P526 (JM) P764 (DT) P765 (JR) $HPRT_{Coulsden}$ (Family 4) Family 8 (DAG25) DAG33 DL	deletion exon 7 (nt 485 to 532)	165 amino acids	same mutation in 7 different patients	this study this study this study Mckeran et al, 1975; Watts et al, 1982; ; Gibbs et al, 1986; Davidson et al, 1991; Gibbs et al ,1986; Davidson et al, 1991 Sege-Peterson et al, 1992
HJ	duplication of exons 7 and 8	315 amino acids	Lesch-Nyhan Alu-Alu recombination	Marcus et al, 1993
RJK 974 Patient 4 (Family 3 $HPRT_{North\ Mymms}$) 1321 NB family GS	C 508 to T	Arg 169 to Stop 169 amino acids	same mutation in 5 different patients normal mRNA 2.2% activity	Gibbs et al, 1989; Watts et al, 1982; Gibbs et al, 1986; Davidson et al, 1991; Tarle et al, 1991 Marcus et al, 1992; Burgemeister et al, 1995
1266	insertion GT in repeat sequence between nt 511 and 517	189 amino acids		Tarle et al, 1991
RJK 1894 (PK)	deletion GTT 514-517	217 amino acids		Gibbs et al, 1990
RJK 1210	deletion of 5 bases insertion of 6 bases	153 amino acids		Gibbs et al, 1989
$HPRT_{Chemside}$ (RW)	deletion exon 6 (nt 402 to 484)	146 amino acids	splice junction mutation, no RNA 0.5% CRM	Keough et al, 1988; Gordon et al, 1991

Variant	cDNA Change	Predicted Change in Protein	Comment	Reference
$HPRT_{Connersville}$ (HD) RJK 888 (GM 7092)	deletion exon 8 (nt 533 to 609)	182 amino acids	normal mRNA no CRM Same mutation in 2 patients	Wilson et al, 1986a; Davidson et al 1989a; Gibbs et al, 1989; Gibbs et al, 1990
$HPRT_{Michigan}$ (DA, RJK 855)	deletion GTT 535-537 or TTG 536-538	217 amino acids	normal mRNA no CRM	Wilson et al, 1986a: Davidson et al, 1989a; Gibbs et al, 1989
RJK 906 (GM 1899)	deletion 17 bp, cryptic splice site	203 amino acids	normal mRNA 1.3% CRM	Wilson et al, 1986a; Gibbs et al, 1989; Gibbs et al, 1990
Case 5	deletion 58 bp 5'-end of exon 9 (nt 610 to 567). Insertion of 26 bp of 3'-end of intron 8	233 amino acids	74 bp genomic deletion from intron 8 to exon 9 Alternative splice site utilisation	Yamada et al, 1992
$HPRT_{Brierly\ Hill}$	deletion GT 617, 618	127 amino acids		Davidson et al, 1991
$HPRT_{Evansville}$ (BS, RJK 894)	deletion (nt 643 to 663	242 amino acids	normal mRNA no CRM	Wilson et al, 1986a; Davidson et al, 1989a; Gibbs et al, 1990
Japan 3	deletion nt 648-698	216 amino acids	partially deficient	Igarashi et al, 1989

The amino acid sequence is numbered with the methionine coded by the ATG start codon as residue 1.
The HPRT cDNA sequence is numbered with the A of the ATG start codon numbered as nucleotide 1.
The sequence of the HPRT gene is numbered according to Edwards et al (1990).
Abbreviations: nt , nucleotide; crm, HPRT immunoreactive material.

All of the mutations described in the patients investigated in this study resulted in cDNA insertion or deletion events. Premature termination of the translated sequence due to an early encounter with a nonsense codon resulted in a change in the predicted size of the protein in those cell lines with an amplifiable HPRT mRNA (Figure 3.10). Premature translation termination has been reported to trigger deadenylation-independent mRNA decapping and consequently, an increased rate of mRNA degradation (Muhlrad and Parker, 1994). The qualitative decrease in the levels of HPRT mRNA noted in the amplification of HPRT cDNA from F526 using primers P1b-P2 and the low levels of

HPRT mRNA reported in many Lesch-Nyhan patients (Table 3.2), may well be an illustration of this phenomenon.

3.4.1 Null Mutations.

The defect in two of the Lesch-Nyhan cell lines, F748 and F750, appears to be the result of structural deletions affecting either one or both of the PCR primer binding sequences located in exons 1 and 9. Although the extent of the deletion has still to be determined, the experimental evidence suggests that the defect is not confined to a local area about either exon 1 or exon 9. A segment of intron 6 near the center of the HPRT gene could not be amplified in these two cell lines which indicates that the deletion is very large. Complete deletions of the HPRT gene appear to be relatively rare mutational events, with only two such mutations having been previously reported (see Table 3.2). However, a deletion of exons 6, 7, 8 and 9 has been reported.

3.4.2 Single Base Insertions.

The single base insertions found in F766 and F768 are novel mutations which result in a shift in the reading frame and premature termination of the predicted amino acid sequence (Figure 3.11).

In F766, the frame shift due to the insertion of a T within the sequence 293-ATTTTA-298, results in a predicted protein of 106 amino acids (Figure 3.10) compared to the normal predicted protein of 218 amino acid residues. A review of *in vivo* somatic and germinal mutations at the HPRT locus by Cariello and Skopek (1993b), showed that 23 of 34 single base insertions or deletions shifts were found in runs of two or more identical nucleotides. The data presented in Table 3.2 shows that single base pair insertions previously reported in the Lesch-Nyhan syndrome are more common than single base pair

deletions (5 single base deletions compared to 2 insertions). Four of these mutations occur within two or more mononucleotide runs and 6 of the 7 mutations involve the insertion or deletion of a single T.

The insertion found in F766 is consistent with the Streisinger strand slippage model of frameshift mutagenesis (Streisinger and Owen, 1985). Streisinger proposed that during DNA replication, should the polymerase stall at a run of identical nucleotides, the DNA strands could misalign. When DNA replication resumes, an insertion or deletion of a single nucleotide would result.

The single base insertion defined in F768 results in a predicted protein of 11 amino acids (Figure 3.11). The insertion of a T between nucleotides 22-G and T-23 or 23-T and 24-C occurs within the context of the sequence 21-CGTCG-25, which has the potential to form a small hairpin loop. Two to seven base repeats have been associated with spontaneous deletions in *E. coli* (Nalbantoglu et al, 1986), in human HPRT (Cariello and Skopek, 1993b) and human mitochondrial DNA (Mita et al, 1990) and are associated with two of the GT deletions ($GT_{289,290}$ and $GT_{317,318}$) previously described in Lesch-Nyhan patients (Table 3.2). Insertions within hairpin loops have not previously been reported in Lesch-Nyhan syndrome patients. It is likely that the sequence context of the insertion defined in L768 is fortuitous and the presence of a hairpin loop does not imply a particular mutational mechanism.

```
                10          20          30          40
HPRT     MATRSPGVVI SDDEPGYDLD LFCIPNHYAE DLERVFIPHG
F751-B   MATRSPGVV- ---------- ---------- ----------
F751-A   MATRSPGVV- ---------- ---------- ----------
F749     MATRSPGVVI SDDEPGYDLD LFCIPNHYAE DLERVFIPHG
F526     MATRSPGVVI SDDEPGYDLD LFCIPNHYAE DLERVFIPHG
F766     MATRSPGVVI SDDEPGYDLD LFCIPNHYAE DLERVFIPHG
F768     MATRSPGVRD *

                50          60          70          80
HPRT     LIMDRTERLA RDVMKEMGGH HIVALCVLKG GYKFFADLLD
F751-B   ---------- ---------- ---------- ----------
F751-A   ---------- ---------- ---------- ----------
F749     LIMDRTERLA RDVMKEMGGH HIVALCVLKG GYKFFADLLD
F526     LIMDRTERLA RDVMKEMGGH HIVALCVLKG GYKFFADLLD
F766     LIMDRTERLA RDVMKEMGGH HIVALCVLKG GYKFFADLLD
F768

                90          100         110         120
HPRT     YIKALNRNSD RSIPMTVDFI RLKSYCNDQS TGDIKVIGGD
F751-B   ---------- ---------- ---------- ----------
F751-A   ---------- ---------- ---------- ----------
F749     YIKALNRNSD RSIPMTVDFI RLKSYCNDQS TGDIKVIGGD
F526     YIKALNRNSD RSIPMTVDFI RLKSYCNDQS TGDIKVIGGD
F766     YIKALNRNSD RSIPMTVDFY QTEELL*
F768

               130         140         150         160
HPRT     DLSTLTGKNV LIVEDIIDTG KTMQTLLSLV RQYNPKMVKV
F751-B   --------NV LIVEDIIDTG KTMQTLLSLV RQYNPKMVKV
F751-A   ---------- ----DIIDTG KTMQTLLSLV RQYNPKMVKV
F749     DLSTLTGKNV LIVEDIIDTG KTMQTLLSLV RQYNPKMVKV
F526     DLSTLTGKNV LIVEDIIDTG KTMQTLLSLV RQYNPKMVKV
F766
F768

               170         180         190         200
HPRT     ASLLVKRTPR SVGYKPDFVG FEIPDKFVVG YALDYNEYFR
F751-B   ASLLVKRTPR SVGYKPDFVG FEIPDKFVVG YALDYNEYFR
F751-A   ASLLVKRTPR SVGYKPDFVG FEIPDKFVVG YALDYNEYFR
F749     ARYMLWN*
F526     ASCWI*
F766
F768

               210
HPRT     DLNHVCVISE TGKAKYKA*
F751-B   DLNHVCVISE TGKAKYKA*
F751-A   DLNHVCVISE TGKAKYKA*
```

Figure 3.11: A comparison of the predicted amino acid sequence due to the insertion or deletion events defined in HPRT cDNA of 7 Lesch-Nyhan patients. HPRT, normal predicted HPRT amino acid sequence with methionine coded by the ATG start codon numbered as residue 1. F751-A and F751-B, Type A and Type B cDNA transcripts respectively. The predicted amino acid sequence in F526 is identical to that of F764 and F765.

3.4.3 Large Deletion or Insertion Events.

3.4.3.1 Deletions of Exon 7.

The 47 bp deletion of exon 7 in three patient cell lines F526, F764 and F765 cause a shift in the reading frame and premature termination, resulting in each case, in a predicted protein of 165 amino acids (Figure 3.11). The cDNA deletions in F764 and F765 have not been defined at the gene level. It is possible that a genomic deletion including one or both of the splice junctions defining exon 7 is responsible for the deletion in these two patients. Preliminary results suggesting that the cDNA deletions of exon 7 in F764 and F765 are due to a genomic DNA deletion of exon 7, are not totally convincing. The technical difficulties experienced in amplifying exon 7 from genomic DNA of controls points to the need for alternative PCR primers to reliably amplify exon 7. Only then can it be determined whether the cDNA deletions of exon 7 defined in F764 and F765 are due to splice junction mutations, or due to deletions of the exon at the gene level.

The dinucleotide AG at the intron-exon boundary of a 3' splice site or splice acceptor is highly conserved (Mount 1982). The A of the dinucleotide is not invariant and a pyrimidine in this position has been occasionally reported in the non-consensus splice acceptors of some alternatively spliced exons (Jackson, 1991). The G of the AG dinucleotide is however, absolutely conserved and is necessary for splicing to occur. The cDNA deletion of exon 7 in F526 is the result of a 39815-G to T transversion in the invariant G of the terminal AG of the intron 6 splice acceptor. The mutation destroys the intron 6 splice acceptor and results in the skipping of exon 7 during HPRT pre-mRNA splicing.

Four cDNA deletions of exon 7 have been reported in the literature (see Table 3.2) and together with the three apparently unrelated patients reported in this study, represent the largest single group of deletion mutants in the Lesch-Nyhan syndrome. Until the mutations responsible for the deletion of exon 7 in the patients in this study and those

reported in the literature have been defined at the genomic level, it is not possible to determine whether the cDNA deletion of exon 7 represents a mutational hot spot.

3.4.3.2 The Creation of a New Exon.

The 36221-T to A single base transversion in intron 6 defined in F749 effectively creates a new exon. The detection of this mutation is an illustration of the power of screening for mutations at the cDNA level as opposed to genomic exon by exon screening. The amplification of a larger than predicted PCR product from HPRT cDNA is an indication from the outset that an insertion has occurred. DNA sequencing of the amplified cDNA provides the information necessary to determine the origin of the inserted fragment. PCR primers for exon by exon screening of genomic DNA are usually located within 200 bp of the intron-exon boundaries and are unlikely to be positioned so as to amplify a segment of DNA located thousands of bases from any exon boundary. In essence, if an exon by exon screening strategy had been used to screen HPRT genomic DNA from this patient, no mutation would have been detected.

Although the insert is in-frame, stop codons within the intron derived sequence result in premature termination after coding for 6 incorrect amino acids. A shortened protein of 167 amino acids is predicted (Figure 3.11). The T to A transversion occurs within a pyrimidine rich region bounded by TGG at the 3' end (Figure 3.12).

A number of *cis* acting sequence elements and *trans* acting factors are required for the splicing of an intron (see reviews by Aebi and Weissman, 1987; Smith et al, 1989; Horowitz and Krainer, 1994; Norton 1994). The 5' splice site consensus sequence is exon-(C or A)AG/GTRAGT-intron with the vertical line indicating the exon-intron boundary. The GT dinucleotide at the exon-intron boundary is strictly conserved. The 3' splice site is composed of 3 elements: the conserved splice sequence intron-YAG/G-exon, a stretch of pyrimidines typically found immediately adjacent and upstream of the 3' splice

site and a loosely defined branch point with the consensus sequence YNYTRAY, typically found 20-40 nucleotides upstream from the 3' splice site. The only highly conserved bases are the AG at the intron-exon boundary of the 3' splice site.

In addition, downstream purine-rich exonic enhancer elements may act as cis acting modulators of intron splicing efficiency (Dirksen et al, 1995; Chiara and Reed, 1995; Takeshima et al, 1995). G rich sequences present in the 5' part of introns may also enhance the splicing reaction (Sirand-Pugnet et al, 1995).

```
     36010       36020       36030       36040       36050
ATAGATTTGG GACAGGTACT ATGAGAGTAT ATAAGTGATA CGTTATAGGA

     36060       36070       36080       36090       36100
CACTAACTAG TATCCTATGA AATGGCAAAA ACTGCAATCA CTTTTGCACC

     36110       36120       36130       36140       36150
AACCAAATAG AAACTAATCA GTGCACTTGC TTATTTTTCT ACATGCTCTT

     36160       36170       36180       36190       36200
TAGGGTTTTA AATGTCAACC TACTGTGGCA TAGACTTTAA TCCTCTGGGT

     36210       36220       36230       36240       36250
ATTCTTTTGT TGTTCTTTCC AGGTATATGC TGTGGAATTG AGATAGACTG

     36260       36270       36280       36290       36300
GTTCGTGAGC GAGAGATTTT GTGTTGCCAC AGGTAGGACA TGCTCAAACA

     36310       36320       36330       36340       36350
ATACTTGGGT CATTTCTTGA CCCAAGTCAT CTATTCACCA TAGTTTTGTA

     36360       36370       36380       36390       36400
GCACCGATCT TGCATACATT TCATGTATCT TCTTTGAACC CCACGTCAGT
```

Figure 3.12: The sequence context of the T to G transversion at nucleotide 36221 within intron 6 which creates a new exon in F749. The mutation is indicated by an arrow. The sequence inserted within HPRT cDNA is shown in the rectangle. Components of the 3' splice site and downstream 5' splice site are double underlined. A cryptic upstream 3' splice site and possible branch site, which are not used in splicing are shown single underlined. The sequence and numbering are according to Edwards et al (1990).

Within this context, the mutation creates an AG dinucleotide at bases -2 and -1 from the insert boundary, which is characteristic of the highly conserved 3' splice site or splice acceptor. The insert is bounded at the 3' end by a sequence with homology to the consensus sequence for a 5' splice site or splice donor. Only one abnormally large species of HPRT cDNA could be amplified from F749 in a highly sensitive nested primer amplification system and direct sequencing showed only one sequence. This evidence suggests that both the newly created splice acceptor and cryptic splice donor brought into use are "tight", in the sense that only a single mRNA species is spliced. In addition, the clinical features of the Lesch-Nyhan syndrome reported in the patient and the demonstration of severely impaired [^{14}C] hypoxanthine incorporation by the cell line F749, argue against the synthesis of any detectable amount of normal HPRT mRNA in F749.

A sequence 36130-CTTATTTTTCTACATGCTCTTTAG GGT-36156 with good homology to a splice acceptor already exists 48 bases 5' to the newly created splice acceptor. While this sequence has less homology to the consensus splice acceptor than the new splice acceptor, it is a better fit to the consensus sequence than the true intron 6 acceptor (sequence intron 6-TTTTGTAATTAACAG/CTT-exon 7). This raises the question: why is the existing cryptic splice acceptor sequence at nt 36130 to nt 36154 not used in splicing HPRT pre-mRNA, considering that the sequence 36280-CAG/GTAGGA-36288 is shown as able to act as a splice donor in the variant HPRT pre-mRNA of F749?

Splicing of an intron from a pre-mRNA is thought to occur in two steps involving successive transesterification reactions (see reviews by Smith et al, 1989; Horowitz and Krainer, 1994). The first step involves cleavage at the 5' exon and creation of a lariat intermediate by an attack of the 2'OH of the internal branch site adenosine on the 5' splice site. The second step is thought to involve an attack of the 3'OH of the 5' exon on the 3' splice acceptor, ligation of the exons and the release of the lariat intron from the mature mRNA.

The mechanisms by which splice site pairs are recognised and distinguished from cryptic splice sites are not clear. A number of *trans*-acting factors are involved in the recognition of a splice site and assemble into a highly ordered spliceosome. Initial recognition of the 5' splice site is primarily by base pairing and binding of U1 small nuclear ribonucleoprotein (snRNP). Identification of the 5' splice site takes place early in the splicing pathway and may occur in parallel with recognition of the 3' splice site (Horowitz and Krainer, 1994).

Recognition of the 3' splice site and branch site is promoted by the binding of several proteins, including U2AF which directs U2 snRNP towards the 3' splice site. The U2 snRNP base pairs with the branch site, although often these RNA sequences have limited complementarity. U2 binding is mediated by U1 snRNP but does not depend strictly on the presence of a 5' splice site. Interaction of U1 snRNP with a downstream splice site or exonic enhancer may target components to the 3' splice site (see references in Tarn and Steitz, 1995). The pre-spliceosome composed of U1 and U2 snRNPs and other proteins then binds to a complex of U4, U5, and U6 snRNPs to form the spliceosome. In mammalian systems, Ser/Arg rich (SR) proteins may be involved in recruiting U1 snRNP to the 5' splice site and are also involved in promoting the binding of U2 snRNP to the 3' splice site, even in the absence of U1 snRNP (Tarn and Steitz, 1995).

There is still uncertainty as to whether recognition of the 5' splice site of an intron occurs first and then directs recognition of the downstream 3' splice site of the intron. There is however, accumulating evidence that 3' splice site choice can occur first and direct across an exon, the choice of a downstream 5' splice site. In many pre-mRNAs, the closest downstream 5' splice site to a 3' splice site is used in preference to more distant candidate 5' splice sites (Horowitz and Krainer, 1994). This is in line with the exon definition model of splice site choice (proposed by Roberson et al (1990) and reviewed by Stephens and Schneider, 1992; Horowitz and Krainer, 1994; Norton, 1994) which proposes that the spliceosome binds the 3' splice site first and then searches 5' to 3' across the adjacent downstream exon for the next 5' or donor splice site. Once two exons have been located, the intervening intron is removed. However, the model cannot be generalised to all

pre-mRNAs (Horowitz and Krainer, 1994) and other factors are likely to play a role in defining both exons and introns.

Nevertheless, there is accumulating evidence that 3' splice site choice may direct 5' splice site choice across an exon. Interactions mediated by SR proteins between U1 snRNP and components assembled at the 3' splice site may direct 5' splice site selection (Tarn and Steitz, 1995), while Chiara and Reed (1995) provided further evidence from *trans* splicing experiments that selection of the 5' splice site can occur after assembly of the 3' splice site complex, if the 3' splicing substrate contains a downstream exonic enhancer or 5' splice site.

The cryptic 5' splice site 36280-CAG/GTAGGA-36288 used in splicing of the insertion in F749 HPRT pre-mRNA, has reasonable homology to the consensus 5' splice site sequence exon-(C or A)AG/GTRAGT-intron. An identical cryptic splice site is located 160 nucleotides downstream. The absence of any amplifiable mRNA transcripts utilising the second downstream cryptic 5' splice site suggests that the splice site sequence has sufficient strength to avoid alternative use of this downstream cryptic 5' splice site. The use of the closest downstream 5' splice site in preference to other splice sites located further downstream is consistent with the observations of other investigators (see references in Horowitz and Krainer, 1994).

The selection of the new pair of splice sites which define the insert in F749, may be the result of the creation of a 3' splice site which is "stronger" than a nearby upstream cryptic 3' splice site. The first component of this added "strength" is the greater homology to the consensus sequence of the newly created 3' splice site. Only 2 purines are present in the 19 nucleotide polypyrimidine tract compared to 4 purines in the 21 nucleotide polypyrimidine tract of the upstream cryptic 3' splice site. Although the intrinsic strength of a splice site sequence is not absolutely related to the degree of homology to the consensus sequence (Lear et al 1990; also see review by Smith et al, 1989), Dirksen et al

(1995) have shown that mutating splice sites towards the consensus sequence can lead to complete splicing of introns which are normally alternatively spliced.

A second element adding to the strength of the new 3' splice site is the potential branch site sequence 36185-CTTTAAT-36191 located within 30 bases of the 3' splice site which has 100% homology to the consensus sequence YNYTRAY. In contrast, the potential branch point sequence 36112-AACTAAT-36118 located 34 nucleotides upstream of the cryptic 3' splice site, differs from the consensus branch sequence by the presence of a purine at the 5' end. Sub-optimal branch site sequences have been shown to decrease the intrinsic strength of a 3' splice site (Champion-Arnaud et al, 1995) and have been implicated in mechanisms of alternative splicing (Dirksen et al, 1995; Andreadis et al, 1995).

It is interesting that the insertion contains a 10 nucleotide purine-rich sequence, 36257-GAGCGAGAAGA-36266. It is possible that this sequence could act as an exonic enhancer element. Although this element would be included in the "exon" were the cryptic 3' splice site to be used, the element could be a contributor to raising the strength of the newly recognised splice site pair above a splicing threshold.

The defining of the new exon in the variant HPRT pre-mRNA is consistent with a splicing mechanism which depends on the initial recognition of the 3' splice site, followed by scanning downstream across the exon and identification of the 5' splice site. The creation of a 3' splice site which leads to pre-mRNA splicing of a new exon thus provides further *in vivo* evidence in support of the exon definition model.

In summary, a single nucleotide substitution within intron 6 has led to the creation of a new 3' splice site. The good homology of the polypyrimidine tract and branch point sequence of the new 3' splice site in F749 to the consensus sequence, are likely to contribute to committing the variant HPRT pre-mRNA to the splicing pathway.

3.4.3.3 A Deletion of Exon 2, 3, 4 and 5.

Both HPRT cDNA transcripts sequenced in F751 share a deletion of exons 2, 3 and 4. Exon 5 is spliced out in the lower molecular weight transcript or Type A transcript, but is included in the higher molecular weight cDNA or Type B species. It would thus appear that a deletion of exons 2, 3, and 4 modulates the splicing of exon 5.

Alternative splicing of an exon is dependent on the interplay between the splicing elements defining the exon, the intrinsic strength of the exon inherent in the exon nucleotide sequence and the splicing context of the exon.

The relative strength of elements of the splice junctions is an important determinant of whether an exon will be alternatively spliced. The majority of alternatively spliced exons have suboptimal or unusually placed splicing elements (Norton, 1994). Donor splice sites tend to have poor complementarity to U1 snRNA, while 3' splice sites feature unusually long polypyrimidine tracts and multiple or unusual branch sites.

If it is assumed that the deletion of exons 2, 3 and 4 in HPRT cDNA is the result of a large deletion in the HPRT gene which encompasses these exons, then exons 1 and 5 will be joined by an intervening hybrid intron derived from intron 1 and intron 4. Splicing of the hybrid intron will be dependent on the recognition of the intron 1 splice donor and the intron 4 splice acceptor. In terms of the exon definition model, exon 5 is defined by the upstream hybrid intron splice acceptor and the downstream intron 5 splice donor sequences (Figure 3.13).

The intron 5 splice donor (downstream of exon 5) has the sequence 31633-AA/GTAAGT-31641, which differs from the consensus donor sequence at nt 31633-G and nt 31635-A in the exonic nucleotides of the splice site. The last nucleotide of the exon (31635-A) is probably the more important of the two nucleotides in influencing splice site strength. The G at this position in the consensus sequence is well conserved.

```
     31510       31520       31530       31540       31550
GCATCTAAAA ACAAGAGTTT GGATAATTCC TTAGGGTTGT TATGATGTGA

     51560       31570       31580       31590       31600
TTTGACTTAT AATTGGAAAT ACCGTTTTAT TCATTGTACT GATTTTCATT

     31610       31620       31630       31640       31650
TCTCTTTTTC TTCTAGAATG TCTTGATTGT GGAAGTAAGT TCACATTTAC

     31660       31670       31680       31690       31700
TTTTAATATA ACATTTATGA CTTTTCTAAC TTAGTATGCA CCATCCTAAA

     31710       31720       31730       31740       31750
GGTAAGCCAG GGAGAGAAAT TCCTCTGCAT CAGTTTTAAT GGTGGGCTTG
```

Figure 3.13: The sequence context of exon 5. Nucleotides of exon 5 are shown within the rectangle. Components of the 3' splice site and downstream 5' splice site are double underlined. A potential branch site located close to the polypyrimidine tract, but with poor homology to the consensus branch site sequence, is shown single underlined. The sequence and numbering are according to Edwards et al (1990).

An analysis of 1800 authentic splice donor sequences by Stephens and Schneider (1992) showed only 169 splice donor sequences with an A in this position.

The intron 4 splice acceptor which is used in splicing the hybrid intron in F751 has the sequence 7294-TTTTCATTTCTCTTTTTCTTCTAG/A-7318, which with the exception of the first nucleotide of the exon, compares favourable to the consensus splice acceptor intron-Y_nAG/G-exon. The 22 nucleotide polypyrimidine tract has only one purine within the sequence. The only difference between the authentic splice acceptor and the consensus sequence is at the first nucleotide of the downstream exon. This position is not particularly conserved and 25% of the 1800 authentic splice acceptors analysed by Stephens and Schneider (1992) had an A nucleotide in this position. The consensus branch site sequence is YNYTRAC. Two potential branch site sequences exist upstream of the 3' splice site. The sequence 7285-ATTGTAC-7290 has poor homology to the consensus branch site sequence and is located within 40 base pairs of the splice junction. The second sequence, 7251-ATTTGAC-7257, has 100% homology to the consensus

branch site sequence and is located within 60 base pairs of the splice site. The *cis* acting splicing elements identified which could potentially effect alternative splicing have, with the exception of the exonic components of the elements, good homology to the consensus sequences. This is to be expected as exon 5 is constitutively included in the normal mature HPRT mRNA.

It is possible that intrinsic features of the nucleotide sequence of exon 5 contribute to alternative splicing in F751. In this regard, it may be significant that at 18 bp, exon 5 is the smallest of the HPRT exons . Alternatively spliced short cassette exons are usually excluded in default pre-mRNA splicing, but are constitutively spliced if the exon is lengthened (Black, 1992). Exon 5 also lacks an identifiable purine rich element which may promote constitutive splicing (Dirksen et al, 1995; Chiara and Reed, 1995; Takeshima et al, 1995). The non-consensus nucleotides constituting the exon located components of the splice sites may also contribute to the decreased intrinsic strength of exon 5.

Andreadis et al (1995) showed that the context of an alternatively spliced exon can influence splicing. Splicing of a small cassette exon was dependent on the presence of a pre-spliced upstream exon. Splicing of exon 5 in normal HPRT pre-mRNA does not appear to be dependent on the presence of exon 4. Two previously reported deletions of exon 4 (see Table 3.2) did not apparently affect exon 5 splicing. There is however, a precedent in HPRT for mutations in one exon to affect the splicing of another exon. Two *in vitro* single base nucleotide substitutions within the coding sequence of exon 3 have been reported to result in the loss of both exons 2 and 3 in some mRNA transcripts (Steingrimsdottir et al, 1992). Mutations which alter the relative strength of an exon could alter the pattern of splicing and result in some exons being alternatively spliced. The juxtaposition of exon 1 and exon 5 in F751 may lead to a decrease in the relative strength of exon 5 which results in exon 5 being alternatively spliced. Kessler et al (1993) observed a highly preferred, non-linear order in the splicing of introns in APRT pre-mRNA. A similar, preferred order of intron removal may ensure that exon 5 is constitutively spliced in normal HPRT pre-mRNA splicing.

The two mRNA transcripts identified in F751 result in predicted proteins with a deletion of either amino acid residues 10 to 128 or residues 10 to 134 (Figure 3.11). The cDNA deletions of exons 2, 3 and 4 common to both transcripts are likely to be the result of a structural deletion of the HPRT gene with breakpoints located in intron 1 and intron 5. Edwards (1990) points out that 30% of the HPRT gene is composed of repetitive sequence elements and it is possible that the structural deletion responsible for the deletion of 3 exons in the two transcripts amplified from F751 is associated with two of these repetitive elements. It is interesting that more than half the HPRT structural deletions defined in somatic cells of new-born infants are due to a deletion of exons 2 and 3 and are likely to be the result of inappropriate V(D)J recombinase activity, since the breakpoints of the deletions show strong similarity to the consensus sequence for V(D)J recombinase (Cariello and Skopek, 1993b). The breakpoints of the structural deletion in F751 need still to be defined, but it will be interesting to see whether at least the 5'-end of the deletion in intron 1 is associated with a V(D)J recombinase type recognition sequence.

In summary, a deletion of exons 2, 3 and 4 leads to alternative splicing of exon 5. Despite good homology of the splice sites defining exon 5 to the consensus sequence, exon 5 may be an intrinsically weak exon. Constitutive splicing of exon 5 in normal HPRT pre-mRNA may be dependent on a preferred order of intron removal.

3.5 Conclusion.

All of the mutations in the nine Lesch-Nyhan patients investigated resulted in a truncated predicted amino acid sequence and consequent disruption of enzyme structure and function. The definition of the molecular defects in these patients enables appropriate genetic counselling based on carrier detection within affected families and adds to a compendium of mutations

4. MOLECULAR AND BIOCHEMICAL CHARACTERISATION OF FOUR PATIENTS WITH PARTIAL HPRT DEFICIENCY.

4.1 Introduction.

Partial HPRT deficiency results in the Kelley-Seegmiller syndrome (Kelley et al, 1969). Patients present with hyperuricemia due to purine overproduction, symptoms of gouty arthritis and occasionally, mild neurological symptoms. The degree of neurological impairment is inversely proportional to the residual HPRT activity measured in intact erythrocytes (Page et al, 1981; Fairbanks et al, 1987; Sege-Peterson et al, 1992). Patients with partial HPRT activity are spared the symptoms of compulsive self-mutilation characteristic of the Lesch-Nyhan syndrome. Partial HPRT deficiency is rare in the gouty population and Yu et al (1972) reported a frequency of approximately 1 patient with partial HPRT deficiency for every 150 patients with hyperuricemia.

In vivo mutations at the HPRT locus show marked genetic heterogeneity (Wilson et al, 1986a; Davidson et al 1989a; Davidson et al, 1991; Tarle et al, 1991; Sege-Peterson et al, 1992; Sculley et al, 1992; Cariello and Skopek, 1993). There is some clustering of mutations in exons 3 and exon 5 (Tarle et al, 1991; Cariello and Skopek, 1993) which may represent functionally important areas of the enzyme or alternatively, a sequence dependent predisposition to mutation.

The definition of the crystal structure of HPRT with bound GMP (Eads et al, 1994) has been a major step in understanding HPRT structure and function. However, the derived model is static and represents HPRT in a single conformation.

Nature's experiments in the form of naturally occurring mutations can provide insight into the role of individual amino acids in HPRT. Patients with partial HPRT deficiency are

particularly important in this regard, since the molecular defect can be correlated with a measurable change in enzyme function, providing insight into the function of individual amino acids within the enzyme.

Four patients presenting with the features of partial HPRT deficiency were investigated biochemically to confirm partial HPRT deficiency and at the molecular level to determine the nature of the defect in the HPRT gene.

4.2 Materials and Methods.

4.2.1 Patients.

Patients (P) are coded in the text by cell line reference numbers (Cell Bank, Department of Chemical Pathology, University of Cape Town, South Africa). Cell line numbers prefixed by "L" are Epstein Barr virus transformed lymphoblast cultures and cell line numbers prefixed by "F" are fibroblast cultures derived from forearm skin biopsies.

4.2.1.1 Cell line F45 (Patient TK).

$HPRT_{Cape\ Town}$ is an unusual biochemical variant of HPRT described from a patient with gout. Steyn and Harley (1984) showed that the HPRT enzyme in haemolysates from this male patient was subject to marked inhibition by the purine base substrates hypoxanthine and guanine. This purine base substrate inhibition was not associated with changes in the values of the K_m for hypoxanthine, guanine or PRPP, nor in the V_{max}. Galloon and Harley (1988) showed that the property of substrate inhibition in $HPRT_{Cape\ Town}$ was not restricted to the patient's erythrocytes and was also demonstrable in cell free assays of cultured lymphoblasts. Purine base inhibition of HPRT of intermediate character was also shown in cell free extracts of erythrocytes and cultured lymphoblasts of the proband's daughter.

These results suggested that a mutation in the coding region of HPRT itself is the basis for the unusual kinetics of $HPRT_{Cape\ Town}$, rather than a defect in post-translational modification of the enzyme.

4.2.1.2 Cell line L534 (Patient SM).

Patient SM presented at the age of 38 years at Groote Schuur Hospital, Cape Town, South Africa, with recurrent right loin pain since the age of 17 and progressively worsening gout since the age of 24. On examination, he had evidence of tophi, severe extensive polyarthritis and bilateral knee effusions. Both knees were heavily scarred, apparently due to self-inflicted injuries. On questioning, the patient revealed that although the injuries were self-inflicted, this was treatment recommended by a traditional healer to release "evil spirits" from his painful joints and was not the compulsive self-mutilation characteristic of the Lesch-Nyhan syndrome. Further investigations revealed that he had moderate renal impairment, with a urea of 18.3 mmol/l (control range 1.7-6.7 mmol/l), creatinine of 255 µmol/l (75-115 µmol/l), creatinine clearance of 32 ml/min (100-125 ml/min), an elevated urate of 0.71 mmol/l (0.12-0.50 mmol/l) and a normal urinary urate excretion of 3.3 mmol/day (1.5-4.4 mmol/day). He also had a urinary tract infection, evidence on ultrasound of bilateral hydronephrosis and dilated pelvicalyceal system, but no discrete stones. The knee effusion yielded negatively birefringent urate crystals.

4.2.1.3 Cell line L867 (Patients AW) and cell line L868 (Patient GT).

L867 and L868 were derived from patients in the United Kingdom with biochemical evidence of partial HPRT deficiency and were kindly supplied by John Duley and Anne Simmonds of the Purine Research Laboratory, Guy's Hospital, London. These cell lines were established by The European Collection of Animal Cell Cultures, PHLS Centre for Applied Microbiology and Research, Porton Down, UK and are stored in this repository

under the codes FS0001 for L867 and FS0002 for L868. Cell lines used as controls had no known defect in purine or pyrimidine metabolism.

4.2.2 Materials.

Dulbecco's Modified Eagle Medium was purchased from Gibco BRL, Gaithersburg, Maryland, USA or from Highveld Biological, Kelvin, South Africa. Foetal calf serum and Hanks Balanced Salt solution was purchased from Highveld Biological, Kelvin, South Africa. Sterile plastic pipettes, centrifuge tubes, flasks and petri dishes were of tissue culture grade.

[8-^{14}C] hypoxanthine, [8-^{3}H] adenine and L-[2,3,4,5,6-^{3}H] phenylalanine were purchased from Amersham International, UK. 5-phosphoribosyl-1-pyrophosphate (sodium salt) and hypoxanthine were purchased from Sigma Chemical Corporation, St. Louis, Missouri, USA. Hionic-Fluor was from Packard, Downers Grove, Illinois, USA; Biorad reagent from Bio-Rad Laboratories, München, Germany; dTTP from Boehringer Mannheim, Germany.

4.2.3 Methods.

4.2.3.1 Tissue Culture.

Fibroblast and transformed lymphoblast cultures were maintained in Dulbecco's Modified Eagles medium supplemented with 10% foetal calf serum, in an atmosphere of 10% CO_2 at 37°C. Cultures were grown in 250 ml tissue culture flasks without antibiotics and screened at intervals for *Mycoplasma* infection using bisbenzamide fluorochrome stain (Hoechst No. 33258), (Chen, 1977). Cultures were fed twice weekly.

4.2.3.2 Assay of HPRT Activity in Erythrocyte Lysates.

Overview of Method.

HPRT activity was assayed using a kinetic method described by Wohlhueter (1975) and modified according to Steyn and Harley (1984). HPRT activity was measured as the rate of [^{14}C] IMP formation from [^{14}C] hypoxanthine. The product, [^{14}C] IMP, was trapped on Whatmans DE81 paper which had been treated with EDTA to chelate free magnesium and stop the reaction. Unreacted substrate was removed by suspending the strips of anion exchange paper in running water and the amount of bound product determined by liquid scintillation counting.

Preparation of Erythrocyte Lysates.

The buffy coat was removed from 10 ml heparinised blood after centrifugation at 3000g for 10 min. The erythrocytes were then washed twice with saline and lysed by the addition of 4 volumes of cold distilled water. The stroma was removed by centrifugation and the haemolysate dialysed overnight against two 5 l changes of 50 mM Tris-HCL pH 7.8 containing 1 mM dithiothreitol. The dialysed haemolysates were stored at -20°C. Haemolysates stored at -20°C showed a 10% loss of activity after 4 weeks storage (Steyn, 1983).

Preparation of DE81 Paper.

Whatmans DE81 anion exchange paper was ruled into 2.5x2.5 cm squares, cut into a 2x4 array and soaked in 20 mM EDTA (pH 8.0). The paper was dried before use.

Determination of Lysate Protein Concentration.

Protein concentrations were determined from a standard curve by the method of Bradford (1976) using Biorad protein reagent.

HPRT Enzyme Assay

The enzyme assays were performed at 37°C in duplicate. Each 100 µl reaction volume contained approximately 100 µg of lysate protein, 50 mM Tris-HCL (pH 7.8), 14 mM $MgCl_2$ and [^{14}C] hypoxanthine and PRPP at appropriate concentrations. Assay tubes were preincubated for 2 min before the reaction was started by the addition of the lysate. At four 1 min timed intervals, 20 µl of the reaction mixture was spotted onto EDTA treated DE81 anion exchange paper. Unreacted substrate was removed by suspending the paper strips in a 5 l beaker and allowing tap water to flow through at a rate of approximately 1 l per minute for 1 hour. The DE81 paper was dipped into absolute ethanol to reduce fragility and cut into squares, each square representing a single time point. The squares were transferred to scintillation vials, 10 ml of scintillant added and the bound [^{14}C] IMP determined by scintillation counting using an open window. The rate of [^{14}C] IMP formation was estimated from the slope of a linear regression line fitted to the averaged duplicate data points using the method of least squares (Instat V2.05a, Graphpad Software, San Diego, USA). The reaction was regarded as linear when a correlation coefficient of greater than 0.99 was obtained. Counts per minute were converted to dpm taking into account the efficiency of the scintillation counter and quenching due to the DE81 paper. Units of enzyme activity were defined as 1 U = µmol IMP produced/min/mg protein. Kinetic parameters were estimated by fitting the data directly to the Michaelis-Menten rate equation (1) using a non-linear iterative method of least squares. Preliminary estimates of the apparent K_m and V_{max} were obtained from Lineweaver-Burk plots.

$$v = V_{max} \frac{[S]}{K_m + [S]} \qquad (1)$$

4.2.3.3 Assay of HPRT Activity in Cultured Lymphoblasts.

Lymphoblasts were grown to a density of approximately 10^6 cells/ml. Approximately 50 ml of the cell suspension was pelleted at 1000g for 10 min and washed twice in normal saline. The cell pellet was resuspended in 100 µl Tris-HCL pH 7.8 and transferred to a

microfuge tube. The cells were lysed by 6 freeze-thaw cycles. Cell membranes were removed by centrifugation at 10000g for 30 min. The membrane free supernatant was passed through a modified Penefsky column (Grubmeyer and Penefsky, 1981) packed with Sephadex G50 resin. Enzyme activity in the lysates was assayed immediately.

The HPRT assay described above was modified by the inclusion of 1.5 mM dTTP in the reaction to inhibit 5'-nucleotidase activity present in nucleated cells (Fujimoto and Seegmiller (1970); Adams and Harkness, 1976), the activity of which would otherwise result in an underestimation of IMP product formation. Shin-Buehring et al (1980) reported 5'-nucleotidase activity of 37 - 160 nmol phosphate produced per min per mg protein in various tissues as measured by the release of phosphate from IMP during conversion to inosine. HPRT assay time points of 15 min, 30 min, 45 min and 60 min were used for cell lysates with less than 10% activity. Assay time points for controls were at 1 min, 2 min, 3 min and 4 min. The data was analysed as described above.

4.2.3.4 Heat Stability of HPRT Activity in Lymphoblast Lysates.

200 µl aliquots of a prepared lymphoblast lysate from each cell line were incubated for 5, 10, 15, or 20 min at 75°C and immediately placed on ice until assayed. HPRT activity was assayed as described above, with hypoxanthine concentration constant at 100 µM and the PRPP concentration at 1.6 mM.

4.2.3.5 Double Label Experiments: Uptake of [^{14}C] Hypoxanthine and [^{3}H] Phenylalanine by Cultured Fibroblasts.

Confluent flasks of fibroblasts were trypsinised (0.1% trypsin in 0.5 mmol/l EDTA in phosphate buffered saline) and plated in duplicate into 60 mm diameter tissue culture dishes and allowed to recover overnight. The medium was then replaced with 1 ml of

Hanks Balanced Salt solution supplemented with 15 mmol/l Hepes (pH 7.4) 0.5 μCi/ml [^{14}C] hypoxanthine and 1.5 μCi/ml [^{3}H] phenylalanine. Cells were incubated for 1.25 hr at 37°C without CO_2. Each dish was then washed 3 times with 2 ml ice cold 5% trichloroacetc acid (TCA), the precipitated material redissolved in 1.3 ml 0.1 N NaOH, and neutralised with glacial acetic acid. 1 ml was counted in 10 ml scintillant in a Beckman LS6001C scintillation counter using windows of 0 to 200 keV for [^{3}H] and 400 to 1000 keV for the [^{14}C] label.

4.2.3.6 Molecular Methods.

Molecular methods are described in detail in Section 2.

Briefly, total RNA was extracted from tissue cultured cells, reverse transcribed with AMV reverse transcriptase using an oligo dT_{15} primer and amplified using HPRT cDNA specific PCR primers. cDNA prepared from F45 and L534 was amplified using primer pair P1b and P2, while HPRT cDNA from L867 and L868 were amplified using a nested primer system (initial amplification was with primers OPF and OPR, followed by nested amplification with primer pair NPF and NPR). PCR products amplified from F45 and L534 were purified using Millipore Ultrafree-MC 100 000 NMWL filter units and directly sequenced. In order to read sequences close to the 3'-end of the PCR primers, the PCR products were also cloned into pUC 18 using the Klenow-Kinase-Ligase method and the areas close to the PCR primers sequenced using vector primers. Amplified cDNA from L867 and L868 was cloned into pGEM-T and then sequenced.

4.3 Results.

4.3.1 HPRT Activity in Erythrocyte Haemolysates of Patient P534.

Erythrocytes were available from only one patient, P534. Substrate-velocity curves and the derived Lineweaver-Burk plots of HPRT activity in erythrocyte haemolysates of P534 and a control are shown in Figure 4.1. With PRPP concentration saturating at 1.6 mM and hypoxanthine concentration varied from 5 μM to 90 μM, the Lineweaver-Burk plots derived from substrate velocity curves of P534 and the control intersect at the same point on the X-axis, but at differing points on the Y-axis. These results are consistent with an altered apparent V_{max}, but unchanged apparent K_m for hypoxanthine. Similar results were obtained when the concentration of PRPP was varied in the range 0.05 to 1.6 mM with hypoxanthine at a constant concentration of 200 μM. The Lineweaver-Burk plots of patient and control intersect at the same point on the X-axis, but at different points on the Y-axis and are consistent with an altered apparent V_{max}, but unchanged apparent K_m for PRPP.

The apparent Michaelis constants for P534 and the control are shown in Table 4.1. Each value is the mean of duplicate determinations performed on blood specimen drawn on two separate occasions. The apparent K_m for hypoxanthine of both the patient (mean 5.1 μM) and the control (mean 5.2 μM) are within the control range reported by Wilson (1986a) and are within the control range of 1.3 μM to 20 μM reported in the literature (Shin-Buering et al, 1980; Steyn and Harley, 1984; Snyder et al, 1989). The apparent K_m for PRPP for the patient P534 (0.02 mM) and the control (0.02 mM) are identical and are also within the control range of 0.006 mM to 0.25 mM reported in the literature (Shin-Buering et al, 1980; Steyn and Harley, 1984; Snyder et al, 1989). However, the apparent V_{max} of P534 was decreased to 20 to 30% of the control value.

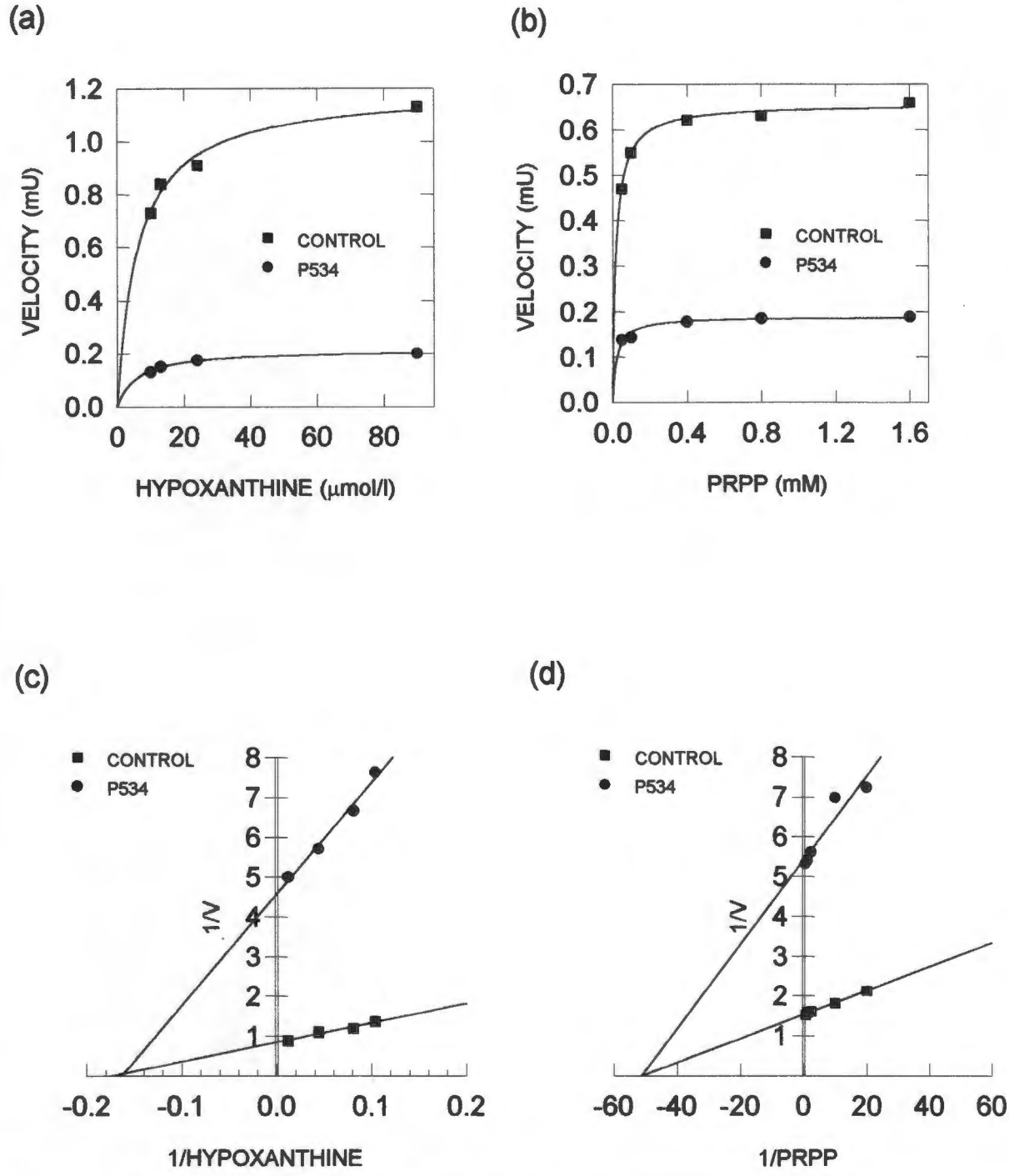

Figure 4.1: Substrate-velocity curves and the derived Lineweaver-Burk plots of HPRT activity in haemolysates of P534 and a control. (a) Substrate-velocity curve with hypoxanthine as the varied substrate. Hypoxanthine concentrations were 10, 15, 25 and 90 μM with PRPP saturating at 1.6 mM . The derived Lineweaver-Burk plot is shown in (c). (b) Substrate-velocity curve with PRPP as the varied substrate. PRPP concentrations were 0.05, 0.1, 0.4, 0.8, and 1.6 mM with hypoxanthine constant at 100 μM. The derived Lineweaver-Burk plot is shown in (d). Values are the mean of duplicate determinations.

Table 4.1: Apparent kinetic parameters for HPRT in erythrocyte lysates of patient p534.

KINETIC PARAMETER			CONTROL	PATIENT
K_m	hypoxanthine	(μmol/l)	4.7; 5.5	5.4; 5.0
	PRPP	(mmol/l)	0.02; 0.02	0.02; 0.02
V_{max}	hypoxanthine	(mU)	0.97; 1.10	0.19; 0.21
	PRPP	(mU)	0.55; 0.79	0.16; 0.19

Patient P534 had received a blood transfusion a day prior to blood being drawn for HPRT determination. The possible effects of this blood transfusion on the measurement of HPRT activity in haemolysates prepared post-transfusion were assessed by measuring HPRT activity in erythrocyte haemolysates prepared from stored blood transfusion units. HPRT activity in haemolysates, prepared from units of blood (from different donors) stored at 4°C for 0 days to beyond the expiry date of a unit, were assayed and the results are shown in Figure 4.2. There was no appreciable decrease in HPRT activity in blood transfusion units stored for up to 36 days. On the contrary, HPRT activity in blood stored with citrate, phosphate, glucose and adenine as an anticoagulant appeared to increase with time.

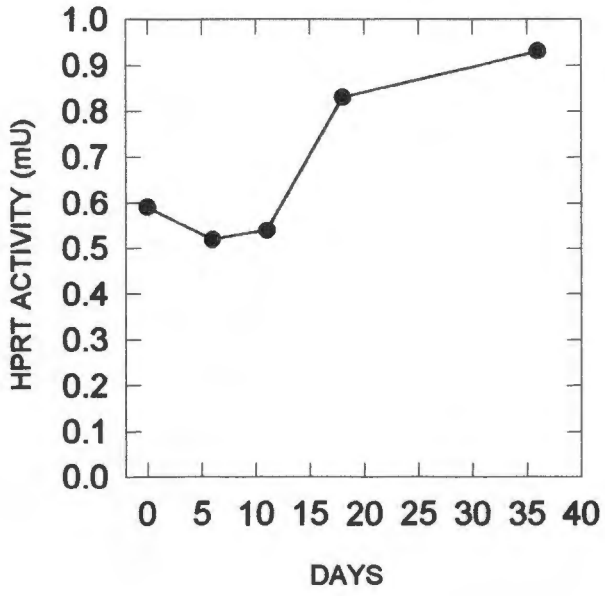

Figure 4.2: HPRT activity in blood transfusion units stored for up to 36 days. Hypoxanthine concentration was constant at 100 μM with PRPP saturating at 1.6 mM. Values are the mean of duplicate determinations.

4.3.2 The Incorporation of [^{14}C] Hypoxanthine Relative to [^{3}H] Phenylalanine by Fibroblasts Cultured from P534.

The incorporation of [^{14}C] hypoxanthine relative to [^{3}H] phenylalanine by fibroblasts cultured from P534 was compared to a Lesch-Nyhan cell line (F526) and two control cell lines and is shown in Table 4.2. The values shown are the means of duplicate determinations. The ratio of [^{14}C] hypoxanthine to [^{3}H] phenylalanine in the cell line F534 was approximately 30% of control values, which supported the finding of partial HPRT deficiency in the erythrocytes of this patient.

Table 4.2: Ratio of [^{14}C] hypoxanthine to [^{3}H] phenylalanine incorporation by cultured fibroblasts.

Fibroblast cell line	Ratio
Control 1	0.07
Control 2	0.07
F526 (Lesch-Nyhan)	<0.0001
F534	0.026

Values are the mean of duplicate determinations.

4.3.3 HPRT Activity in Cultured Lymphoblast Lysates.

Transformed lymphoblast cultures were available from patients P534, P867 and P868. The substrate-velocity curves and derived Lineweaver-Burk plots of HPRT activity in lymphoblast lysates with hypoxanthine as the varied substrate are shown in Figure 4.3. The substrate-velocity curve and Lineweaver-Burk plots derived when the concentration of PRPP was varied are shown in Figure 4.4. The apparent kinetic parameters calculated by fitting the data to the Michaelis-Menten equation are shown in Table 4.3.

Table 4.3: Apparent kinetic parameters for HPRT in cultured lymphoblast lysates.

	HYPOXANTHINE		PRPP	
Patient	K_m (μmol/l)	V_{max} (mU)	K_m (μmol/l)	V_{max} (mU)
control	16.6+/-7.0*	3.34+/-0.76*	59.7+/-9.0*	3.54+/-0.91*
L534	12.9+/-7.6**	3.83+/-0.95**	52.9: 38.8	4.25: 2.21
L867	27.9: 33.9	0.07: 0.09	49.1: 52.4	0.07: 0.06
L868	20.3: 10.3	0.07: 0.06	42.7: 50.7	0.03: 0.09

* Mean +/- 1SD from 3 control cell lines, each assayed in duplicate in 2 independent experiments.

** Mean +/- 1SD from duplicate values of 3 experiments

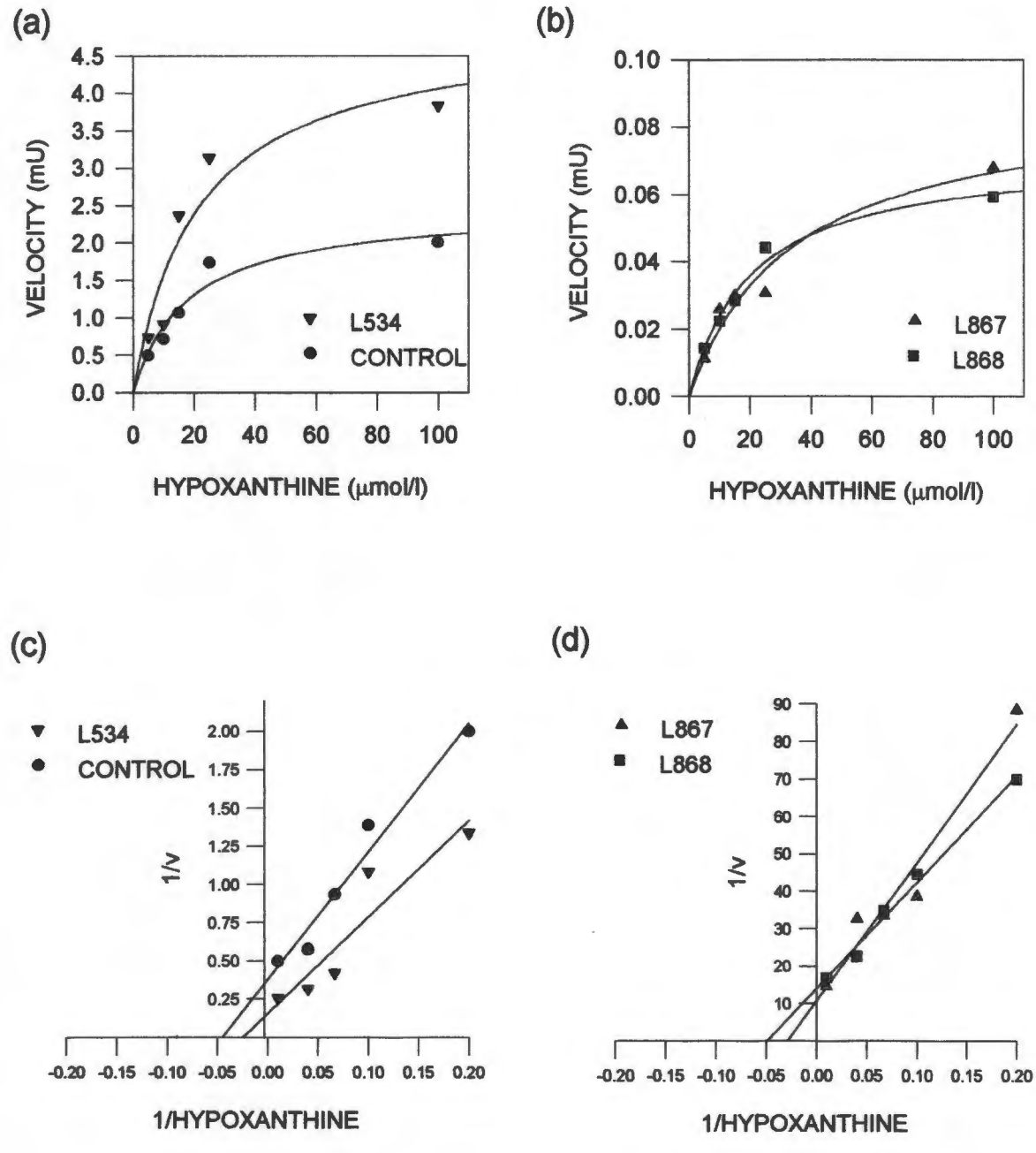

Figure 4.3: Substrate-velocity curves, with hypoxanthine as the varied substrate, of HPRT activity in lymphoblast lysates of L534, a control, L867 and L868.
Hypoxanthine concentrations were 5, 10, 15, 25 and 100 µM with PRPP saturating at 1.6 mM. (a) and (c) Substrate-velocity curve and derived Lineweaver-Burk plot of L534 and a control. (b) and (d) Substrate-velocity curve and derived Lineweaver-Burk plot of L867 and L868. Values are the mean of duplicate determinations.

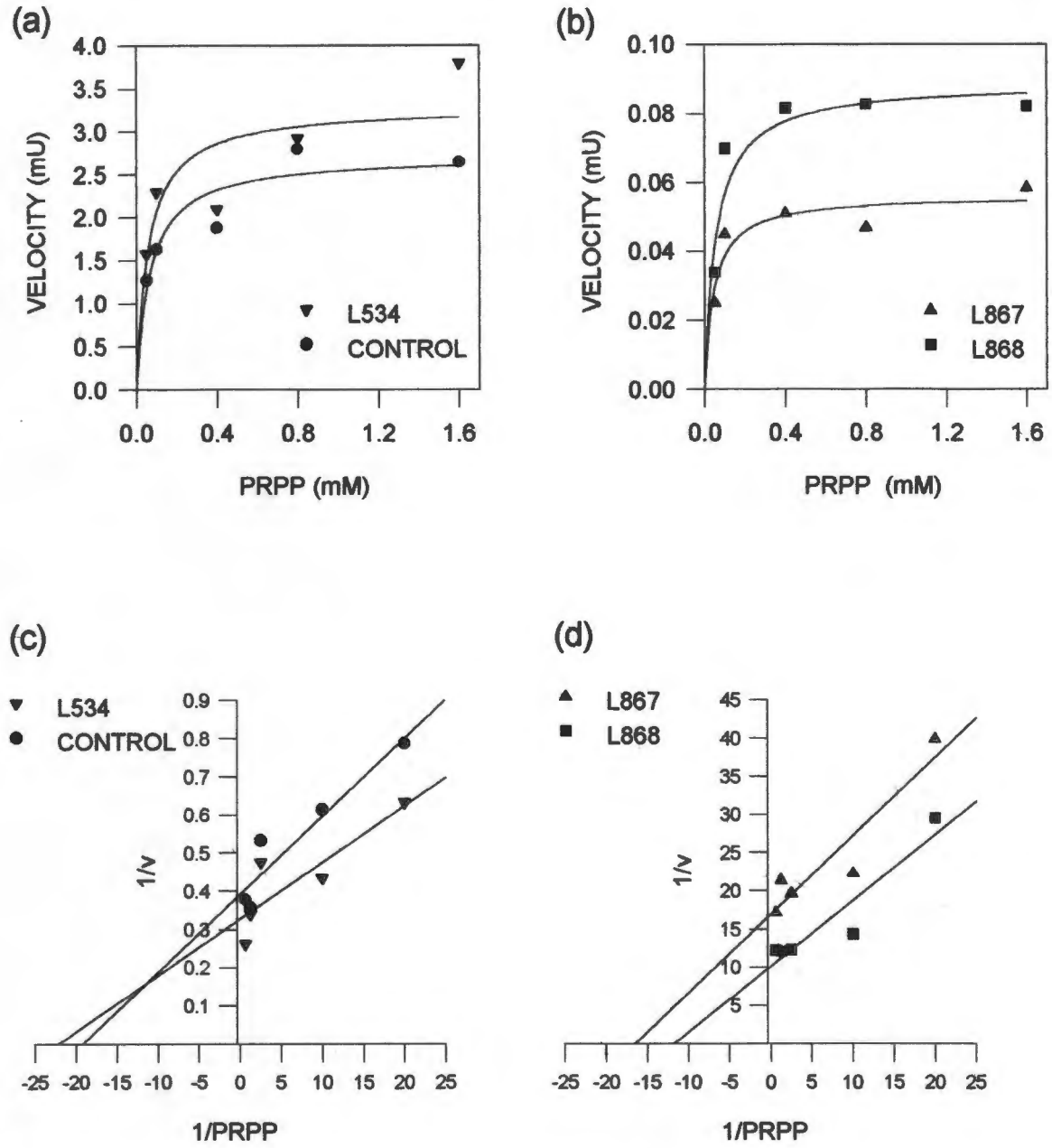

Figure 4.4: Substrate-velocity curves, with PRPP as the varied substrate, of HPRT activity in lymphoblast lysates of L534, a control, L867 and L868. PRPP concentrations were 0.05, 0.1, 0.4, 0.8 and 1.6 mM with hypoxanthine concentration constant at 100 μM. (a) and (c) Substrate-velocity curve and derived Lineweaver-Burk plot of L534 and a control. (b) and (d) Substrate-velocity curve and derived Lineweaver-Burk plot of L867 and L868. Values are the mean of duplicate determinations.

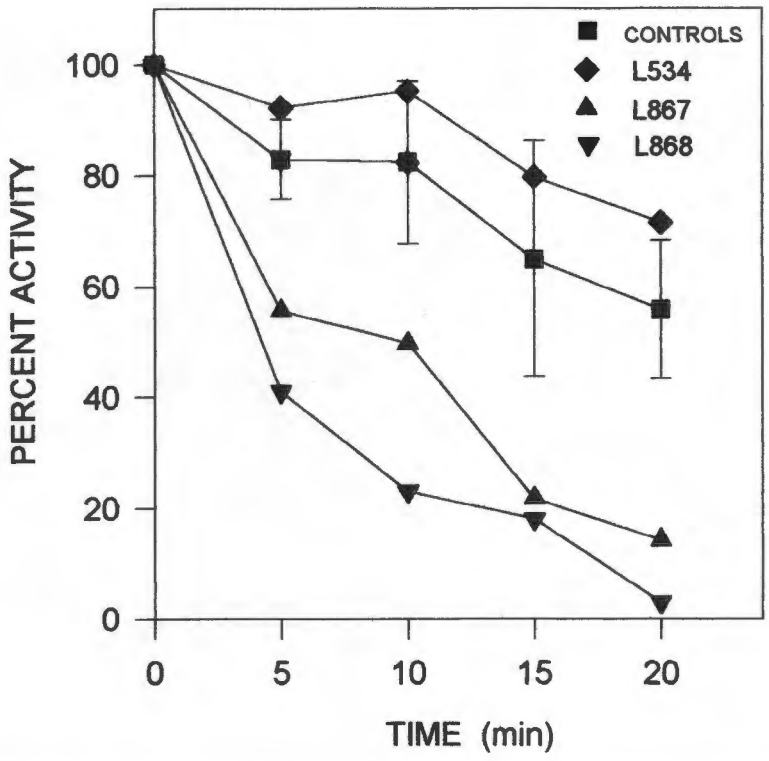

Figure 4.5: Heat stability of HPRT in lymphoblast lysates of L534, L867, L868 and controls. HPRT activity was assayed with hypoxanthine and PRPP concentrations at 100 μM and 1.6 mM respectively. HPRT activity at each time point was determined in duplicate. Data points for the controls represent the mean (+/-1SD) of duplicate determinations of HPRT activity in three control lymphoblast cell lines.

HPRT activity in lymphoblast lysates of the cell lines L867 and L868 were less than 2% of the mean of the control range, while the apparent K_m for hypoxanthine and PRPP were normal. The V_{max} and apparent substrate affinities for L534 were normal, a result which contradicted the finding of a decreased V_{max} in erythrocyte lysates and the decreased incorporation of [^{14}C] hypoxanthine by fibroblasts. Apparent K_m values for HPRT determined in lymphoblast lysates showed greater variability than in erythrocytes, which is consistent with the experience of other investigators (Adams and Harkness, 1976).

HPRT activity in lymphoblast lysates of L867 and L868 showed marked heat lability (Figure 4.5). Enzyme activity in both cell lines had a half-life of 10 min at 75°C compared to a mean half-life of 23 min for the controls. HPRT activity in L534 showed a similar heat stability profile to that of controls, with a half-life of 37 min.

4.3.4 Results of the Molecular Investigations.

Amplification of HPRT cDNA prepared from F45 and L534 using primers P1b and P2, yielded a single PCR product of approximately the predicted size of 725 bp (Figure 4.6c, L534 not shown). Amplification of HPRT cDNA from L867 and L868 using the nested primer system yielded PCR products of approximately the predicted size with both outer primers (798 bp) and nested primers (741 bp) (Figure 4.6a and 4.6b respectively).

The entire coding region of HPRT cDNA amplified from each of the three patient cell lines was sequenced. An A to G transition at nt 307 due to a Taq polymerase error was found in a single clone of L867 HPRT cDNA. This nucleotide transition was distinguished from a true mutation by the presence of a normal base at the same position in two other clones.

DNA sequencing of cloned PCR products amplified from HPRT cDNA of L867 showed a G to T transversion at nt 481 in two independent clones (Figure 4.7a). The mutation resulted in an Ala_{161} to Ser amino acid substitution (the methionine coded by the ATG start codon is numbered as residue 1). Interestingly, a C to G transversion at the adjacent nucleotide nt 482, was found in L868. This mutation alters the same amino acid Ala_{161} but to Gly instead of Ser.

Direct sequencing of cDNA amplified from F45 showed a G to A transition at nt 403, which resulted in the amino acid substitution of Asn for Asp_{135} (Figure 4.7b).

The entire coding region of HPRT cDNA amplified from L534 was sequenced directly. PCR products were also cloned and sequenced. No mutations within the coding region of the HPRT cDNA in this patient were found.

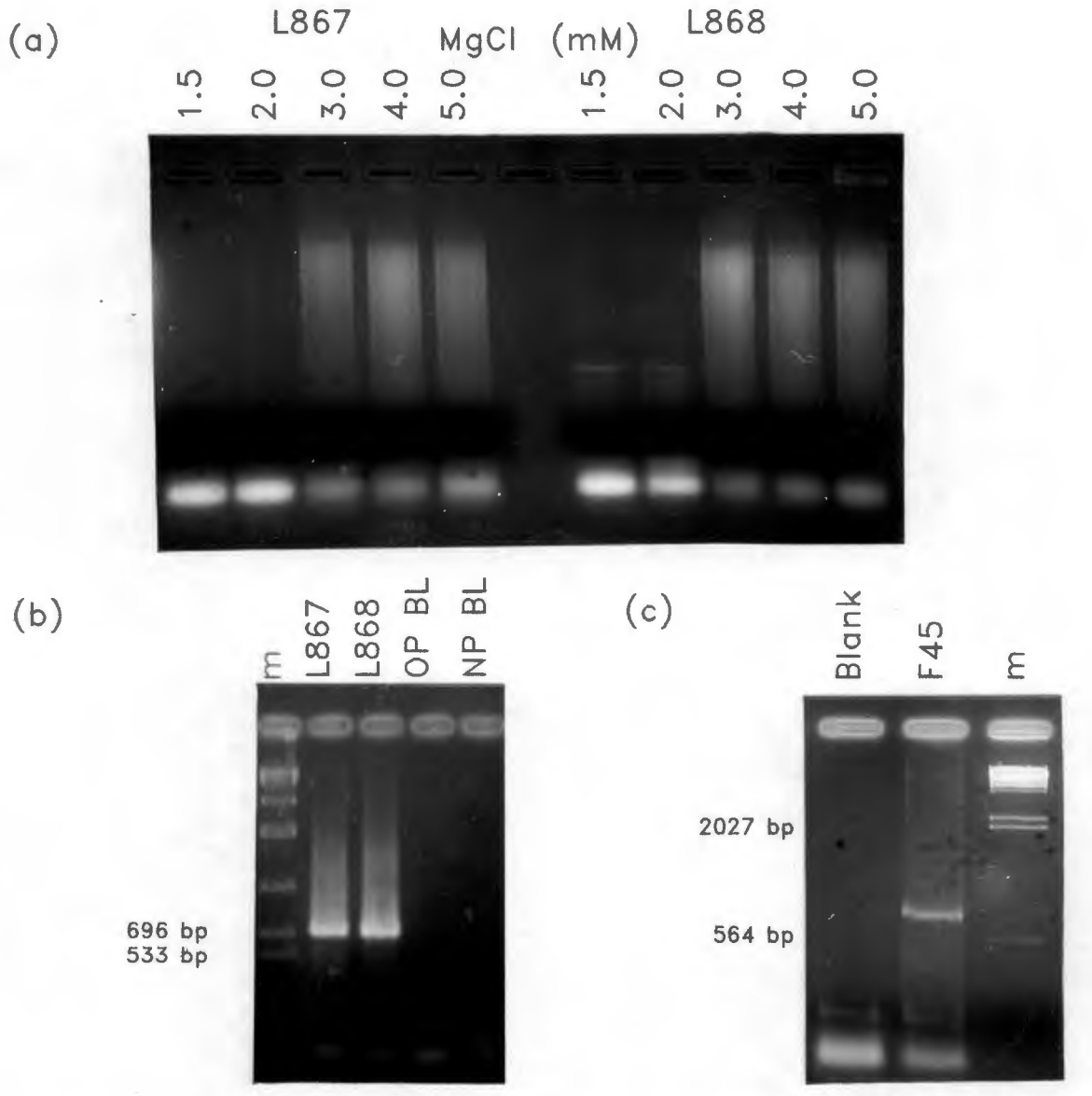

Figure 4.6: HPRT cDNA amplified from L867, L868 and F45. (a) and (b) Nested primer amplification of HPRT cDNA from L867 and L868. **(a) Amplification with outer primers OP1 and OP2 at different $MgCl_2$ concentrations.** Amplification was optimal at 1.5 and 2 mM $MgCl_2$. **(b) Nested primer amplification of L867 and L868 HPRT cDNA with nested primers NP1 and NP2 at a $MgCl_2$ concentration of 1.5 mM.** 1 µl of the outer primer PCR reaction was amplified with primers NP1 and NP2.in a PCR reaction containing 1.5 mM $MgCl_2$. Lane OP BL, a PCR reaction blank carried through both outer and nested PCR. Lane NP BL, nested PCR reaction blank. Lane m, lambda DNA digested with *Dra*I, the 696 bp and 533 bp pair bands are indicated. **(c) HPRT cDNA amplified from F45 with primers P1b and 2**, lane labelled F45. A PCR blank is shown in the lane Blank . Lambda DNA digested with *Hind*III was used as a molecular weight marker in lane m. The 564 bp and 2027 bp bands of the marker are indicated.

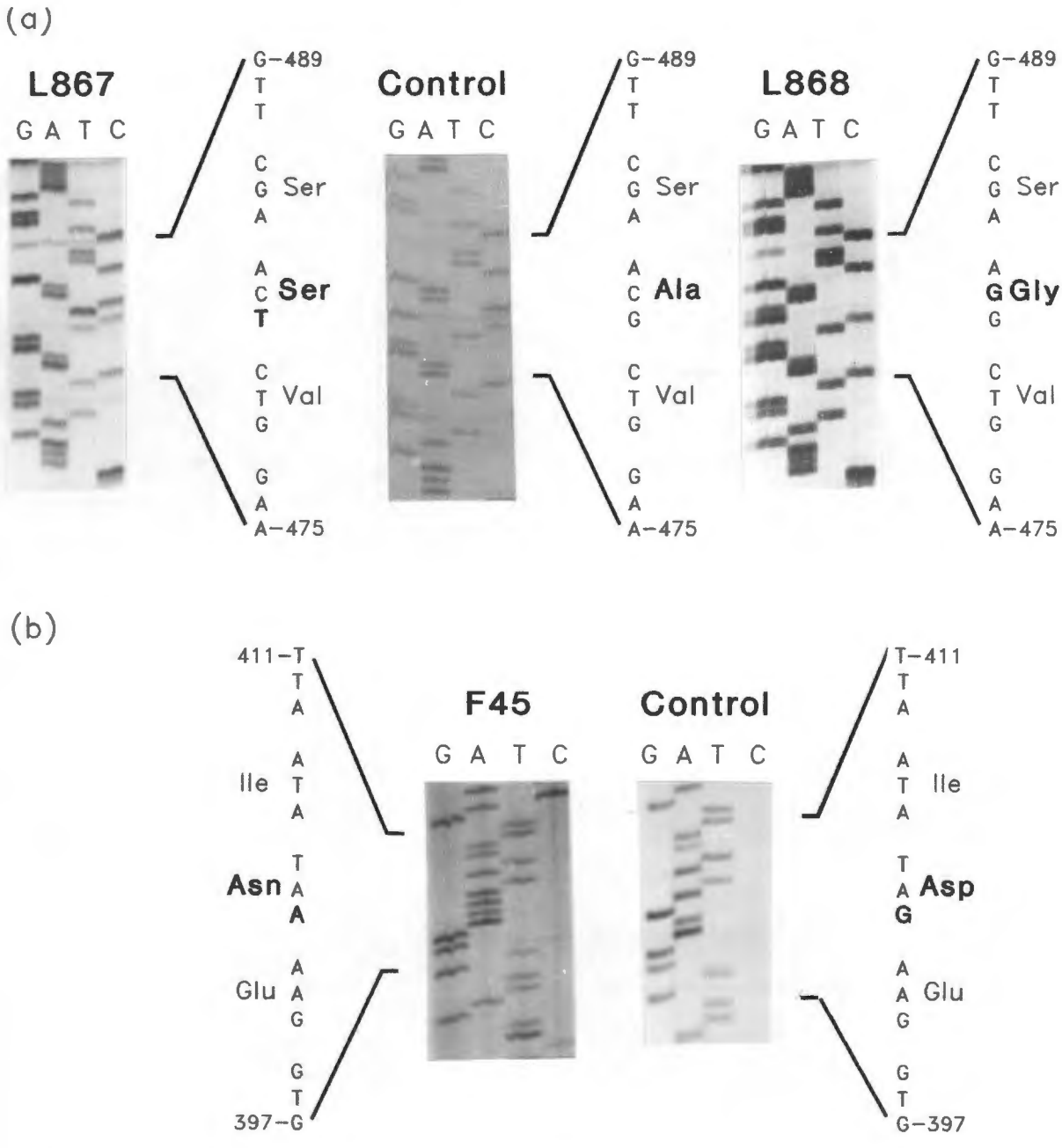

Figure 4.7: The molecular defect in L867, L868 and F45. (a) In L867, a G to T transversion at nt 481 alters the codon for Ala_{161} to Ser. In L868, a C to G transversion at nt 482 alters the codon for Ala_{161} to Gly. (b) The molecular defect in F45 is a G to A transition at nt 403 which results in the substitution of Asp_{135} by Asn.

4.4 Discussion.

The recent determination of the crystal structure of HPRT with GMP bound (Eads et al, 1994) is a major advance in the understanding of HPRT structure. The model however, characterises the enzyme in a single conformation, with GMP bound. *In vivo* mutations causing partial HPRT deficiency thus present an opportunity to gain insight into the role of individual amino acids within the functioning protein.

A survey of *in vivo* amino acid substitutions reported in HPRT is shown in Table 4.4 and a graphical representation of this data is shown in Figure 4.8. The linear representation of the HPRT protein shows a distinct clustering in the occurrence of amino acid substitutions. The clusters of amino acid substitutions may point to either functionally important region of the enzyme, or provide evidence for mutational hot spots at the DNA level. Clustering of mutations at the DNA level in exon 3 and exon 5 have been noted by Tarle et al (1991) and Cariello and Skopek (1993) respectively.

A clustering of amino acid substitutions occurs between amino acid residues 40 and 60. These residues are within α helix A2 of the crystal structure defined by Eads et al, 1994 (see Figure 4.9). This large helix is located away from the catalytic site of the enzyme and appears to have a structural function. It is possible that this clustering of amino acid substitutions which are encoded by exon 3, represent a DNA sequence predisposition to mutation. However, 8 of the 12 amino acid substitutions reported have occurred only once at residues within this region. This heterogeneity would suggest functional sensitivity of the protein to amino acid substitutions in α helix A2 rather than a nucleotide sequence susceptibility to mutation.

In contrast, the amino acid substitutions clustered at residue 70 to 73, also encoded by exon 3, are more likely to have resulted from a DNA sequence predisposition to mutation. G to A transitions at nucleotide G_{208} or the adjacent G_{209} both alter the codon for Gly_{70} and these two mutations have occurred independently in five patients.

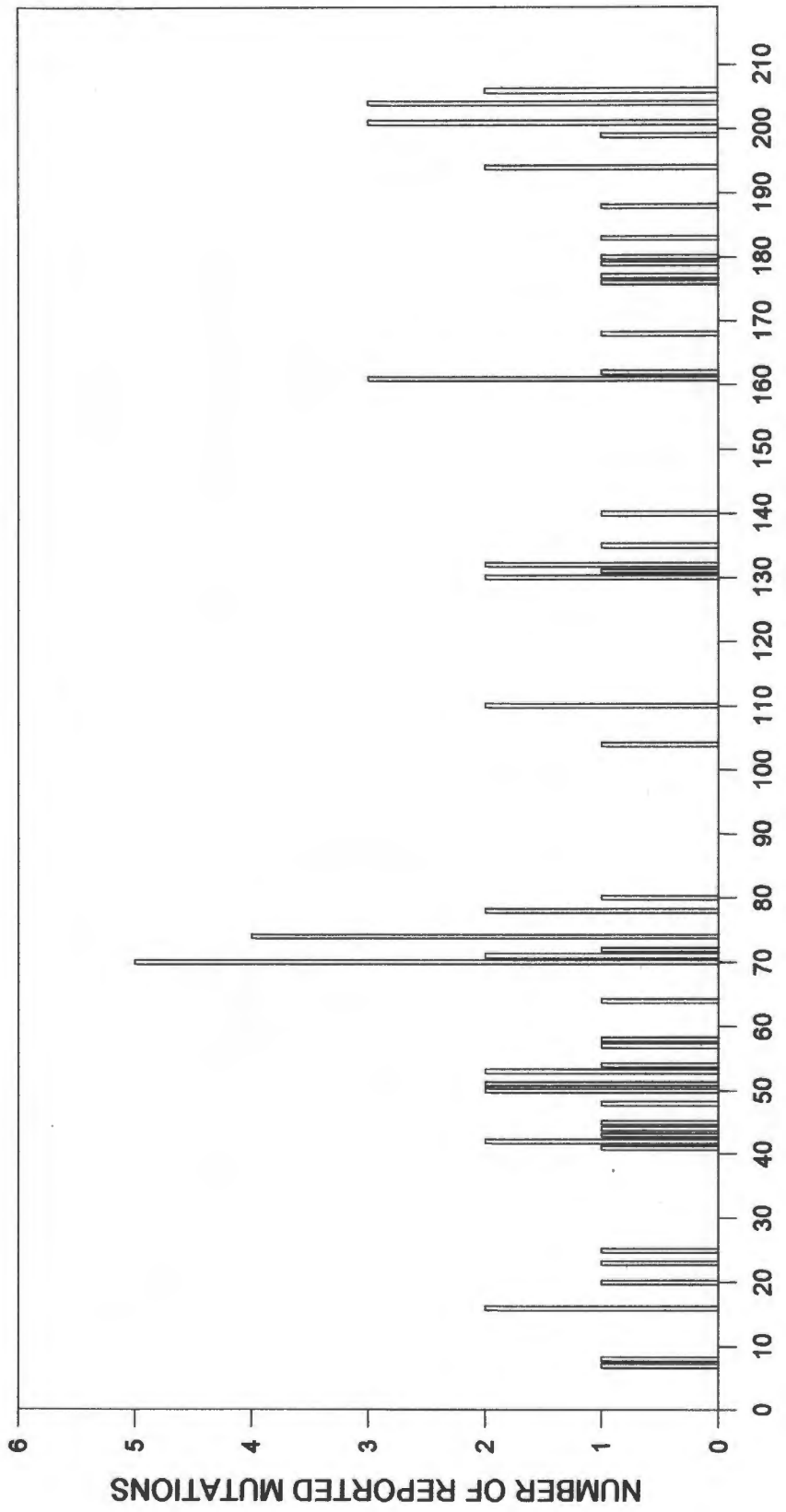

Figure 4.8: **The distribution of *in vivo* amino acid substitutions in HPRT.** Each bar on the chart represents the total number of amino acid substitutions at a single amino acid residue. All patients are apparently unrelated.

Mutations at G_{211} and G_{212} have resulted in differing amino acid substitutions in two patients at residue Gly_{71}. The occurrence of seven amino acid substitutions due to mutations within the run of G nucleotides between nt 207 and nt 212, may reflect a DNA mutational hot spot. Five of the seven mutations are G to A transitions and it is possible that guanine nucleotides within mono-nucleotide runs may have an increased propensity for this type of mutation. Amino acid residues 70 to 73 occur within a loop of residues connecting the ß strand B3 and α helix A3 and are in close proximity to the catalytic site of HPRT. Mutations at these residues may thus be the result of an increased DNA sequence susceptibility to mutation which affects functionally important residues of the protein. The substitution of Phe_{74} by Leu in four apparently independent patients are due to C_{222} to A transversions. These four identical mutations are the most common of the amino acid substitutions reported in HPRT. The high rate of identical mutations at nucleotide C_{222} suggests that a DNA sequence dependent cause for the observed increase in mutations cannot be excluded.

Exon 5 (nt 385 to nt 402) codes for the amino acid residues 129 to 135. These residues form part of the conserved PRPP binding motif (residues 129 to 140). Amino acid substitutions occur at four of the six residues encoded by exon 5, but these substitutions are probably a reflection of the functional importance of these residues in the catalytic site (discussed in more detail below), rather than a DNA sequence predisposition to increased rates of mutation. Similarly, substitutions in the 30 amino acids at the carboxyl terminal of the protein are evenly spaced and point to a heterogeneous mutational origin in a functionally important region of the enzyme.

Table 4.4: A review of *in vivo* mutations in HPRT which result in amino acid substitutions.

Variant	cDNA Change	Predicted Change in Protein	Comment	Reference
$HPRT_{Gravesend}$ (Family D)	G 20 to A	Gly 7 to Asp	partial, 0.9% activity	McKeran et al, 1975; Davidson et al, 1991
HB	T23 to G	Val 8 to Gly	partial, 6.9% activity	Sege-Peterson et al, 1992
$HPRT_{Uraqan}$ (GL)	G 46 to A	Gly 16 to Ser	partial, <0.1% activity 0.7% CRM	Keough et al, 1988; Sculley et al, 1991
FG	G 47 to A	Gly 16 to Asp	Lesch-Nyhan 1.4% activity	Sege-Peterson et al, 1992
$HPRT_{Mashad}$	A 59 to T	Asp 20 to Val	partial, 0.7% activity	Davidson et al, 1991
JS	C 69 to G	Cys 23 to Trp	partial, 30% activity	Sege Peterson et al, 1992
$HPRT_{Yonago}$	C 73 to A	Pro 25 to Thr	partial, 4.2% activity, normal mRNA	Tohyama et al, 1994
$HPRT_{Detroit}$ (KM)	T 122 to C	Leu 41 to Pro	Lesch-Nyhan	Davidson et al 1989a
$HPRT_{Isar}$ (KM)	A 124 to T	Ile 42 to Phe	Lesch-Nyhan 0.37 to 3.2 % residual activity	Burgemeister et al, 1995
$HPRT_{Heapy}$	T 125 to C	Ile 42 to Thr	activity not reported	Davidson et al, 1991
$HPRT_{Salamanca}$ (AA)	T 128 to G G 130 to A	Met 43 to Arg Asp 44 to Asn	Partial, 7.5% activity, K_m for hx increased 2 amino acid substitutions in same patient	Sege-Peterson et al, 1992
RJK 2163 (TD)	G 134 to A	Arg 45 to Lys	Lesch-Nyhan	Gibbs et al, 1990
AG DD	G 143 to A	Arg 48 to His	partial, 20% activity same mutation in 2 patients	Sege-Peterson et al, 1992
LW	G 148 to C	Ala 50 to Pro	partial, 1.6% activity	Sege-Peterson et al, 1992
1265	C 149 to T	Ala 50 to Val	Lesch-Nyhan	Tarle et al, 1991
$HPRT_{Toronto}$ (LP)	C 151 to G	Arg 51 to Gly	partial, 33% activity normal mRNA 52% CRM, normal K_m	Wilson et al, 1982c; Kelley and Wilson, 1982; Wilson et al, 1983b; Wilson et al, 1983c; Wilson et al, 1986a
$HPRT_{Benbury}$ Family 2	G 152 to C	Arg 51 to Pro	Lesch-Nyhan	Gibbs et al, 1986; Davidson et al, 1991
$HPRT_{Edinburgh}$	A 155 to G	Asp 52 to Gly	partial	Lightfoot et al, 1992
TE	G 157 to A	Val 53 to Met	partial, 20% activity	Sege-Peterson et al, 1992
MG	T 158 to C	Val 53 to Ala	partial, 15% activity	Sege-Peterson et al, 1992

Variant	cDNA Change	Predicted Change in Protein	Comment	Reference
Japan 1	A 160 to C	Met 54 to Leu	Lesch-Nyhan	Igarashi et al, 1989
$HPRT_{Montreal}$	T 170 to C	Met 57 to Thr	Lesch-Nyhan	Skopek et al, 1990
$HPRT_{Toowong}$ (PH)	G 172 to A	Gly 58 to Arg	partial, 10% activity normal mRNA 49% CRM	Keough et al, 1988; Sculley et al, 1991
Case 2	G 190 to C	Ala 64 to Pro	Lesch-Nyhan <1% activity	Yamada et al, 1992
$HPRT_{Utrecht}$ (K-Kindred) Case 1	G 208 to A	Gly 70 to Arg	Lesch-Nyhan same mutation in 2 patients normal mRNA	Bowens-Rombouts et al, 1993; Tohyama et al, 1994
$HPRT_{New\ Haven}$ (DG) 1510 955-2	G 209 to A	Gly 70 to Glu	Lesch-Nyhan Normal mRNA 50% CRM, same mutation in 3 different patients	Wilson et al, 1986a; Davidson et al, 1989a; Tarle et al, 1991
$HPRT_{Yale}$ (KT)	G 211 to C	Gly 71 to Arg	Lesch-Nyhan normal mRNA 92% CRM	Wilson et al, 1986a; Fujimori et al, 1989
$HPRT_{Madrid}$ (S-Kindred)	G 212 to T	Gly 71 to Val	partial	Bowens-Rombouts et al, 1993
$HPRT_{Seoul}$	A 215 to G	Tyr 72 to Cys	partial, <0.2% activity	Choi et al, 1993
$HPRT_{Flint}$ (AC, RJK 892) $HPRT_{Perth}$ 1522 DW	C 222 to A	Phe 74 to Leu	Lesch-Nyhan no mRNA no CRM Same mutation in 4 different patients	Wilson et al, 1986a: Davidson et al, 1988b; Gibbs et al, 1989; Sculley et al, 1991; Tarle et al, 1991; Sege-Peterson et al, 1992
$HPRT_{Swan}$	C 232 to G	Leu 78 to Val	partial, 10% activity	Sculley et al, 1991
Case 3	T 233 to A	Leu 78 to Gln	Lesch-Nyhan 2% activity	Yamada et al, 1992
$HPRT_{Arlington}$ (MS and WB)	A 239 to T	Asp 80 to Val	partial	Davidson et al, 1989a
$HPRT_{Munich}$ (IV)	A 310 to G	Ser 104 to Arg	partial, 3% activity normal mRNA 79% CRM increased K_m for hx, decreased V_{max}	Wilson et al, 1982c; Kelley and Wilson, 1982; Wilson and Kelley, 1984; Wilson et al, 1986a
$HPRT_{London}$ (GS) DB	C 329 to T	Ser 110 to Leu	partial, 59% to 69% activity normal mRNA 35% to 52% CRM, increased K_m for hx, same mutation in 2 different patients	Wilson et al, 1982c; Kelley and Wilson, 1982; Wilson et al, 1983a; Wilson et al, 1986a; Davidson et al, 1988c

Variant	cDNA Change	Predicted Change in Protein	Comment	Reference
$HPRT_{Midland}$ (JH, RJK 896)	T 389 to A	Val 130 to Asp	Lesch-Nyhan Normal mRNA no CRM same mutation in 2 different patients	Wilson et al, 1986a; Davidson et al , 1988a, 1989a; Gibbs et al, 1989; Tarle et al, 1991
375				
RJK 1784	T 392 to C	Leu 131 to Ser	Lesch-Nyhan	Gibbs et al, 1989
$HPRT_{Runcorn}$	T 395 to C	Ile 132 to Thr	activity not reported	Davidson et al, 1991
$HPRT_{Ann\ Arbor}$ (KC and TC)	T 396 to G	Ile 132 to Met	10% activity increased K_m for hx and PRPP, normal V_{max} normal mRNA 11% CRM	Wilson et al 1982c; Kelley and Wilson, 1982; Wilson et al, 1986a; Fujimori et al, 1988
$HPRT_{Cape\ Town}$ (TK) (P45)	G 403 A	Asp 135 to Asn	substrate inhibition, normal K_m for hx and PRPP	Steyn and Harley, 1984; this study
$HPRT_{Tokyo}$ YY (WR 194)	G 419 to A	Gly 140 to Asp	Lesch-Nyhan	Fujimori et al, 1992
$HPRT_{Milwaukee}$ (JM, RJK 949)	G 481 to T	Ala 161 to Ser	partial, 1.4% activity normal mRNA 3% CRM	Wilson et al, 1986a; Davidson et al, 1989a; Gibbs et al, 1989; this study
P867 (AW)			<2% activity, normal K_m, decreased V_{max} same mutation in 2 different patients	
P868 (GT)	C 482 to T	Ala 161 to Gly	<2% activity, normal K_m, decreased V_{max}	this study
$HPRT_{Farnham}$	C 486 to G	Ser 162 to Arg	activity not reported	Davidson et al, 1991
$HPRT_{Brisbane}$ (FC)	C 503 to T	Ile 168 to Thr	partial, !0% activity K_m for PRPP increased normal mRNA, 26% CRM	Gordon et al, 1987b; Keough et al, 1988; Gordon et al, 1990
$HPRT_{Marlow}$	C 527 to T	Pro 176 to Leu	0.8% activity	Davidson et al, 1991
RJK 2185	G 529 to T	Asp 177 to Tyr	Lesch-Nyhan	Gibbs et al, 1990
Japan 2	T 536 to G and G 538 to A	Val 179 to Gly and Gly 180 to Arg	partial two mutations in same patient	Igarashi et al, 1989
1734 (JF)	T 548 to C	Ile 183 to Thr	partial, 8% activity	Tarle et al, 1991 Sege-Peterson et al, 1992
Case 1	T 563 to C	Val 188 to Ala	5% activity	Yamada et al, 1992
$HPRT_{Kinston}$ (ES, RJK 2188)	G 580 to A	Asp 194 to Asn	Lesch-Nyhan normal mRNA 72% CRM increased K_m for hx and PRPP	Wilson et al, 1982c; Kelley and Wilson, 1982; Wilson et al, 1986a

Variant	cDNA Change	Predicted Change in Protein	Comment	Reference
$HPRT_{Moose\ Jaw}$	C582 to G	Asp 194 to Glu	partial 5 to 12% activity, K_m for hx and PRPP increased	Lightfoot et al, 1994
$HPRT_{New\ Briton}$ (EC, RJK 950	T 595 to G	Phe 199 to Val	Lesch-Nyhan normal mRNA no CRM	Wilson et al, 1986a; Davidson et al, 1989a; Gibbs et al, 1989
RB	G 601 to A	Asp 201 to Asn	60% activity	Sege-Peterson et al, 1992
GM	G 601 to T	Asp 201 to Tyr	Lesch-Nyhan	Sege-Peterson et al, 1992
$HPRT_{Ashville}$ (PC)	A 602 to G	Asp 201 to Gly	Partial <0.1% increased K_m for hx and PRPP, normal mRNA 4% CRM	Wilson et al, 1986a; Davidson et al, 1989b
RJK 1874 RJK 2079	C 610 G	His 204 to Asp	Lesch-Nyhan same mutation in 2 different patients	Gibbs et al, 1989; Gibbs et al, 1990
779	A 611 to G	His 204 to Arg	Lesch-Nyhan	Tarle et al, 1991
RJK 1727 $HPRT_{Reading}$ (Patient 6, Family 7)	G 617 to A	Cys 206 to Tyr	Lesch-Nyhan same mutation in 2 different patients	Gibbs et al, 1989; Watts et al, 1982; Gibbs et al, 1986; Davidson et al, 1991

HPRT cDNA is numbered with the A of the ATG start codon numbered as base 1. The amino acid sequence is numbered with the Met residue coded by the start codon as residue 1.
Abbreviations: hx, hypoxanthine; crm, HPRT imunoreactive material. Partial, partial HPRT deficiency; normal mRNA, normal mRNA size and levels.

In contrast, only three amino acid substitutions, one at residue Ser_{104} and two at Ser_{110}, have been reported in the 50 amino acid run from residue 81 to the start of the PRPP binding domain at residue 129. These substitutions occur in partial HPRT variants with altered affinity for the substrate hypoxanthine. This mutationally silent region corresponds to the flexible loop region linking strand B4 with B5. Both Ser_{104} and Ser_{110} are located close to the catalytic site of the enzyme. The paucity of amino acid substitutions in the flexible loop region suggests that this structure may be fairly tolerant of amino acid substitutions.

In summary, a review of mutations causing amino acid substitutions in HPRT suggests that the majority of mutations are not the result of DNA mutational hotspots, but reflect instead, structurally and functionally important regions of the protein. There is however,

evidence to support the existence of two DNA mutation hotspots, the first at the run of G nucleotides encoding amino acid residues 70 and 71, and the second at nucleotide C_{222}.

4.4.1 The Biochemical Genetics of L867 and L868.

The differences found in the values for the apparent K_m of hypoxanthine and PRPP between control haemolysates and control lymphoblast lysates do not reflect tissue specific isoforms of HPRT. Differing K_m values in different tissue has been well described (Adams and Harkness 1976; Shin-Buehring et al 1980) and probably reflect differences in the metabolism of the substrates hypoxanthine and PRPP, or the product IMP, by other enzymes present in the crude lysate preparations.

The kinetic characteristics of HPRT in L867 and L868 were similar with essentially normal substrate affinities for hypoxanthine and PRPP, but a severely decreased V_{max}.
The similarity between the two HPRT variants extended to the nature of the genetic defect, with single base substitutions affecting adjacent nucleotides in the codon for Ala_{161}.

The G_{481} to T transversion and the resulting Ala_{161} to Ser amino acid substitution found in L867 occur within the context of a CpG dinucleotide on the non-coding strand. CpG dinucleotides represent potential sites of cytosine methylation in mammalian cells (Wolf and Migeon, 1985) and spontaneous deamination of 5-methylcytosine to thymine (Ehlrich, 1990) has been reported to lead to the occurrence of a disproportionate number of C to T transitions at these sites (Rideout et al, 1990; Skandalis et al, 1994). The G_{481} to T transversion in L867 could not have occurred by spontaneous deamination of a 5-methylcytosine residue on the non-coding strand, as this mechanism would have led to a G_{481} to A transition on the coding strand and a change in the codon GCA (Ala) to ACA (Thr).

The identical G_{481} to T transition and resulting Ala_{161} to Ser substitution has been described in an apparently unrelated patient with gout (Patient JM of Davidson et al (1989a), cell line RJK 949 derived from JM of Gibbs et al, 1989). Davidson et al (1989a) named the variant $HPRT_{Milwaukee}$. In the original description of JM, Wilson et al (1986a) reported 1.4% residual HPRT activity in cultured lymphoblasts, but did not measure any kinetic parameters. The level of HPRT immunoreactive protein was decreased to 3% of control values.

The C_{482} to G transition and the resulting Ala_{161} to Gly amino acid substitution found in P868 is a novel mutation.

With the exception of the PRPP binding domain, the phosphoribosyltransferases show little amino acid sequence homology between enzymes. However, a comparison of HPRT amino acid sequences from various organisms shows that Ala_{161} occurs within an evolutionary conserved region of HPRT and is absolutely conserved in organisms as diverse as the rat, *Schistosoma mansoni* and *Plasmodium falciparum* and is conserved in character in *Leishmania donovani* (Figure 4.9).

```
                    150        160        170        180
Human[1]        KTMQTLLSLV RQYNPKMVKV ASLLVKRTPR SVGYKPDFVG
L867            .......... .......... S......... ..........
L868            .......... .......... G......... ..........
Mouse[2]        .......... K..S..... ........S. ....R.....
Hamster[3]      .......... KR..L..... ........S. ....R.....
Rat[4]          .......... K..S..... ........S. ....R.....
S. mansoni[5]   ..ITK.I.HL DSLST.S... ........SP RND.R.....
P. falciparum[6] ..LVKFCEYL KKFEI.T.AI .C.FI....L WN.F.A....
L. donovani[7]  I.L.Y.MRFM LAKK.ASL.T VV..D.PSG. K.EVLV.YPV
```

Figure 4.9: A between species comparison of the amino acid sequence of HPRT from residue 141 to 180. Numbering is according to the human sequence with the methionine coded by the ATG start codon numbered as residue 1. Only amino acids which differ from the human sequence are shown. Sequences were aligned using DAPSA (Harley, 1994). References: [1]Jolly et al, 1983; [2,3] Konecki et al, 1982; [4]Chiaverotti et al, 1991; [5]Craig et al, 1988; [6]Vasanthakumar et al, 1989; [7]Allen et al, 1993.

Figure 4.10: Ribbon diagram of human HPRT structure with GMP bound (reproduced from Eads et al, 1994).

The exact position of Ala_{161} within the crystal structure of HPRT was determined by using the shareware programme RasMol v2.5 (Sayle, 1994) to view the X-ray diffraction data lodged by Eads et al (1994) in the Brookhaven Protein Data Base.

Ala_{161} is located near the end of the ß strand B6, which together with strand B5, α helix A5 and strand B7 comprise the second half-sheet of the core of the enzyme. Strand B6 ends with Ser_{162}, then leads into a distinct bend followed by a short secondary strand B6' (Figure 4.10). Ala_{161} is some distance from the active site and appears to have a structural role.

It is generally recognised that protein secondary structure prediction models based on local amino acid sequence information which do not take into account global effects, rarely produce a predictive score of greater than 65% (Nishikawa and Noguchi, 1991). Nevertheless, where the local structure predicted by singlet-type methods such as Chou and Fasman (CF) (Chou and Fasman, 1978) and the quasi-doublet method of Garnier et al (1978) (GOR method) are in agreement with the structure defined by X-ray crystallography, simple models such as CF and GOR can prove useful in modelling the effects of an amino acid substitution on the predicted local structure.

Secondary structure predictions using the programmes PepPlot (Gribskov and Devereux, 1986), PeptideStructure and PlotStructure (Wolf et al, 1988) which form part of the Sequence Analysis Software Package (Genetics Computer Group) were used to predict the local structure about the residue Ala_{161} in the normal protein, as well as the affect on the predicted normal sequence of the amino acid substitutions, Ala_{161} to Ser in P867 and Ala_{161} to Gly in P868. Secondary structure predictions based on the GOR method differed from structures derived using the CF method. The GOR method predicted that Ala_{161} falls within an α helix. The substitution of Ala_{161} by either Ser or Gly resulted in the predicted loss of an α helix and the gain of a ß strand.

Conflicting predictions were obtained using CF based methods which predicted Ala_{161} to fall within a short ß strand (Figure 4.11). This prediction is consistent with the model of HPRT structure derived from the crystal structure of OPRT by Scapin et al (1994) as well as the position of Ala_{161} within the crystal structure of HPRT as defined by Eads et al (1994). This support for the local secondary structure predicted by the CF method lends credibility to the use of CF secondary structure predictions in the analysis of the effects of amino acid substitutions at Ala_{161}.

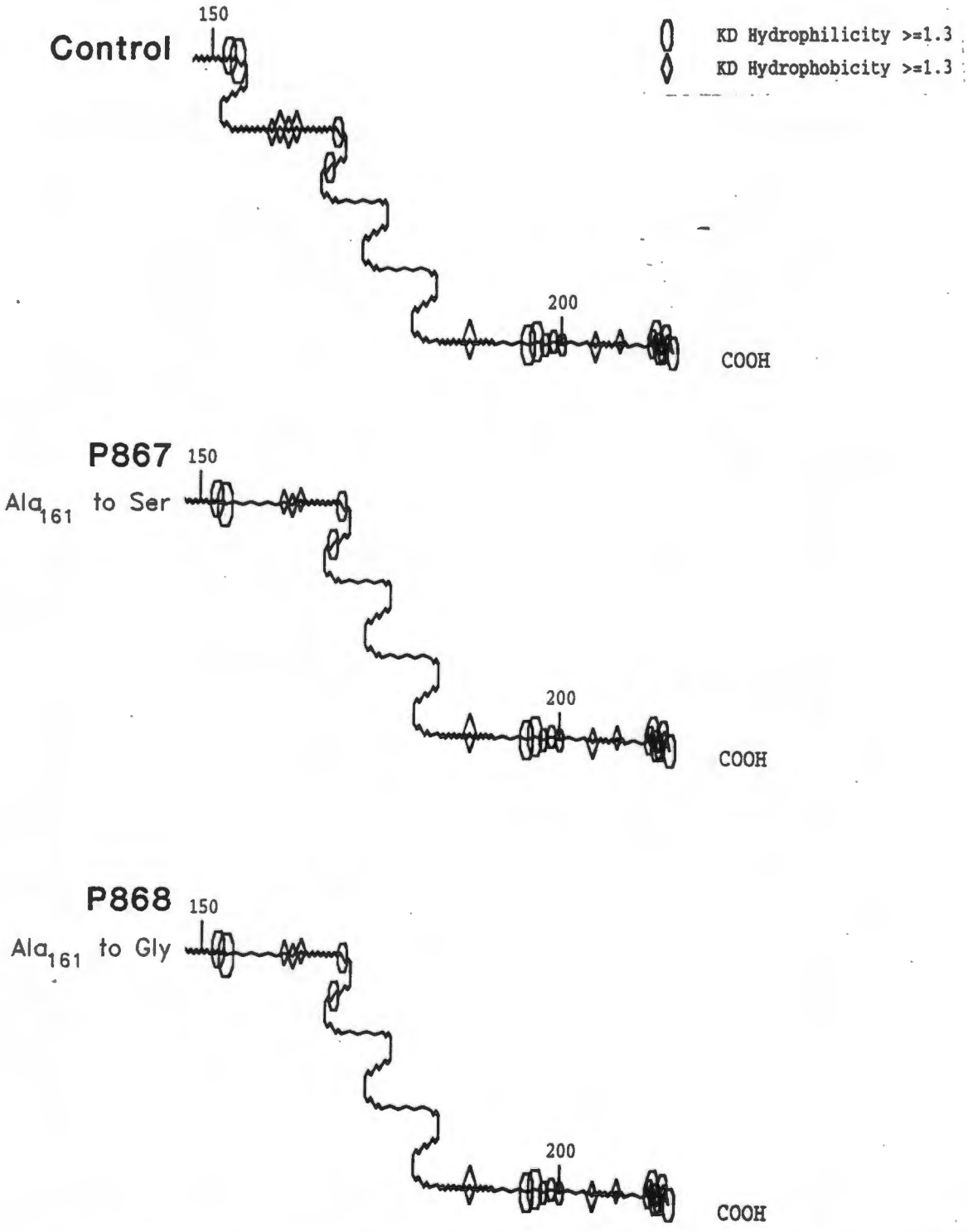

Figure 4.11: Effect of substituting Ser or Gly for Ala_{161} on the predicted local secondary structure of HPRT. PeptideStructure and PlotStructure (Wolf et al, 1988) were used to predict the local structure about the residue Ala_{161}. α-Helices are shown with a sine wave, β-strands with sharp saw-tooth waves, turns with 180 degree turns and coils with dull saw- tooth waves.

The substitution of the non-polar hydrophobic Ala_{161} residue by a polar hydrophilic Ser in P867 may affect packing within the hydrophobic core of the enzyme and also raises the possibility of changes in the secondary structure through the potential of Ser to form hydrogen bonds with other amino acid residues brought into close proximity by the change in secondary structure.

These disruptions to the structure of the enzyme may lead to partial unfolding. Partially unfolded proteins are thought to have higher rates of proteolytic degradation *in vivo* (Goldberg and St. John, 1976). The marked decrease in immunoreactive HPRT protein reported in $HPRT_{Milwaukee}$ (Wilson et al, 1986a) and the decreased thermal stability of HPRT noted in L867, are evidence of increased enzyme degradation *in vivo*. The normal apparent substrate affinities found in L867 supports the view that the defect in $HPRT_{Milwaukee}$ and L867 affects a structurally important amino acid residue with no direct role in substrate binding or catalysis.

In HPRT of L868, Ala_{161} is substituted by Gly. The effect of the substitution on secondary structure predictions using the CF method (Figure 4.11) was identical to those predicted for the Ala_{161} to Ser mutation. A predicted ß turn and ß strand are lost and replaced by an α helix. Ala_{161} to Gly is a relatively conservative amino acid change in that both Gly and Ala are hydrophobic non-polar amino acids. However, Gly differs from Ala by the absence of a methyl side chain, resulting in greater conformational freedom, a decreased hydrophobic surface relative to Ala and an intrinsic capacity to destabilise both α helix (Chou and Fasman, 1978; Lyu et al, 1990; Horovitz et al, 1992; Blaber et al, 1994) and ß strand structures (Minor and Kim, 1994).

Substituting Gly near the end of strand B6 could result in premature termination of the ß strand, increasing flexibility in the bend linking B6 and B6' and possibly allowing the bend to fall into an α helix. Increased flexibility in the bend could allow B6 to float and may possibly have an effect on strand B6'. Lys_{166} is located in B6' and interacts with GMP through side chain hydrogen bonding to the purine base, whilst the main chain oxygen is

hydrogen bonded to the side chain oxygen of Thr_{168}, presumably stabilising this region of the enzyme (Eads et al, 1994). The normal apparent substrate affinities found in L867 and L868 suggests that the destabilising effects of both the Gly and Ser substitutions at Ala_{161} do not significantly affect strand B6' and the position of Lys_{166} within the active site. The effect of both substitutions at Ala_{161} appears to be focused on the ß strand structural element B6.

Two HPRT variants have been reported with amino acid substitutions in the immediate vicinity of Ala_{161} (Table 4.4). Davidson et al (1991) reported the substitution of Ser_{162} by Arg in $HPRT_{Farnham}$. No residual activity was detected in this enzyme variant using a gel-based assay system, but the sensitivity of this assay in detecting low levels of residual activity was not discussed and it was not reported whether the variant resulted in the Lesch-Nyhan phenotype. The substitution of the small neutral, polar, mildly hydrophilic residue side chain of Ser_{162} by the bulky, highly hydrophilic, positively charged side chain of Arg has the potential for a major disruption of the core structure of the enzyme. The substituted Arg side chain would probably disrupt the bend between B6 and B6'. The effect could be transmitted to the nearby residue Lys_{166} affecting substrate binding within the active site. The non-conservative nature of the amino acid substitution and the consequent disruption to the core of the enzyme, as well as the potential for displacement of residues with side chains located within the active site, are consistent with a possible complete loss of enzyme activity in $HPRT_{Farnham}$. Eads et al (1994) discussed the effect of the Thr_{168} to Ilu substitution found in a partially deficient HPRT variant, $HPRT_{Brisbane}$ (Gordon et al, 1990) and pointed out that the mutation would be expected to interfere with the hydrogen bond between Thr_{168} and Lys_{166} leading to an increased K_m for the purine base substrates. Contrary to expectations, the reported K_m for guanine was normal while that of PRPP was elevated fivefold (Keough et al (1988).

The three mutations affecting Ala_{161} described in L868, $HPRT_{Milwaukee}$ and the identical mutation in L867, as well the mutation at Ser_{162} found in $HPRT_{Farnham}$, suggest that the end of ß strand B6 and the bend between strand B6 and B6' are key structural elements within

the core of HPRT. The severe impact on residual activity of the two relatively conservative amino acid substitutions in L867 and L868, and the absence of any effect on substrate affinities, provides further evidence that Ala_{161} plays a crucial role in maintaining the integrity of HPRT structure.

4.4.2 The Molecular Defect in $HPRT_{Cape\ Town}$.

The molecular defect in $HPRT_{Cape\ Town}$ results in the substitution of Asp_{135} by Asn. Secondary structure predictions using the CF and GOR methods predicted no changes in local secondary structure as a result of the residue substitution. Asp_{135} is located at the center of the highly conserved PRPP binding motif which in HPRT comprises the residues 129-VLIVEDIIDTGK-140 (Wilson et al, 1983d; Hove-Jensen et al 1986). The character of the motif has been conserved through all known phosphorybosyltransferases, in species as diverse as humans and *E. coli* and is also identifiable in PRPP synthetase (Table 4.5). Asp_{135} is the only amino acid within the PRPP binding motif which is absolutely conserved.

Within the HPRT crystal structure, Eads et al (1994) described the PRPP binding motif as starting with the hydrophobic residues of strand B5 within the core of the enzyme (Figure 4.10). These hydrophobic residues have no direct interactions with the active site. The ß strand makes a sharp turn at Asp_{135} and leads into a loop composed of residues Asp_{138} to Thr_{142} which encircle the phosphate group of GMP. The carboxylate side chains of Glu_{134} and Asp_{135} are located below the ribose in HPRT, as are the equivalent amino acids in the crystal structure of OPRT (Scapin et al, 1994).

The kinetics of $HPRT_{Cape\ Town}$ in haemolysates has been described in detail by Steyn and Harley (1984). This unusual HPRT variant has normal substrate affinities and V_{max}. However, at hypoxanthine concentrations above 70 µM, enzyme activity decreased with increasing purine base substrate concentration.

TABLE 4.5 COMPARISON OF AMINO ACID SEQUENCES AROUND POSITION 135 IN THE PRPP BINDING DOMAIN

							135						
$HPRT_{CapeTown}$	Asn	Val	Leu	Ile	Val	Glu	**Asn**	Ile	Ile	Asp	Thr	Gly	Lys
HPRT													
Human[1]	Asn	Val	Leu	Ile	Val	Glu	**Asp**	Ile	Ile	Asp	Thr	Gly	Lys
Mouse[2]	Asn	Val	Leu	Ile	Val	Glu	**Asp**	Ile	Ile	Asp	Thr	Gly	Lys
P. fal.[3]	His	Val	Leu	Ile	Val	Glu	**Asp**	Ile	Ile	Asp	Thr	Gly	Lys
XGprt (gpt)													
E. coli[4]	Gly	Phe	Ile	Val	Ile	Asp	**Asp**	Leu	Val	Asp	Thr	Gly	Gly
APRT													
Human[5]	Arg	Val	Val	Val	Val	Asp	**Asp**	Leu	Leu	Ala	Thr	Gly	Gly
E. coli[6]	Lys	Val	Leu	Val	Val	Asp	**Asp**	Leu	Leu	Ala	Thr	Gly	Gly
OPRT(pyrE)													
E. coli[7]	Arg	Val	Met	Leu	Val	Asp	**Asp**	Val	Ile	Thr	Ala	Gly	Thr
AmPRT(purF)													
E. coli[8]	Asn	Val	Leu	Leu	Val	Asp	**Asp**	Ser	Ile	Val	Arg	Gly	Thr
AnthrPRT													
E. coli[9]	Asp	Tyr	Leu	Phe	-	Ala	**Asp**	Ile	Val	Gly	Thr	Gly	Gly
ATP-PRT													
S. typh.[10]	Leu	Ala	Asp	Ala	Ile	Cys	**Asp**	Leu	Val	Ser	Thr	Gly	Ala
PRPP-synthetase													
E. coli[11]	Asp	Cys	Val	Leu	Val	Asp	**Asp**	Met	Ile	Asp	Thr	Gly	Gly
Human[12]	Val	Ala	Ile	Leu	Val	Asp	**Asp**	Met	Ala	Asp	Thr	Cys	Gly

References : [1]Wilson et al (1982) [2]Konecki et al (1982) [3]Vasanthakumar et al (1989) [4]Richardson et al (1983) [5]Wilson et al (1986) [6]Hershey and Taylor (1986) [7]Poulsen et al (1983) [8]Tso et al (1982) [9]Horowitz et al (1982) [10]Piszkiewiez et al (1979) [11]Hove-Jensen et al (1986) [12]Iizasa et al (1989)
Abbreviations : PRT, phosphoribosyltransferase AmPRT, glutamine PRT AnthrPRT, anthranilate PRT

The pattern of inhibition was uncompetitive and was characteristic of an ordered sequential reaction, with PRPP binding before hypoxanthine. On the basis of double inhibition studies (using the inhibitory substrate hypoxanthine and the product PPi) Steyn and Harley proposed the reaction mechanism shown in Figure 4.12. In both the normal enzyme and $HPRT_{Cape\ Town}$, PRPP binds before hypoxanthine. Catalysis occurs and IMP is released. In the normal enzyme PPi is released. But in $HPRT_{Cape\ Town}$, before PPi is released, hypoxanthine binds to the enzyme pyrophosphate intermediate forming a dead end product-substrate-enzyme complex.

$HPRT_{Cape\ Town}$ is a unique HPRT variant and no other variant phosphoribosyltransferase characterised by substrate inhibition has been previously reported. However, a similar pattern of apparent substrate inhibition to that found in $HPRT_{Cape\ Town}$ was reported in rat liver by Wohlhueter (1975). There is no evidence for tissue specific HPRT isoenzymes in the rat or any other species and it seems likely that the apparent substrate inhibition shown by Wolhueter in rat liver may be a consequence of using crude undialysed enzyme preparations. The assay method used by Wolhueter did not include TTP as an inhibitor of 5'-nucleotidase and it is possible that this may have contributed to the decreased product formation at high substrate concentrations in the crude rat liver preparation.

Early models of phosphoribosyltransferase structure suggested that the two carboxylate residues at the center of the PRPP binding motif in HPRT (Busetta, 1988) and OPRT (Ashton et al, 1989) play a role in binding the pyrophosphate moiety of the PRPP-Mg^{2+} substrate complex.

The absence of PPi or PRPP in the crystal structures of HPRT and OPRT has resulted in difficulties in clarifying the functional role of the two conserved carboxylate residues. Eads et al (1994) and Scapin et al (1994) showed no direct interaction between the carboxylate residue of Asp_{135} in HPRT (and the equivalent residue in OPRT) and the ribose of the bound mononucleotide.

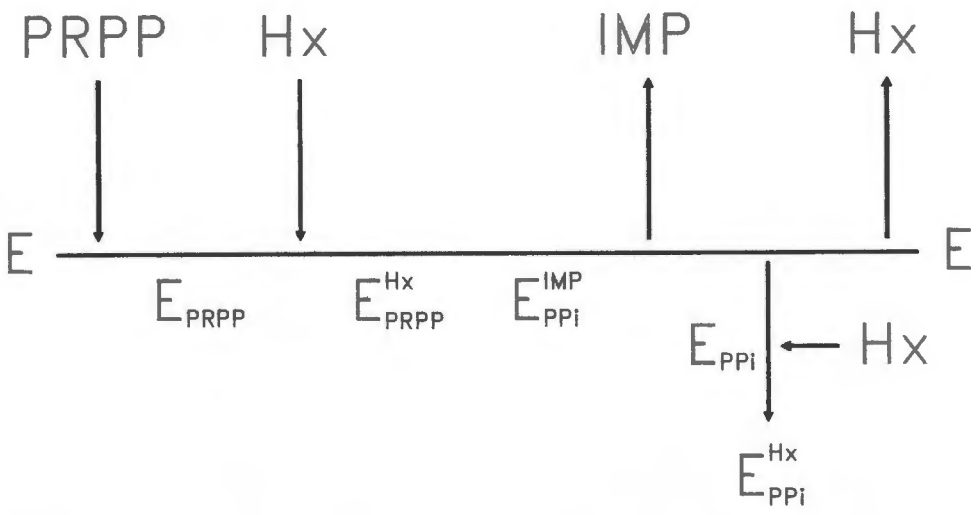

Figure 4.12: Proposed reaction mechanism of catalysis in $HPRT_{Cape\ Town}$. In the reaction mechanism proposed by Steyn and Harley (1984), PRPP binds to the enzyme (E) before hypoxanthine (Hx). Catalysis occurs and IMP is released. In $HPRT_{Cape\ Town}$ hypoxanthine then binds to the enzyme pyrophosphate intermediate forming a dead end product-substrate-enzyme complex.

This is consistent with the normal substrate affinities described in $HPRT_{Cape\ Town}$ by Steyn and Harley (1984), since direct interaction between Asp_{135} and the ribose of PRPP would be expected to result in an increased K_m for PRPP with a change to Asn_{135}.

Both Eads et al (1994) and Scapin et al (1994) speculate that the two carboxylate residues may be involved in stabilising the transition state of oxocarbonium character which is believed to develop during phosphoribosyl transfer. A weak positive charge is expected to develop on the ribose. Scapin et al (1994) speculated further that in OPRT, the two carboxylate residues may act as a Mg^{2+}-PPi binding site. Although the distance between the nucleoside and the possible PPi binding site is greater than expected for nucleophilic displacement, Scapin et al (1994) suggested that during the transition state, the bond length between the ribose group and the incoming nucleophile or leaving base during group (ribosyl) transfer may lengthen, bringing the Mg^{2+}-PPi complex and the nucleotide

into close proximity. Alternatively, PPi may bind to one of the conserved basic residues found within the active site of both HPRT and OPRT.

Thus there are two proposed roles for Asp_{135} and the neighbouring carboxylate residue in HPRT: either stabilising the oxocarbonium transition state, or acting as a Mg^{2+}-pyrophosphate binding area, or both.

An alternative mechanism of substrate inhibition in $HPRT_{Cape\ Town}$ based on the assumption that Asp_{135} is not involved in PPi binding, takes into account the Recovery Model of substrate inhibition proposed by Kühl (1994). The model postulates that after the catalytic act, an obligatory recovery phase is necessary before the new operation cycle can start. The recovery phase has a fixed finite time *t* of negligible variance. At high concentrations of substrate, inappropriate binding of substrate to the refractory state of the enzyme may occur. Binding of a substrate molecule during this recovery phase gives rise to substrate inhibition. It is possible that the negative charge associated with Asp_{135} may play a role in the enzyme recovery phase of HPRT. Such a mechanism would be consistent with the placement of Asp_{135} within the crystal structure of HPRT below the ribose ring of bound IMP with no direct interaction with PPi. However, this model does not explain Steyn and Harley's (1984) observation that hypoxanthine and PPi are not independent inhibitors of $HPRT_{Cape\ Town}$.

The proposed formation of a dead-end hypoxanthine-enzyme-PPi complex in $HPRT_{Cape\ Town}$ (Steyn and Harley, 1984) suggests that Asp_{135} interacts in some way with PPi. The release of the products IMP and PPi by the normal enzyme has been reported to be ordered sequential by Krenitsky and Papaioannou (1969), while Giacomello and Salerno (1978) proposed a random sequential release of products based on assays of the reverse reaction. Both mechanisms would result in an E^{PPI} intermediate. The bond lengthening during the transition state may place PPi within close proximity to the negatively charged area of Glu_{134} and Asp_{135}. The release of PPi from the active site of HPRT would then be hastened by repulsion between the carboxylate residues and the

negatively charged PPi. The substitution of the carboxylate residue Asp_{135} by neutral Asn could reduce the leaving impetus of pyrophosphate, increasing the time spent by PPi within the active site and allowing the purine base substrates to bind to form a dead-end product-substrate-enzyme complex. This proposed model thus includes some elements of the Recovery model.

A number of mutations affecting the conserved PRPP binding motif have been reported (Table 4.4). The Val_{130} to Asp in the Lesch-Nyhan variant $HPRT_{Midland}$ (Davidson et al 1988a) and the Leu_{132} to Met in partially deficient $HPRT_{Ann\ Arbor}$ (Wilson et al 1986a) are both in the ß strand B5 at the core of the enzyme. Both variants have decreased intracellular levels of HPRT protein. The Val_{130} to Asp substitution would destabilise the entire core structure, while the substitution in $HPRT_{Ann\ Arbor}$ is more conservative, but could result in altered residue packing within the hydrophobic core of the enzyme (Eads et al, 1994). The implication of the Gly_{140} to Asp substitution in the Lesch-Nyhan variant $HPRT_{Tokyo}$ (Fujimori et al, 1992) is also discussed by Eads et al (1994). The substitution would be expected to alter the conformation and charge of the phosphate binding loop affecting the binding of the 5'-phosphate of PRPP.

It is tempting to speculate that the phenomenon of substrate inhibition due to the Asp_{135} to Asn in $HPRT_{Cape\ Town}$ can be generalised to other phosphoribosyltransferases. De Boer and Glickman (1991) reported the equivalent mutation in an APRT variant isolated from a Chinese hamster ovary cell line. Although the enzyme was not characterised kinetically, it is interesting that this variant APRT showed 10% residual activity.

4.4.3 Patient P534.

The clinical presentation of patient P534 was consistent with partial HPRT deficiency. The "self-mutilation" reported by the clinicians is of anecdotal interest and should not be confused with the compulsive self-mutilation characteristic of the Lesch-Nyhan syndrome. The self-inflicted injuries observed in the patient represented a cognitive attempt by the patient at treatment as recommended by a traditional healer.

The results of the biochemical and molecular investigations of patient P534 are contradictory: HPRT assays on two independently blood specimens were typical of a V_{max} variant, but kinetic parameters and the heat stability profile of HPRT in lymphoblast lysates were normal.

It is possible that the decreased HPRT activity in haemolysates of P534 is artifactual. As Fairbanks et al (1987) pointed out, the assay of HPRT activity in haemolysates may dramatically underestimate the amount of residual HPRT activity as measured in intact erythrocytes. Similar, but as yet undefined factors, may have contributed to an underestimation of normal HPRT activity in haemolysates of P534. The interpretation of the decreased haemolysate HPRT activity in P534 is complicated by the blood transfusion the patient had received a day prior to blood being drawn for HPRT determination. There have been reports of a blood transfusion restoring HPRT activity in a Lesch-Nyhan infant (Simmonds, 1994) and this is in line with the finding that HPRT activity in blood transfusion units was stable to beyond the expiry date of the units. It seems unlikely that the blood transfusion could have led to the decreased HPRT activity seen in haemolysates of the patient, as evidence suggests that a blood transfusion would have led, on the contrary, to an increase and consequent overestimation of HPRT activity in P534.

The double label experiment on intact cultured fibroblasts appeared to support a diagnosis of partial HPRT deficiency, but only a single experiment with two control cell lines was performed and no confirmed partial HPRT fibroblast cell lines were available for the study.

Baumgarten and Harley (1995) stressed the variability of purine label incorporation between experiments by cultured fibroblasts and predicted that the results of a single experiment with few control fibroblasts cell lines, could result in an erroneous diagnosis of partial HPRT deficiency. These reservations are of general relevance and were substantiated by the double label studies on cultured lymphoblasts, which included the cell lines L534, L867 and L868, described in Section 5. In this study, L534 was not significantly different in [^{14}C] hypoxanthine incorporation from the partially HPRT deficient lymphoblast cell lines L867 and L868, but was significantly lower than three of the six control cell lines. These results are also ambiguous and may be taken to support either the hypothesis that P534 has a partial deficiency in HPRT, or that P534 is normal.

The genetic status of P534 remains uncertain. No mutations could be found in the coding region of L534 HPRT cDNA. It is possible that a mutation in a HPRT gene regulatory element could result in decreased transcription and consequently, decreased HPRT activity predominantly in erythrocytes. A lower than normal rate of HPRT enzyme synthesis in nucleated cells could be compensated by the stability of the enzyme and it is conceivable that normal or near normal levels of the enzyme can be maintained. The mature erythrocyte on the other hand, has lost the capacity for protein synthesis. An impaired rate of HPRT enzyme synthesis in the nucleated red cell precursor could result in decreased HPRT enzyme levels in the mature erythrocyte. Without evidence of decreased levels of HPRT mRNA however, the defect in P534 remains speculative.

4.5 Conclusion.

Ala_{161} has an important structural role in maintaining the integrity of HPRT enzyme structure. The biochemical effects of mutations at this residue have not been previously defined. Three mutations have now been reported to affect this residue. The Ala_{161} to Ser substitution in L867 is identical to $HPRT_{Milwaukee}$, while the Ala_{161} to Gly substitution in L868 is a novel mutation.

The role of the extremely conserved residue Asp_{135} in the PRPP binding motif remains uncertain. The Asp_{135} to Asn substitution in $HPRT_{Cape\ Town}$ is associated with substrate inhibition and a proposed dead-end hypoxanthine-PPi-enzyme complex. This suggests that role of Asp_{135} in HPRT lies in the expulsion of PPi from the catalytic site of the enzyme.

The defect in P534 remains unclear. A defect in a HPRT gene regulatory element would be consistent with the profile of impaired enzyme activity in haemolysates and normal activity in lymphoblast lysates.

5. VARIATION IN PURINE LABEL METABOLISM BY CULTURED LYMPHOBLASTS: [^{14}C] HYPOXANTHINE INCORPORATION AS A PREDICTOR OF PARTIAL HPRT DEFICIENCY.

5.1 Introduction.

A number of investigators have suggested that a single measure of HPRT activity is not sufficiently reliable to diagnose partial HPRT deficiency. Reservations have been expressed about the accuracy of assay methods based on the incorporation of [^{14}C] hypoxanthine by cultured fibroblasts (Willers et al, 1984), or intact erythrocytes (Gordon et al, 1987) and the direct assay of HPRT activity in erythrocyte lysates (Fairbanks et al, 1987). Our experience with the patient P534 has confirmed that reliance on a single diagnostic system such as the measurement of HPRT activity in haemolysates, may prove misleading.

Rozen et al (1977) pioneered the use of a double label approach to the diagnosis of inborn errors of metabolism in fibroblasts. The activity of the pathway under investigation can be determined by measuring the incorporation of a [^{14}C] labelled substrate into the product of the pathway relative to a [^{3}H] substrate which is incorporated into a separate, unrelated pathway. The incorporation of the [^{3}H] substrate by the unrelated pathway serves as a control for cell viability and cell number in the assay system. Rozen was able to demonstrate severely decreased [^{14}C] hypoxanthine incorporation relative to normal [^{3}H] thymidine incorporation by fibroblasts derived from a Lesch-Nyhan patient. The value of a similar double label approach, using the ratio of [^{14}C] hypoxanthine incorporation to the control substrate [^{3}H] phenylalanine, in demonstrating complete HPRT deficiency in Lesch-Nyhan patients was shown in Section 3.

Recently our laboratory defined the components of the major physiological variation found in the uptake of the purine bases adenine and hypoxanthine by human and other mammalian fibroblasts (Baumgarten and Harley, 1995; Vreede, 1994)). Although cell lines partially deficient in HPRT were not included in these studies, the finding of a large variation in the uptake of labelled hypoxanthine between individual fibroblast cell lines within the same experiment over a time scale of a few days, has cast doubt on the validity of using the incorporation of labelled hypoxanthine by nucleated cells as a means of diagnosing partial HPRT deficiency.

Cultured lymphoblasts are an easily obtainable, renewable source of patient material and are often, as in the case of P867 and P868, the only material available for investigation by a reference laboratory. Little is known of the components and extent of variation of whole cell purine base uptake in these cells. The validity of an intact lymphoblast double label assay as a method of diagnosing partial HPRT deficiency in nucleated cells merited further investigation.

Two label pairs were assessed as predictors of HPRT deficiency: [^{14}C] hypoxanthine and [^{3}H] phenylalanine and in a modification of the method described by Rozen et al (1977), [^{14}C] hypoxanthine and [^{3}H] adenine. In the first label pair, [^{3}H] phenylalanine enters an independent control pathway and serves as a measure of cell viability within the assay system and corrects for variables such as cell number. In contrast, the salvage of [^{3}H] adenine and [^{14}C] hypoxanthine are not independent. The salvage pathways of hypoxanthine and adenine converge at AMP. The first step of both salvage pathways are catalysed by a phosphoribosyltransferase which requires PRPP as a co-substrate.

APRT activity has been reported to be increased in erythrocytes of partially and completely HPRT deficient patients (Kelley et al, 1967, 1969; Seegmiller et al, 1967; Shin-Buehring, 1980; Snyder et al, 1984), while Zoref et al (1978) showed increased adenine salvage in intact fibroblasts from a patient with partially deficient HPRT activity. However, APRT activity in fibroblast lysates (Kelley, 1971) and lymphoblast lysates

(Snyder et al 1989) was found to be normal. In an analogous approach to a whole cell double label method, Stout et al (1985) used the ratio of HPRT activity to APRT activity in cell free chorionic villus material in the prenatal diagnosis of the Lesch-Nyhan syndrome. The measure of APRT activity served as an internal control.

On the basis of increased APRT activity reported in HPRT deficiency, we postulated that if [^{3}H] adenine was used instead of the traditional [^{3}H] phenylalanine or [^{3}H] thymidine as a measure of the control pathway, the dynamics of [^{14}C] hypoxanthine and [^{3}H] adenine uptake by a partially deficient lymphoblast cell line could act to increase the differential in the uptake of [^{14}C] hypoxanthine relative to the control pathway label. An analysis of variance was used to define the components of variation within the two assay systems, and a pair-wise comparison of patients and controls was used to test the predictive power of both label pairs in detecting partial HPRT deficiency in cultured lymphoblasts.

5.2 Methods.

5.2.1 Cell Lines.

The transformed lymphoblast cell lines used in the double label experiments are shown in Table 5.1. All cell lines were free of *Mycoplasma* contamination.

Table 5.1: Transformed lymphoblast cell lines used in the double label experiments.

CELL LINE	DEFECT
L516	obligate heterozygote variegate porphyria
L517	obligate heterozygote variegate porphyria
L634	acute intermittent porphyria
L844	possible porphyria
L863	normal individual
L864	normal individual
L534	possible partial HPRT deficiency
L867	partial HPRT deficiency
L868	partial HPRT deficiency

5.2.2 Incorporation of [^{14}C] Hypoxanthine Relative to [^{3}H] Adenine or [^{3}H] Phenylalanine by Cultured Lymphoblasts.

Lymphoblast cultures were fed twice weekly with 20 ml of DMEM supplemented with 10% foetal calf serum. Experiments were timed to occur the day after the cells were fed. All experiments were performed in triplicate. Cell densities of lymphoblast cultures were estimated on a Coulter Model Z cell counter (Coulter Electronics, Florida, USA). A volume of the cell suspension equivalent to $1x10^6$ cells was transferred to a centrifuge tube

and the cells pelleted at 1000g for 10 min. The medium was discarded and replaced with normal saline, the cells pelleted and then resuspended in 1 ml of a labelling medium consisting of 15 mM Hepes buffered Hanks Balanced Salt solution (pH 7.4) supplemented with 0.2 μCi [^{14}C] hypoxanthine and 0.8 μCi [^{3}H] phenylalanine or [^{3}H] adenine. The cells were then incubated with shaking at 37°C without CO_2 for 2 hours. After labelling, the cells were pelleted at 1000g for 10 min and the cell pellet washed with 4 ml ice cold saline. The cells were pelleted again, the saline discarded and the tubes allowed to drain for a few moments in an inverted position on absorbent paper to remove as much of the saline as possible. 200 μl of ice cold 5% trichloroacetic acid (TCA) was then added to the cell pellet and the precipitate trapped on Whatman GF/C glass microfibre filters (Whatman International, Maidstone, England) mounted in a Millipore vacuum manifold. The filters were washed twice under vacuum with 4 ml ice cold 5% TCA. Care was taken to rinse the edges of the filters after removal of the sealing gasket of the vacuum manifold. Each filter was transferred to a scintillation vial and 200 μl water and 10 ml Hionic-Fluor scintillant added. The vials were counted the next day using windows of 0 to 200 keV for [^{3}H] and 400 to 1000 keV for the [^{14}C] label. The efficiency of counting of each isotope in each window is shown below:

[^{3}H] in the [^{3}H] window	34% efficiency
[^{3}H] in the [^{14}C] window	0% efficiency
[^{14}C] in the [^{3}H] window	5% efficiency
[^{14}C] in the [^{14}C] window	54% efficiency

5.2.3 Statistical Analysis.

5.2.3.1 Analysis of Components of Variance of Labelled Substrate Incorporation by Cultured Lymphoblasts.

The double label experiments have a nested design. Replicate determinations are nested within individual cell lines which are nested within experiments performed on different occasions. Determinations are influenced by random factors derived from each experimental level. The experimental system fits a random effects model with three stages of sampling as shown in Table 5.2. The general structure of the model and formulae for calculations are as described by Snedecor and Cochran (1980).

The k^{th} observation of the j^{th} cell line in the i^{th} experiment has the structure

$$X_{ijk} = \mu + A_i + B_{ij} + e_{ijk}$$

μ = general mean
A_i = random effect of experiments
B_{ij} = random effect of individual cell lines
e_{ijk} = random effect of replicate determinations.

with $i = 1,..,a$; $j = 1,..,b$: $k = 1,..,n$;
and $A_i = N(0,\sigma_a^2)$; $B_{ij} = N(0,\sigma_b^2)$; $e_{ijk} = N(0,\sigma_e^2)$.

The variables A_i, B_{ij} and e_{ijk} are all assumed independent.

Table 5.2: Structure of double label experiments.

Experiment, *i* i=1,...,a	Cell Line, *ij* j=1,...,b	Replicates, *ijk* k=1,...,n		
1	1	X_{111}	.	X_{11n}
.	2	X_{121}	.	X_{12n}
.	.	.	.	.
.	.	.	.	.
.	b	X_{1b1}	.	X_{1bn}
.	.	.	.	.
.	.	.	.	.
.	.	.	.	.
.	.	.	.	.
.	.	.	.	.
a	1	X_{a11}	.	X_{a1n}
	.	.	.	.
	.	.	.	.
	b	X_{1ab}	.	X_{abn}

Total size = abn

Calculations of Sum of Squares (SS):

a = number of experiment; b = number of cell lines;

n = number of replicate

$C = (X..)^2/(abn)$

Total SS*determinations* = $\Sigma X^2_{ijk} - C$

Total SS*cell lines* = $\Sigma X^2_{ij.}/n - C$

Total SS*exp* = $\Sigma X^2_{i..}/bn - C$

SS*ind* (individual cell lines of same experiment)

= SS*cell lines* - SS*experiment*

SS*err* (Replicate in same cell line in same experiment)

= SS*determinations* - SS*cell lines*

An ANOVA table was constructed as shown below (Table 5.3).

Table 5.3: Form of ANOVA tables.

Source of Variation	SS	df	MS	Parameters Estimated
Experiment	SS*exp*	(a-1)	$\frac{SS\textit{exp}}{(a-1)}$	$\sigma_e^2 + n\sigma_B^2 + bn\sigma_A^2$
Individual	SS*ind*	a(b-1)	$\frac{SS\textit{ind}}{a(b-1)}$	$\sigma_e^2 + n\sigma_B^2$
Replicate	SS*err*	ab(n-1)	$\frac{SS\textit{err}}{ab(n-1)}$	σ_e^2

Estimation of the Components of Variance.

Unbiased estimates of the three components of variance were calculated from the mean squares as shown below:

Variance due to replication error:

$s_e^2 = MS\textit{err}$ estimates σ_e^2

Variance due to individual cell lines within an experiment:

$s_B^2 = (MS\textit{ind} - MS\textit{err})/n$ estimates σ_B^2

Variance due to experiments:

$s_A^2 = (MS\textit{exp} - MS\textit{ind})/nb$ estimates σ_A^2

Hypothesis Testing.

H_0: $\sigma_A^2 = 0$, there is no significant difference in the incorporation of a labelled substrate by a cell line between experiments.

$$F = \frac{MSexp}{MSind} \quad \text{estimates} \quad \frac{\sigma_e^2 + n\sigma_B^2 + bn\sigma_A^2}{\sigma_e^2 + n\sigma_B^2}$$

with degrees of freedom v = (a-1),a(b-1)

At large values of F, reject H_0 and accept H_1 that there is a significant difference in the incorporation of a labelled substrate by a cell line between experiments.

H_0: $\sigma_B^2 = 0$, there is no significant difference in the incorporation of a labelled substrate by individual cell lines within the same experiment.

$$F = \frac{MSind}{MSerr} \quad \text{estimates} \quad \frac{\sigma_e^2 + n\sigma_B^2}{\sigma_e^2}$$

with degrees of freedom v = a(b-1),ab(n-1)

At large values of F, reject H_0 and accept H_1 that there is a significant difference in the incorporation of a labelled substrate between individual cell lines within an experiment.

5.2.3.2 Analysis of Variance and Multiple Comparison Testing Between Patients and Control Cell Lines.

An analysis of variance was used to determine whether there were significant ($p<0.05$) differences between the population means of individual cell lines. Replicate data from three experiments for both patient and control cell lines were pooled and analysed with the aid of a statistical computing programme (Instat V2.05a, Graphpad Software, San Diego, USA). If the overall p value was <0.05, a multiple comparison between cell lines was performed using the Student-Newman-Keuls multiple-range test.

Interpretation of results:

$p>0.05$	ns	not significant
$p<0.05$	*	significant
$p<0.01$	**	very significant
$p<0.0001$	***	extremely significant

5.3 Results.

5.3.1 Time Course of Labelled Substrate Incorporation.

The incorporation of [^{14}C] hypoxanthine by a control lymphoblast cell line relative to either [^{3}H] adenine or [^{3}H] phenylalanine, over a time course of 150 min is shown in Figure 5.1. The rate of incorporation of all three labelled substrates was approximately linear between 90 min and 150 min and is shown in Table 5.4. The rate of [^{14}C] hypoxanthine uptake was not affected by the nature of the second [^{3}H] label.

The trend of the ratio with time of each substrate pair is a reflection of the rate of the incorporation of each label. The incorporation of [^{14}C] hypoxanthine and [^{3}H] phenylalanine showed a marked lag phase between 30 min and 90 min, during which the labelled substrates were incorporated into acid precipitable material at a slower rate than between 90 and 150 min. As a result, the ratio of [^{14}C] hypoxanthine to [^{3}H] phenylalanine showed an increasing trend with time (Figure 5.1c). The rate of incorporation of [^{14}C] hypoxanthine was similar to the rate of [^{3}H] adenine uptake which was relatively constant (Figure 5.1b). The slope of the regression line fitted to the ratio of [^{14}C] hypoxanthine to [^{3}H] adenine versus time was not significantly different from zero.

Table 5.4: The rate of incorporation of labelled substrate by cultured lymphoblasts.

LABEL PAIR	CONCENTRATION IN MEDIUM (nM)	RATE OF INCORPORATION* (dpm/min/10^6cells)
[^{14}C] Hypoxanthine	3750 (0.2 μCi/ml)	102.0
[^{3}H] Adenine	38.1 (0.8 μCi/ml)	115.4
[^{14}C] Hypoxanthine	3750 (0.2 μCi/ml)	105.9
[^{3}H] Phenylalanine	6.5 (0.8 μCi/ml)	60.2

* calculated from the slope of a regression line fitted to the data shown in Figure 5.1 for the interval 90 min to 150 min.

5.3.2 Analysis of Variance of Double Label Incorporation by Cultured Lymphoblasts.

The Standard Experiment.

Lymphoblasts at a density of $1x10^6$ cells/ml were incubated for 2 hours in 1 ml medium containing either, 0.2 μCi [^{14}C] hypoxanthine and 0.8 μCi [^{3}H] phenylalanine or 0.2 μCi [^{14}C] hypoxanthine and 0.8 μCi [^{3}H] adenine. The study included 6 control cell lines and the partially HPRT deficient cell lines L867 and L868. The results of the biochemical and molecular studies on L534 (Section 4) did not confirm an HPRT deficiency in this cell line. In an attempt to determine whether HPRT deficiency in this patient could be demonstrated *in vivo*, L534 was included in the double label study.

Three levels of experimental variation were analysed:

- EXPERIMENT: Between experiment variance (variation of individual control cell lines between experiments).
- INDIVIDUAL: Between individual variance (variation between control cell lines within the same experiment).
- REPLICATE: Between replicate variation (variation between triplicate values for an individual control cell line within an experiment).

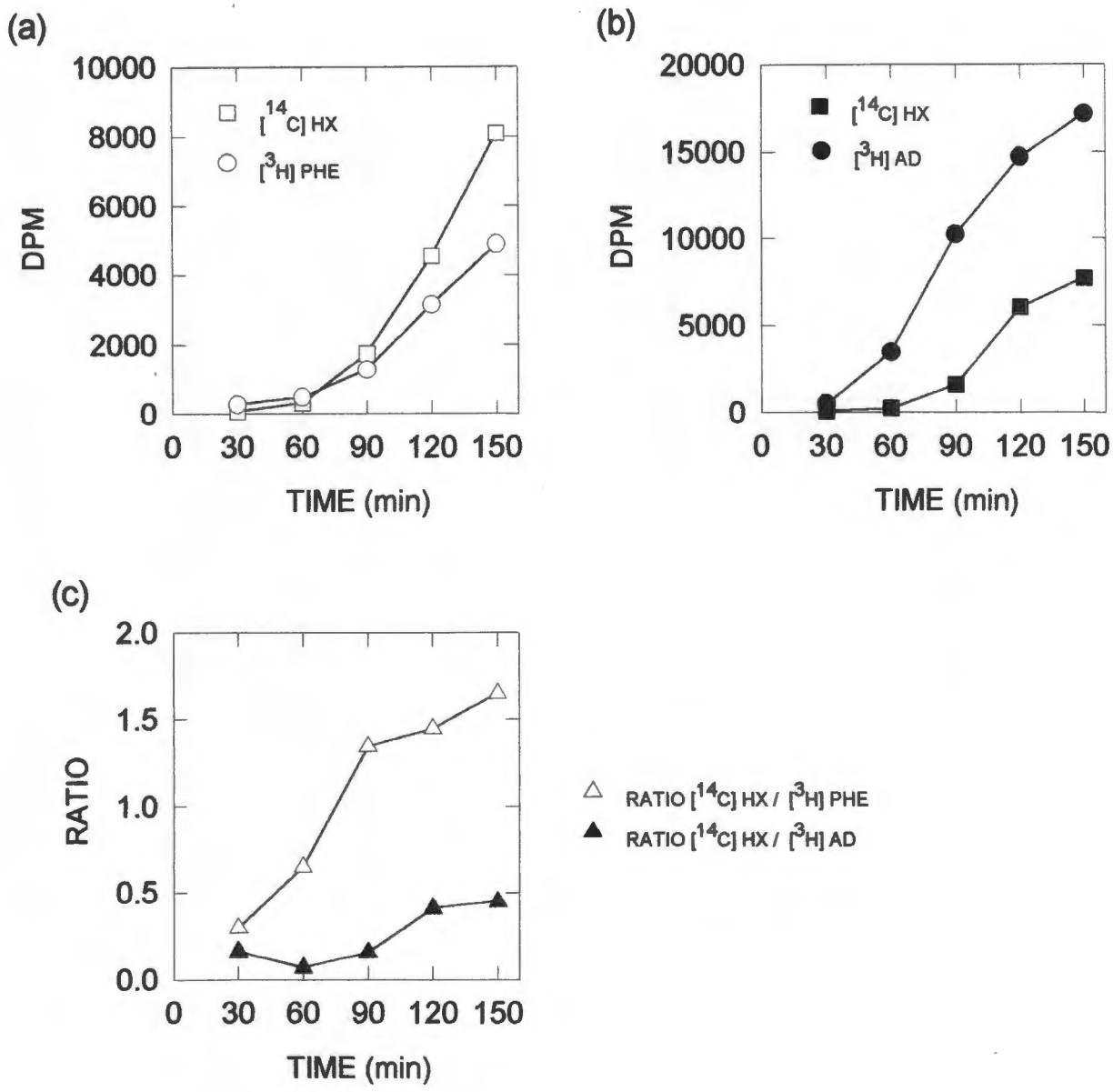

Figure 5.1: Double label time course of [^{14}C] hypoxanthine incorporation relative to the incorporation of either [^{3}H] phenylalanine or [^{3}H] adenine by a normal cultured lymphoblast cell line. (a) Time course of incorporation of [^{14}C] hypoxanthine and [^{3}H] phenylalanine. (b) Time course of incorporation of [^{14}C] hypoxanthine and [^{3}H] adenine. (c) Change in the ratio of [^{14}C] hypoxanthine relative to either [^{3}H] phenylalanine or [^{3}H] adenine over time. Values are the mean of triplicate determinations.

The results of the analysis of variance of three experiments on six control cell lines for each labelled substrate pair are shown in Tables 5.5 to 5.10, and summarised in Table 5.11.

Table 5.5: Analysis of variance of the ratio of [^{14}C] hypoxanthine to [^{3}H] phenylalanine incorporation by six control lymphoblast cell lines in three experiments.

SOURCE	SS	df	MS	% OF VARIANCE
Experiment	17.732	2	8.8860	72.9
Individual	4.636	15	0.3091	10.1
Replicate	3.988	36	0.1108	17.0
Total	26.356	53		100.0

SOURCE	F VARIANCE RATIO	df (v_1,v_2)	$F_{v1,v2}$ (1%)	LEVEL OF SIGNIFICANCE (p)
Experiment	2.87	2,15	6.36	ns
Individual	1.16	15,36	2.58*	ns

* Value between $F_{14,36}$ and $F_{16,36}$ estimated by linear interpolation.

Table 5.6: Analysis of variance of [^{14}C] hypoxanthine (with [^{3}H] phenylalanine as the second label) incorporation by six control lymphoblast cell lines in three experiments.

SOURCE	SS	df	MS	% OF VARIANCE
Experiment	2.666E+09	2	1.333E+09	51.5
Individual	2.126E+09	15	1.417E+08	30.9
Replicate	8.115E+08	36	2.254E+07	17.6
Total	5.604E+09	53		100.0

SOURCE	F VARIANCE RATIO	df (v_1,v_2)	$F_{v1,v2}$ (1%)	LEVEL OF SIGNIFICANCE (p)
Experiment	1.25	2,15	6.36	ns
Individual	184.87	15,36	2.58*	<0.001

* Value between $F_{14,36}$ and $F_{16,36}$ estimated by linear interpolation.

Table 5.7: Analysis of variance of [^{3}H] phenylalanine incorporation by six control lymphoblast cell lines in three experiments.

SOURCE	SS	df	MS	% OF VARIANCE
Experiment	7.238E+09	2	3.619E+09	34.4
Individual	1.192E+10	15	7.947E+08	54.3
Replicate	1.861E+09	36	5.169E+07	11.3
Total	2.102E+10	53		100.0

SOURCE	F VARIANCE RATIO	df (v_1,v_2)	$F_{v1,v2}$ (1%)	LEVEL OF SIGNIFICANCE (p)
Experiment	0.61	2,15	6.36	ns
Individual	6.41	15,36	2.58*	<0.001

* Value between $F_{14,36}$ and $F_{16,36}$ estimated by linear interpolation.

Table 5.8: Analysis of variance of the ratio of [^{14}C] hypoxanthine to [^{3}H] adenine incorporation by six control lymphoblast cell lines in three experiments.

SOURCE	SS	df	MS	% OF VARIANCE
Experiment	0.4137	2	0.2069	30.8
Individual	0.7793	15	0.0520	58.2
Replicate	0.1107	36	0.0031	11.0
Total	1.3037	53		100.0

SOURCE	F VARIANCE RATIO	df (v_1,v_2)	$F_{v1,v2}$ (1%)	LEVEL OF SIGNIFICANCE (p)
Experiment	0.53	2,15	6.36	ns
Individual	7.04	15,36	2.58*	<0.001

* Value between $F_{14,36}$ and $F_{16,36}$ estimated by linear interpolation.

Table 5.9: Analysis of variance of [^{14}C] hypoxanthine (with [^{3}H] adenine as the second label) incorporation by six control lymphoblast cell lines in three experiments.

SOURCE	SS	df	MS	% OF VARIANCE
Experiment	3.325E+08	2	1.663E+08	47.2
Individual	3.647E+08	15	2.431E+07	46.3
Replicate	3.897E+07	36	1.083E+06	6.5
Total	7.362E+08	53		100.0

SOURCE	F VARIANCE RATIO	df (v_1,v_2)	$F_{v1,v2}$ (1%)	LEVEL OF SIGNIFICANCE (p)
Experiment	0.91	2,15	6.36	ns
Individual	9.36	15,36	2.58*	<0.001

* Value between $F_{14,36}$ and $F_{16,36}$ estimated by linear interpolation.

Table 5.10: Analysis of variance of [^{3}H] adenine incorporation by six control lymphoblast cell lines in three experiments.

SOURCE	SS	df	MS	% OF VARIANCE
Experiment	4.836E+08	2	2.418E+08	36.7
Individual	5.564E+08	15	3.709E+07	28.1
Replicate	3.929E+08	36	1.091E+07	35.2
Total	1.433E+09	53		100.0

SOURCE	F VARIANCE RATIO	df (v_1,v_2)	$F_{v1,v2}$ (1%)	LEVEL OF SIGNIFICANCE (p)
Experiment	0.87	2,15	6.36	ns
Individual	1.42	15,36	2.58*	ns

* Value between $F_{14,36}$ and $F_{16,36}$ estimated by linear interpolation.

A summary of the components of variance within the double label experiments is shown in Table 5.11. For the ratio [^{14}C] hypoxanthine / [^{3}H] phenylalanine, variation of cell lines between experiments showed the greatest variance in the experimental system. This is in contrast to the label pair [^{14}C] hypoxanthine / [^{3}H] adenine, where variation between experiments is less than half the between experiment variance of the [^{14}C] hypoxanthine / [^{3}H] phenylalanine label pair. Variation between replicate determinations in both double label systems was low.

Table 5.11: Summary of the components of variance in six control cell lines in three double label experiments with either [^{14}C] hypoxanthine and [^{3}H] phenylalanine, or [^{14}C] hypoxanthine and [^{3}H] adenine as the labelled substrate pair.

	Labelled Substrate Pair			Labelled Substrate Pair		
% Component of variance	[^{14}C] Hx	[^{3}H] Phe	Ratio	[^{14}C] Hx	[^{3}H] Ad	Ratio
Experiment	51.5	34.4	72.9	47.2	36.7	30.8
Individual	30.9	54.3	10.1	46.3	28.1	58.2
Replicate	17.6	11.3	17.0	6.5	35.2	11.0

The significance of the variance of control cell lines between experiments and within an experiment are shown in Table 5.12. The variance of substrate incorporation by individual control cell lines and of the ratio between substrates was not significant between experiments. However, low replicate variance resulted in significant differences between cell lines, when cell lines are compared within an experiment.

Table 5.12: Summary of the significance of control cell line variance between three experiments and within an experiment with either [^{14}C] hypoxanthine and [^{3}H] phenylalanine, or [^{14}C] hypoxanthine and [^{3}H] adenine as the labelled substrate pair.

	Labelled Substrate Pair		Labelled Substrate Pair			
Variation Between:	[^{14}C] Hx	[^{3}H] Phe	Ratio	[^{14}C] Hx	[^{3}H] Ad	Ratio
Experiment	ns	ns	ns	ns	ns	ns
Individual	**	**	ns	**	ns	**

ns not significant, $p>0.05$
** significant at the 1% level

Significant variation between control cell lines within an experiment suggested that a pair-wise comparison between individual control cell lines and patient cell lines within a single experiment, would be unable to discriminate control from patient cell lines with a genuine HPRT deficiency.

Triplicate data for each patient and control cell line over three experiments were combined in an analysis of variance. The data is shown graphically in Figure 5.2 and Figure 5.3. A summary of the analysis of variance of combined patients and controls is compared to that of control cell lines alone and is shown in Table 5.13.

Table 5.13: Significance of the variation between experiment of six control cell lines excluding patients and six control cell lines including patients with either [^{14}C] hypoxanthine and [^{3}H] phenylalanine, or [^{14}C] hypoxanthine and [^{3}H] adenine as the labelled substrate pair.

	Labelled Substrate Pair			Labelled Substrate Pair		
Variation Between:	[^{14}C] Hx	[^{3}H] Phe	Ratio	[^{14}C] Hx	[^{3}H] Ad	Ratio
Controls	ns	ns	ns	ns	ns	ns
Controls + Patients	***	ns	*	**	**	***

ns not significant, $p>0.05$
* significant, $p<0.05$
** very significant, $p<0.01$
*** extremely significant, $p<0.0001$

Between experiment variance for control cell lines was not significant for either of the labelled substrate pairs. When patient cell lines were included in the analysis, significant variance between cell lines was detected.

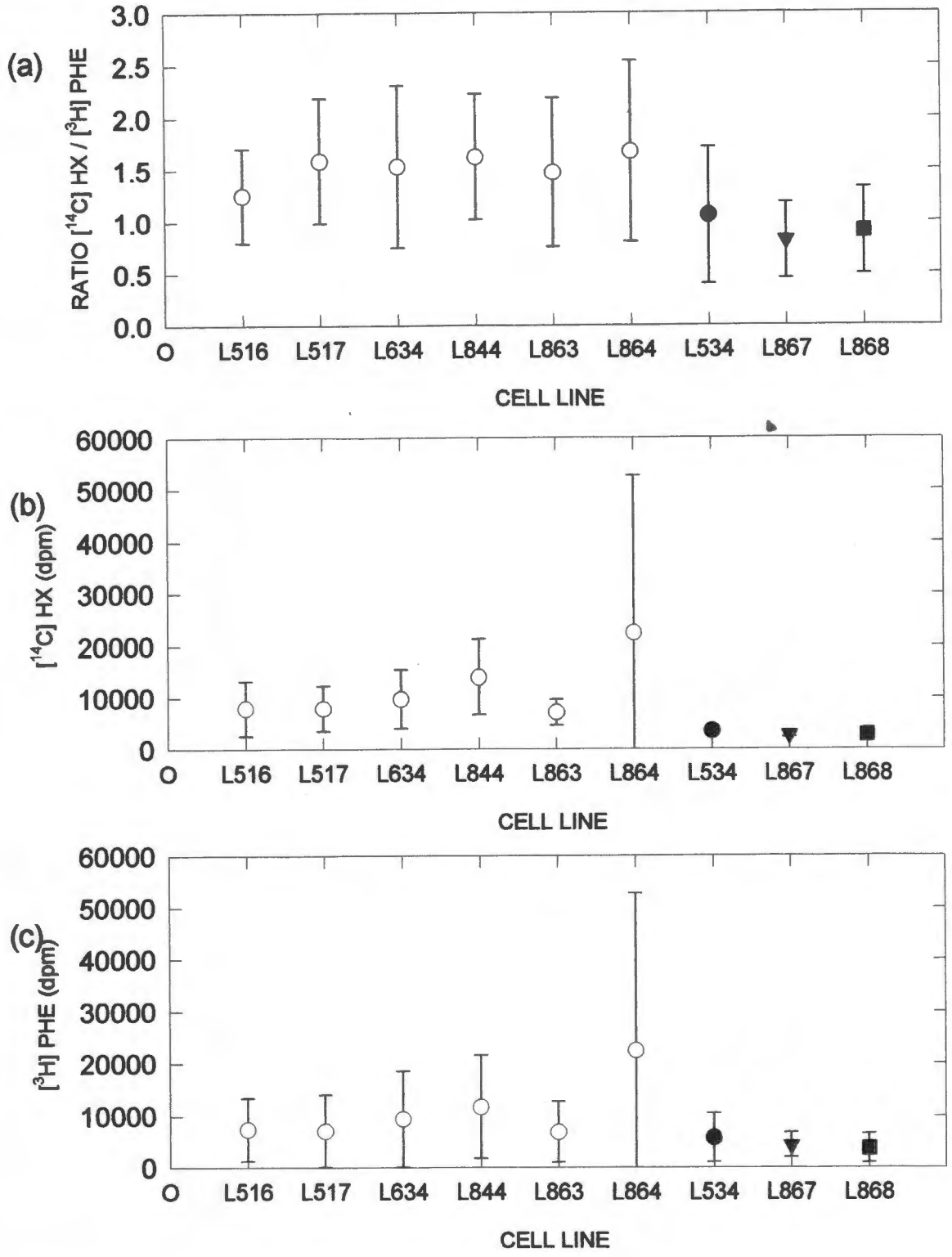

Figure 5.2: The incorporation of [^{14}C] hypoxanthine relative to [^{3}H] phenylalanine by control and patient cultured lymphoblast cell lines. Triplicate values for each cell line from 3 experiments were pooled and are shown as the mean +/-1SD. (a) Ratio of [^{14}C] hypoxanthine to [^{3}H] phenylalanine incorporation. (b) Incorporation of [^{14}C] hypoxanthine. (c) Incorporation of [^{3}H] phenylalanine.

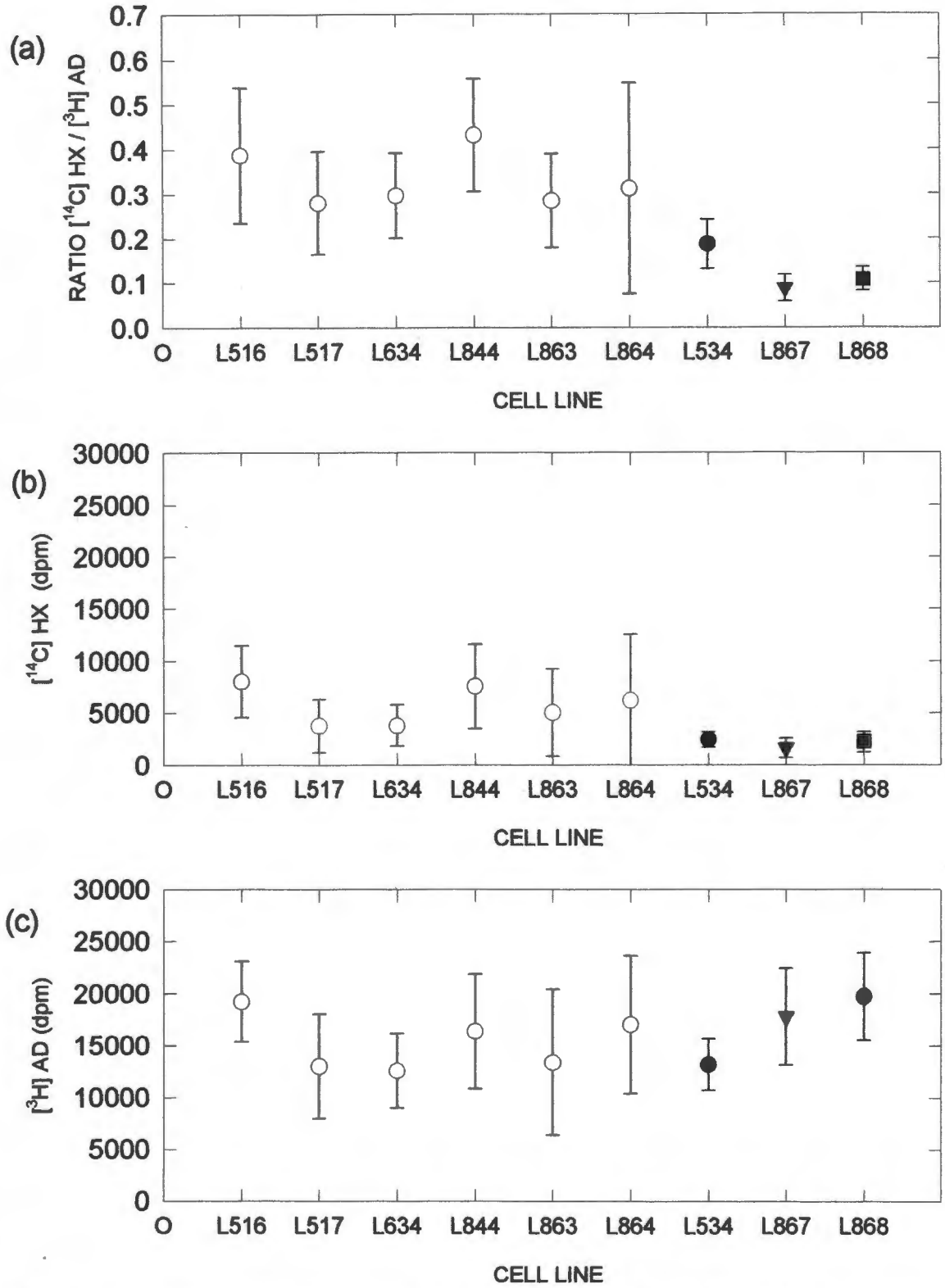

Figure 5.3: The incorporation of [^{14}C] hypoxanthine relative to [^{3}H] adenine by control and patient cultured lymphoblast cell lines. Triplicate values for each cell line from 3 experiments were pooled and are shown as the mean +/-1SD. (a) Ratio of [^{14}C] hypoxanthine to [^{3}H] adenine incorporation. (b) Incorporation of [^{14}C] hypoxanthine. (c) Incorporation of [^{3}H] adenine.

5.3.3 Multiple Pairwise Comparison Between Patient and Control Cell Lines Using the Student-Newman-Keuls Multiple-Range Test.

An analysis of variance determines whether there are differences among the population means of the cell lines being compared, but does not define which cell lines, if any, differ from the others. The Student-Newman-Keuls multiple-range test was used to compare cell lines if the p value was <0.05 as determined by the analysis of variance. The results are shown in Table 5.14.

Table 5.14: Student-Newman-Keuls multiple-range test: comparison between control and patient cell lines using replicate data pooled from three experiments.

LABEL PAIR [^{14}C] HYPOXANTHINE AND [^{3}H] PHENYLALANINE									
Cell Line	[^{14}C] HYPOXANTHINE								
	L516	L517	L634	L844	L863	L864$	L534	L867	L868
L534	ns	ns	ns	**	ns	***	-	ns	ns
L867	ns	ns	ns	*	ns	***	ns	-	ns
L868	ns	ns	ns	*	ns	***	ns	ns	-
[^{3}H] PHENYLALANINE									
No significant difference between patients and controls.									
RATIO									
No significant difference between patients and controls.									

LABEL PAIR [^{14}C] HYPOXANTHINE AND [^{3}H] ADENINE									
Cell Line	[^{14}C] HYPOXANTHINE								
	L516	L517	L634	L844	L863	L864	L534	L867	L868
L534	*	ns	ns	**	ns	ns	-	ns	*
L867	**	ns	**	**	ns	ns	ns	-	**
L868	**	ns	ns	**	ns	ns	*	**	-
[^{3}H] ADENINE									
No significant difference between patients and controls.									
Cell Line	RATIO								
	L516	L517	L634	L844	L863	L864	L534	L867	L868
L534	*	ns	ns	**	ns	**	-	ns	ns
L867	***	**	**	***	*	**	ns	-	ns
L868	***	*	**	***	*	**	ns	ns	-

ns not significant, p>0.05
* significant, p<0.05
** very significant, p<0.01
*** extremely significant p<0.0001
$ L864 was significantly higher than all control and patient cell lines.

The tritriated label entering the control pathway showed no significant differences between patient and control cell lines for both labelled substrate pairs. The incorporation of [^{14}C] hypoxanthine was not a reliable predictor of partial HPRT deficiency. The ratio [^{14}C] hypoxanthine / [^{3}H] phenylalanine failed to statistically distinguish the partial HPRT deficient cell lines from control cell lines. However, the ratio [^{14}C] hypoxanthine / [^{3}H] adenine was a powerful predictor of partial HPRT activity, with significant differences between the confirmed HPRT partially deficient cell lines L867 and L868 and all control cell lines. Of note is that L534 was not significantly different from the two partially HPRT deficient cell lines, L867 and L868.

5.4 Discussion.

5.4.1 The Incorporation of [^{14}C] Hypoxanthine as a Single Measure of HPRT Activity in Cultured Lymphoblasts.

The incorporation of [^{14}C] hypoxanthine by intact lymphoblasts as a single measure of HPRT activity was not able to accurately allocate a particular cell line to either the control or partially HPRT deficient groups. Similar results were found in cultured fibroblasts by Zoref et al (1978) who showed an overlap in the range of [^{14}C] hypoxanthine incorporation by control cell lines and cell lines partially deficient in HPRT.

5.4.2 The Ratio of [^{14}C] Hypoxanthine Relative to [^{3}H] Phenylalanine Incorporation as a Measure of HPRT Activity.

The use of [3H] phenylalanine as an independent metabolic control substrate is in line with the traditional design of double label experiments (Rozen et al 1977). It was surprising that the ratio of incorporation of [^{14}C] hypoxanthine relative to the control substrate [^{3}H] phenylalanine, was unable to discriminate between lymphoblast cell lines partially deficient in HPRT activity and control cell lines.

Factors which may have contributed to this unexpected lack of sensitivity in detecting partial HPRT deficiency are discussed in Section 5.4.4. below.

5.4.3 The Ratio of [^{14}C] Hypoxanthine to [^{3}H] Adenine Incorporation as a Measure of HPRT Activity.

The use of [^{3}H] adenine as a control substrate differs from the traditional double label assay of a metabolic pathway (Rozen et al, 1977). The incorporation of [^{14}C] hypoxanthine and [^{3}H] adenine are not metabolically independent, since both salvage reactions are catalysed by phosphoribosyltransferases and share a substrate in PRPP. Ultimately, both [^{14}C] hypoxanthine and [^{3}H] adenine are incorporated into the same acid precipitable product, nucleic acid.

The incorporation of [^{14}C] hypoxanthine relative to [^{3}H] adenine proved to be an accurate measure of partial HPRT activity and was able to correctly identify the two cell lines L867 and L868 as being partially HPRT deficient. The interpretation of the double label results obtained for the cell line L534 remains problematical. The ratio for L534 showed no significant differences when compared to L867 and L868, which would be consistent with a diagnosis of partial HPRT deficiency in this cell line. However, the ratio for L534 was significantly lower than only three of the six control cell lines, which suggests that L534

may represent the lower extreme of normal physiological variation in purine substrate metabolism. The absence of a mutation within the coding region of HPRT cDNA amplified from L534, the normal activity of HPRT in lymphoblast lysates and the ambiguous results of the double label experiments suggests that any defect in L534 is not the result of an abnormal HPRT enzyme.

The ratio of [^{14}C] hypoxanthine to [^{3}H] adenine incorporation may be a better measure of functional HPRT activity (and phenotype) than the measurement of HPRT activity in lymphoblast lysates. The mean of the ratio of [^{14}C] hypoxanthine to [^{3}H] adenine incorporation over three experiments for L867 and L868 were 27% and 33% respectively of the control mean, while the ratio for L534 was 58% of the control mean. Although these values do not give an indication of the population variance (the ratio mean for L534 falls within the 1 SD control range), they are nevertheless an indication that functional residual HPRT activity in intact cultured lymphoblasts of L867 and L868 was markedly higher than the less than 2% residual activity measured in lymphoblast lysates. These results are equivalent to studies by Fairbanks et al (1987) who reported that intact erythrocyte assays of HPRT are a better indicator of residual HPRT activity and hence phenotype, than HPRT assays on haemolysates. However, it would appear that cell free enzyme assays are still a better method of confirming a genuine HPRT enzyme deficiency.

5.4.4 Sources of Variation.

Mycoplasma infection may lead to increased purine incorporation by infected cell lines (Harley et al, 1970) and could result in an overestimation of residual HPRT activity (Willers et al, 1984). Extreme care was taken to monitor cell lines used in these experiments for the presence of *Mycoplasma* contamination and this is an unlikely source of either variation or increased labelled purine incorporation in the experimental system.

Increased [^{14}C] hypoxanthine incorporation due to unrecognised *Mycoplasma* infection in control cell lines, could give rise to a misdiagnosis of partial HPRT deficiency when compared to uninfected cell lines. Any cell lines used in whole cell assays for the diagnosis of an inborn error of metabolism should be rigorously screened for the presence of *Mycoplasma*. Regular screening of cultured cell lines will reduce the risk of *Mycoplasma* metabolic processes interfering with the pathway under investigation and the possibility of a misdiagnosis.

Baumgarten and Harley (1995) showed low replicate variance in the incorporation of [^{14}C] hypoxanthine and [^{3}H] adenine by cultured fibroblasts. Similarly low replicate variance was found in this study in the incorporation of the two pairs of labelled substrates by cultured lymphoblasts. A consequence of low replicate variance in both double label systems was that within a single experiment, a pair-wise comparison between control cell lines and between control and patient cell lines, resulted in significant differences between nearly all the cell lines. A single experiment was not sufficient to reliably predict whether a cell line was normal or partially deficient in HPRT. It was necessary to pool the results of the three experiments to obtain a statistically significant measure of the differences between patient and control cell lines.

The contribution of the three levels of variation to the variance of the ratio of [^{14}C] hypoxanthine to [^{3}H] adenine in lymphoblasts was strikingly similar to that found by Baumgarten and Harley (1995) in fibroblasts. The largest component of variance in lymphoblasts was between individual cell lines within the same experiment, which was double the variance of cell lines between experiments. The smallest component of variance was between replicates.

The pattern of variation was different for the [^{14}C] hypoxanthine / [^{3}H] phenylalanine label pair. This ratio showed the largest between experiment variance, double the between experiment variance of the [^{14}C] hypoxanthine / [^{3}H] adenine substrate pair. Whilst low replicate variance led to unacceptably high sensitivity in detecting differences between cell

lines, the large between experiment variance in the ratio [^{14}C] hypoxanthine / [^{3}H] phenylalanine resulted in a complete loss of discriminatory power and no significant differences between patient and control cell lines could be seen against the background of between experiment variation.

A possible explanation for the large variability between experiments of the [^{14}C] hypoxanthine / [^{3}H] phenylalanine ratio lies in the observation that the rate of incorporation of [^{14}C] hypoxanthine and [^{3}H] phenylalanine varied over time, with a non-linear lag phase apparent between 30 and 90 min. As a result, the ratio of [^{14}C] hypoxanthine to [^{3}H] phenylalanine showed an increasing trend over time. Any difference between experiments which affects the duration of the lag phase and/or alters the rate of incorporation of one of the labelled substrates, could result in a difference in the ratio and contribute to between experiment variation.

Growth stimulation of lymphoblasts has been reported to rapidly alter HPRT mRNA levels and HPRT enzyme activity in human lymphocytes (Steen et al, 1991). In an effort to reduce the possibility of variation in the metabolism of the labelled substrates due to growth stimulation as a result of medium changes, care was taken to feed cultures twice weekly and maintain lymphoblast cultures at approximately the same cell density. In addition, experiments were timed so as to always occur after a medium change.

[^{14}C] Hypoxanthine and [^{3}H] adenine are incorporated at approximately the same rate into the same acid precipitable product, nucleic acid. Once the two substrate salvage pathways converge at AMP, they share the same pathways and metabolic fates. This may account for the observations that the ratio of incorporation of these two substrates showed no significant trend over time and that between experiment variance was less than half that of the [^{14}C] hypoxanthine / [^{3}H] phenylalanine label pair.

At the between experiment level, the ratio of the labelled purine substrates proved to be a powerful and accurate predictor of partial HPRT deficiency. A pair-wise comparison

between cell lines showed no significant differences between any of the six control cell lines, but significant differences between all six control lines and the two confirmed HPRT variant cell lines, L867 and L868. An increase in adenine incorporation predicted on the basis of increased PRPP pools in partial HPRT activity was, however, not detectable above the background of experimental variation.

5.5 Conclusion.

The double label approach to the diagnosis of partial HPRT deficiency was successful in identifying two HPRT variant cell lines, but the method should be used and interpreted with caution. On the basis of the results described above, a candidate HPRT deficient cell line should be significantly lower than all control cell lines in at least three independent experiments. All defects should be confirmed at the genetic level.

Perhaps the greatest value of the [^{14}C] hypoxanthine / [^{3}H] adenine double label approach is to provide an estimate of functional residual HPRT activity and a more precise prediction of phenotype.

6. BIOCHEMICAL INVESTIGATIONS IN PATIENTS WITH PRIMARY IDIOPATHIC GOUT DUE TO URATE OVERPRODUCTION.

6.1 Introduction.

Gout has been recognised as a clinical entity for more than two thousand years and is characterised by recurrent attacks of acute inflammation in one or more joints (the clinical presentation of gout is comprehensively reviewed by German and Holmes, 1986; Pallela and Fox, 1989; Roubenoff, 1990; Cameron et al, 1993). Crystals of monosodium urate monohydrate are demonstrable in leukocytes of synovial fluid during acute attacks and may accumulate in dense deposits (tophi) in or around the joints of extremities. Only a minority of patients with hyperuricemia may develop gout and then only after 20 to 30 years of sustained hyperuricemia (Pallela and Fox, 1989).

Gout is the most common inflammatory joint disease in men over the age of 40, with estimates of incidence for males ranging from 5/1000 to 86/1000 (Roubenoff, 1990). The incidence of gout in urban Caucasian South Africans has been estimated at 13/1000 for males and 3/1000 for women (Beighton et al, 1977).

6.1.1 Classification of Hyperuricemia.

Hyperuricemia and gout have traditionally been classified into two major groups on the basis of either, increased metabolic uric acid production (urate overproduction) or, decreased renal uric acid excretion (urate underexcretion). A further distinction between primary and secondary gout is made on the basis of whether the principal metabolic abnormality is an elevation of serum urate due to a genetic defect, or whether the

increased serum urate can be ascribed as secondary to a defined pathological entity or the effects of a pharmacological agent.

6.1.1.1 Hyperuricemia due to Urate Overproduction.

Hyperuricemia due to urate overproduction has been reported to occur with a frequency of about 10% in the gouty population (Palella and Fox, 1989). Potential causes of primary overproducing gout have been reviewed by Pallela and Fox (1989) and Henderson (1993) and are discussed below.

6.1.1.2 Increased Purine Breakdown.

In humans, uric acid synthesis occurs primarily in the liver and to a lesser extent in the intestinal mucosa (Palella and Fox, 1989). A possibility that can not be excluded is that decreased inhibition of hepatic AMP deaminase, the rate limiting step of purine catabolism in the liver, could result in an increased rate of purine breakdown and urate overproduction.

Any condition which leads to decreased ATP synthesis such as tissue hypoxia, ischemia and hypophosphatemia will lead to increased rates of purine degradation and ultimately, increased uric acid production.

6.1.1.3 L-Glutamine in Primary Hyperuricemia and Gout.

Together with PRPP, L-glutamine concentration is potentially rate limiting for purine *de novo* synthesis (Palella and Fox, 1989). At present, no specific defect in either glutamine or glutamate metabolism has been implicated in the pathogenesis of primary overproducing hyperuricemia.

6.1.1.4 Decreased Reutilisation of Hypoxanthine.

Decreased salvage or reutilisation of hypoxanthine could act in concert with increased PRPP levels to lead to purine overproduction by a mechanism similar to that which causes hyperuricemia in HPRT deficiency (Palella and Fox, 1989). .

6.1.1.5 Accelerated Rates of Purine Biosynthesis.

PRPP occupies a central role in purine metabolism (see section 1). The link between increased PRPP levels due to PRPP synthetase overactivity or HPRT deficiency and hyperuricemia have been described in sections 1 and 3. Briefly, increased PRPP concentrations in these two enzymopathies activates amidophosphoribosyltransferase, leading to an increased flux through the purine *de novo* synthetic pathway and to increased purine production. As PRPP levels are usually below the K_m for amidophosphoribosyltransferase, the increase in flux through *de novo* purine synthesis is in direct proportion to the increase in PRPP levels.

PRPP metabolism has been implicated in the pathogenesis of idiopathic primary overproducing gout. Increased rates of PRPP turnover in patients with idiopathic primary overproducing gout have been reported *in vivo* (see references in Palella and Fox, 1989), while increased levels of PRPP have been reported in cultured fibroblasts (Becker, 1976).

Measurements of PRPP levels in erythrocytes of gouty overproducers have produced contradictory results. No perturbation in erythrocyte PRPP levels of primary gouty overproducers were found in studies by Fox and Kelley (1971) and Becker et al (1973). These results however, are in conflict with a later study on patients with primary overproducing gout (Becker, 1976), which showed some correlation between increased levels of PRPP in fibroblasts and increased erythrocyte PRPP levels. In the latter study, four out of six patients with overproducing gout and no apparent defect in either HPRT or PRPP synthetase, showed increased levels of PRPP in both fibroblasts and erythrocytes.

There is thus some evidence to suggest that disturbances in PRPP metabolism are implicated in the pathogenesis of primary overproducing idiopathic hyperuricemia and that these disturbances may be detected in erythrocytes.

6.1.2 The Use of Intact Erythrocytes in the Detection of Abnormalities in PRPP Metabolism in Patients with Overproducing Gout.

The intact erythrocyte represents a simple model for the study of the dynamics of PRPP metabolism in primary overproducing gout. Our laboratory has developed a sensitive assay to measure rates of PRPP accumulation in intact erythrocytes. The assay is based on the erythrocyte oxypurine cycle described by Berman et al (1988).

In 1967 and 1969, Hershko et al demonstrated that rabbit and human erythrocytes incubated in a high phosphate medium accumulated PRPP. Berman et al (1988) defined the precise conditions under which PRPP accumulates in intact erythrocytes (Figure 6.1). Briefly, incubation of intact erythrocytes under conditions of pathophysiologically low pH (pH 7.0) and a high concentration of external inorganic phosphate (10 mM) leads to a rise in intracellular Pi. The increase in intracellular Pi at low pH is largely due to the fall in steady state 2,3-bisphosphoglycerate (2,3-DPG) levels induced by acidification.

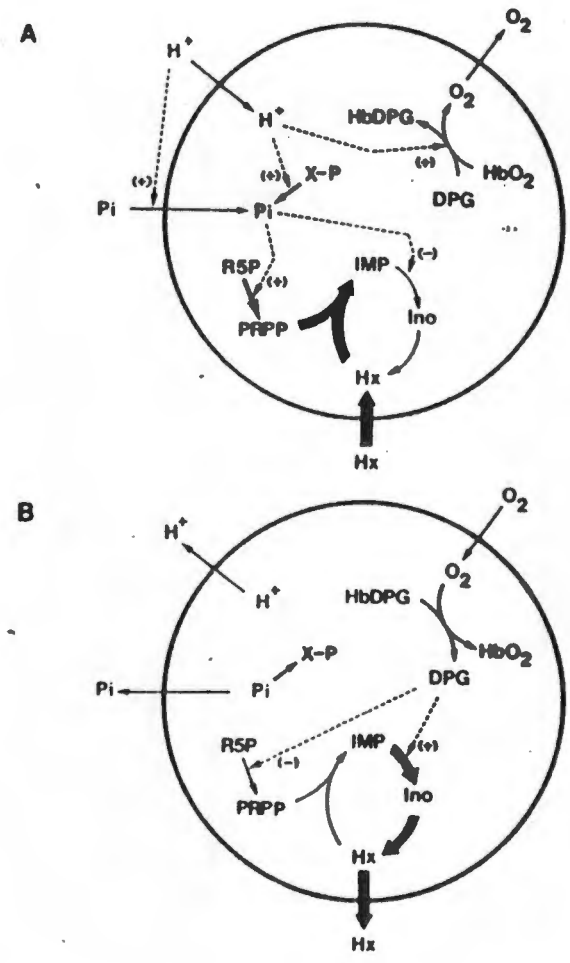

Figure 6.1: The erythrocyte oxypurine cycle. (a) conditions of acid pH, low Po_2, and high external Pi concentration. (b) conditions of neutral or alkaline pH, high Po_2, and low external Pi concentration. DPG, 2,3-bisphosphoglycerate; Hb, hemoglobin; Hx, hypoxanthine: R5P, ribose-5-phosphate; X-P, phosphorylated glycolytic intermediates including 2,3 DPG. Reproduced from Berman et al (1988).

The high level of intracellular Pi inhibits the activity of 5'-nucleotidase and stimulates PRPP synthetase activity. In the absence of any of the phosphoribosyltransferase substrates, PRPP will accumulate. When an excess of [^{14}C] labelled hypoxanthine is added to the medium, hypoxanthine enters the erythrocyte and is rapidly salvaged in a reaction catalysed by endogenous HPRT to form [^{14}C] IMP. Erythrocytes lack adenylosuccinate synthetase, an enzyme needed in the convertion of

IMP to AMP. If conditions of extracellular low pH and high phosphate are maintained, the salvaged [^{14}C] hypoxanthine will remain trapped within the erythrocyte as [^{14}C] IMP. The amount of [^{14}C] IMP formed from [^{14}C] hypoxanthine is related in a 1:1 stoichiometry to the concentration of PRPP which had previously accumulated in the intact erythrocyte.

A preliminary study in our laboratory (P. Cole, 1988) used an assay based on these principles to measure the rate of accumulation of PRPP in the erythrocytes of patients with gout. These provisional results suggested that in 3 patients with overproducing gout, PRPP accumulated at an increased rate.

The aim of the present study was twofold. Firstly, to determine whether the parameters of low pH and high phosphate which promote PRPP accumulation in erythrocytes *in vitro* promote PRPP accumulation in erythrocytes *in vivo*. Patients with physiologically high serum phosphate levels and low blood pH represent an *in vivo* model of the assay system and are predicted to have intrinsically higher levels of PRPP in their erythrocytes. Patients in chronic renal failure fulfil the criteria of low blood pH and high phosphate and were chosen as a group likely to have increased erythrocyte PRPP levels *in vivo*. Secondly, the methodology of the pilot study was refined and the patients noted in that study to have increased rates of PRPP accumulation in erythrocytes, were re-evaluated. The study was broadened to include a larger control group and more patients with gout were included.

6.2 Materials and Methods.

6.2.1 Patient Groups.

All patients and controls were adult males. Informed consent from each patient was obtained before entry into the study. Four groups of patients were selected: normal controls, gouty underexcretors, possible gouty overproducers and patients with chronic renal failure.

Individuals were selected as normal controls on the basis of no clinical or family history of gout and a normal serum urate. Patients with gout were classified as gouty underexcretors on the basis of clinical gout, documented hyperuricemia and a decreased fractional excretion of urate (FE_{ur}) compared to the normal control group (Calabrese et al, 1990). Patients with clinical gout, hyperuricemia and a normal FE_{ur} were classified as being likely to have gout due to urate overproduction. The calculation of the FE_{ur} is shown below:

$$FE_{ur} = \frac{\text{U-urate x P-creatinine}}{\text{P-urate x U-creatinine}} \times 100$$

Where U-urate is urinary urate (mmol/l), P-urate is plasma urate (mmol/l), P-creatinine is plasma creatinine (mmol/l) and U-creatinine is urinary creatinine (mmol/l).

Patients with chronic renal failure were on regular dialysis at the Dialysis Unit, Groote Schuur Hospital, Cape Town, South Africa and had no prior history of hyperuricemia or clinical gout. Plasma creatinine in these patients ranged from 823 µmol/l to 1413 µmol/l (mean 1093 µmol/l). All assays were performed on blood drawn before the start of a dialysis session.

6.2.2 Methods

6.2.2.1 Determination of Plasma and Urinary Uric Acid and Creatinine.

Plasma and urinary uric acid were determined by an automated uricase method. The pH of urine specimens was adjusted to pH 8 before levels of urate were estimated. Plasma and urinary creatinine were measured by an automated method based on the Jaffe reaction. Plasma inorganic phosphate was measured by the acid-molybdate method of Fiske and Subbarow. Whole blood pH was determined on a Radiometer blood gas and pH analyser.

6.2.2.2 Assay of the Rate of PRPP Accumulation in Intact Erythrocytes.

Heparinised blood (10 ml) was centrifuged at 3000g for 10 min, the buffy coat and plasma were removed and the erythrocytes washed twice in cold normal saline. The packed erythrocytes were resuspended in ice cold incubation buffer (10 mM NaH_2PO_4, 10 mM glucose, 130 mM NaCl, 50 mM Hepes, pH to 7.0 with NaOH) to a haematocrit of approximately 30%. Duplicate tubes were incubated at 37°C. At time zero, 1 hr and 2 hr, 300 µl of the suspension was transferred to a prewarmed microfuge tube at 37°C containing 100 µl [^{14}C] hypoxanthine at a specific activity of 6 to 24 dpm/pmol and incubated for a further 5 min. The final concentration of [^{14}C] hypoxanthine in the assay was 200 µM. The reaction was stopped by the addition of 400 µl ice cold 5% TCA. The precipitated protein was removed by centrifugation (5 min at 12000g). The supernatant was transferred to a clean microfuge tube and neutralised by repeated extractions with water saturated ether.

The product of the reaction, [^{14}C] IMP, was separated from unincorporated [^{14}C] hypoxanthine by reverse phase HPLC (System Gold, Beckman Instruments, Fullerton, California, USA). 100 µl of the deproteinised and neutralised supernatant was loaded onto a Beckman Ultrasphere ODS 5 µm 25 cm reverse phase column. The column

was eluted with a buffer containing 1 mM $KHPO_4$ pH 5.2 in 5% MeOH at a flow rate of 1.2 ml/min. Under these isocratic conditions, IMP typically eluted at 3.2 min, while hypoxanthine eluted at 5.6 min. In initial experiments, the column effluent corresponding to the IMP peak were collected in 30 sec fractions directly into scintillation vials, 10 ml of Hionic-Fluor scintillation fluid (Packard Instrument Company, Meriden, Connecticut, USA) was added and radioactivity determined by liquid scintillation counting using an open window. Counts per minute were converted to dpm using appropriate factors to correct for quenching by the eluting buffer and the efficiency of the counter. In later experiments, a Radiomatic Flo-One Beta Series A-100 inline radiochemical detector (Radiomatic, Tampa, Florida, USA) equipped with a 2.5 ml flow cell was used to quantify radioactivity eluted from the column. Scintillant (Flo-Scint IV, Radiomatic, Tampa, Florida, USA) was used at a flow rate four times that of the HPLC buffer. The efficiency of the radiochemical detector was determined by adding a known amount of [^{14}C] label to the scintillant as a standard and monitoring cpm during an HPLC run. This factor was used to convert [^{14}C] IMP cpm to dpm. The results obtained on duplicate specimen using the two different radiochemical detection methods were identical.

The conversion of [^{14}C] hypoxanthine to [^{14}C] IMP consumes a single molecule of PRPP. The rate of PRPP formation in intact erythrocytes was calculated as the difference between the 1 and 2 hr PRPP values and expressed as pmol/hr/10^6 red blood cells (RBC).

Data was analysed using a statistical computing package, Instat V2.05a (Graphpad Software, San Diego, USA).

6.3 Results.

6.3.1 Development of a Standard Method for the Measurement of the Rate of PRPP Accumulation in Intact Erythrocytes.

The influence of extracellular pH and inorganic phosphate on the conversion of [^{14}C] hypoxanthine to [^{14}C] IMP by intact erythrocytes (an indirect measure of intracellular PRPP levels) has been documented by Berman et al (1988). On the basis of this data, a pathophysiologically low pH of 7.0 and a nonphysiologically high concentration of inorganic phosphate (10 mM) were chosen so as to maximise PRPP formation in intact red blood cells.

The following variables were identified as potentially having an effect on the experimental system:

i) The concentration of the substrate [^{14}C] hypoxanthine.

ii) The linearity of PRPP accumulation over time.

iii) The effect of specimen age on PRPP accumulation.

i) The concentration of the substrate [^{14}C] hypoxanthine.

The optimal concentration of the added [^{14}C] hypoxanthine was determined by incubating red blood cells for 1 and 2 hours at pH 7.0 with 10 mM Pi in order to prime the erythrocytes with PRPP. [^{14}C] Hypoxanthine was then added to the incubation medium to give a final concentration of between 50 and 250 μM.

The amount of [^{14}C] hypoxanthine converted to [^{14}C] IMP was maximal at hypoxanthine concentrations above 50 μM (Figure 6.2a(i)). However, after 2 hours PRPP priming followed by incubation with 50 μM [^{14}C] hypoxanthine, more than 60% of the [^{14}C]

hypoxanthine had been converted to [^{14}C] IMP (Figure 6.2a(ii)). This suggested that in patients with high erythrocyte PRPP levels, [^{14}C] hypoxanthine could become limiting, which could result in an underestimation of the rate of PRPP accumulation. At a concentration of 100 μM [^{14}C] hypoxanthine, approximately 30% of the label was converted to [^{14}C] IMP in two hour primed erythrocytes. Labelled hypoxanthine at this concentration was used throughout this study.

ii) Linearity of PRPP Accumulation Over Time.

Erythrocytes were primed at low pH and high phosphate for up to 5 hours and the amount of PRPP determined. After a short initial lag phase, the accumulation of PRPP was effectively linear between 1 hour and 3 hours (Figure 6.2b).

The difference between the 1 hr and the 2 hr PRPP levels (within the linear range of the assay) was used as an estimate of the rate of PRPP accumulation and the results expressed as pmol PRPP formed per hour per 10^6 erythrocytes.

iii) The Effect of Specimen Age on PRPP Accumulation.

The effect of specimen age on the rate of PRPP accumulation was determined by leaving whole blood specimens at room temperature for up to 3 hr. Levels of PRPP accumulated by erythrocytes prepared and assayed 3 hr after venipuncture, were approximately 50% less than the level of PRPP accumulated by erythrocytes prepared and assayed immediately after venipuncture (Figure 6.2c).

Based on these results, the time between venipuncture and the start of the assay was standardised. All specimen were prepared and assayed within 1 hour of blood being drawn from the patient.

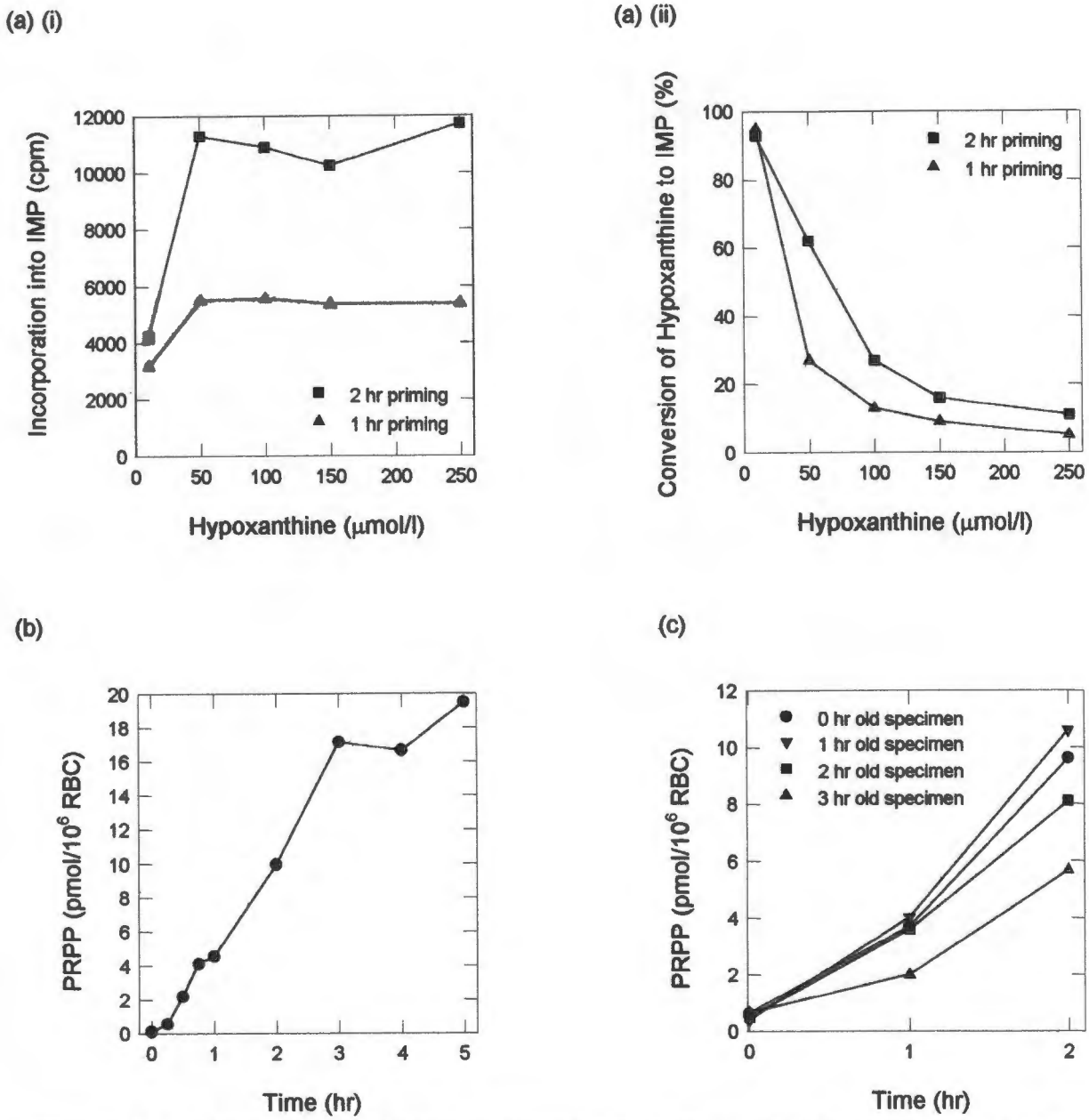

Figure 6.2: Optimisation of the erythrocyte PRPP accumulation assay. (a)(i) The effect of [^{14}C] hypoxanthine concentration on [^{14}C] IMP formation after either 1 hr or 2 hr PRPP priming . (ii) Percent conversion of [^{14}C] hypoxanthine to [^{14}C] IMP after either 1 hr or 2 hr PRPP priming. (b) The linearity of PRPP accumulation over time. (c) The effect of specimen age on PRPP accumulation.

6.3.2 PRPP Accumulation in Patients with Chronic Renal Failure.

The elevated levels of plasma phosphate and mild acidosis associated with chronic renal failure, represent a model to test the validity of the hypothesis that PRPP could accumulate in erythrocytes *in vivo* under conditions of physiologically high phosphate and low pH. The initial PRPP level measured in erythrocytes at time 0 hr is an estimate of the *in vivo* PRPP levels.

The initial erythrocyte PRPP concentration was measured and correlated with plasma phosphate concentration or blood pH (Figure 6.3). Erythrocyte PRPP levels showed an increasing trend ($r=0.81$) with increasing plasma phosphate. Only two of the patients had plasma phosphate levels within the reference range of 0.96 to 1.45 mM, with the highest level of plasma phosphate recorded at 2.90 mM.

The relationship between blood pH and erythrocyte PRPP levels showed a similar but negative correlation ($r=-0.85$). Higher erythrocyte PRPP levels occurred in patients with the lowest blood pH. However, blood pH values of only three patients fell outside the reference range of pH 7.35 to 7.45.

The positive relationship between high initial erythrocyte PRPP levels and high plasma phosphate and the negative correlation of initial PRPP levels with blood pH, thus appear to support the prediction that PRPP will accumulate *in vivo* under physiological conditions of low pH and high phosphate. However, as a group, the PRPP content of erythrocytes of the chronic renal failure patients at time zero were not significantly different from controls (two sided t-test). The PRPP accumulation rate in erythrocytes of the eight patients in chronic renal failure are shown in Figure 6.4 and were not significantly different from the control group (two sided t-test).

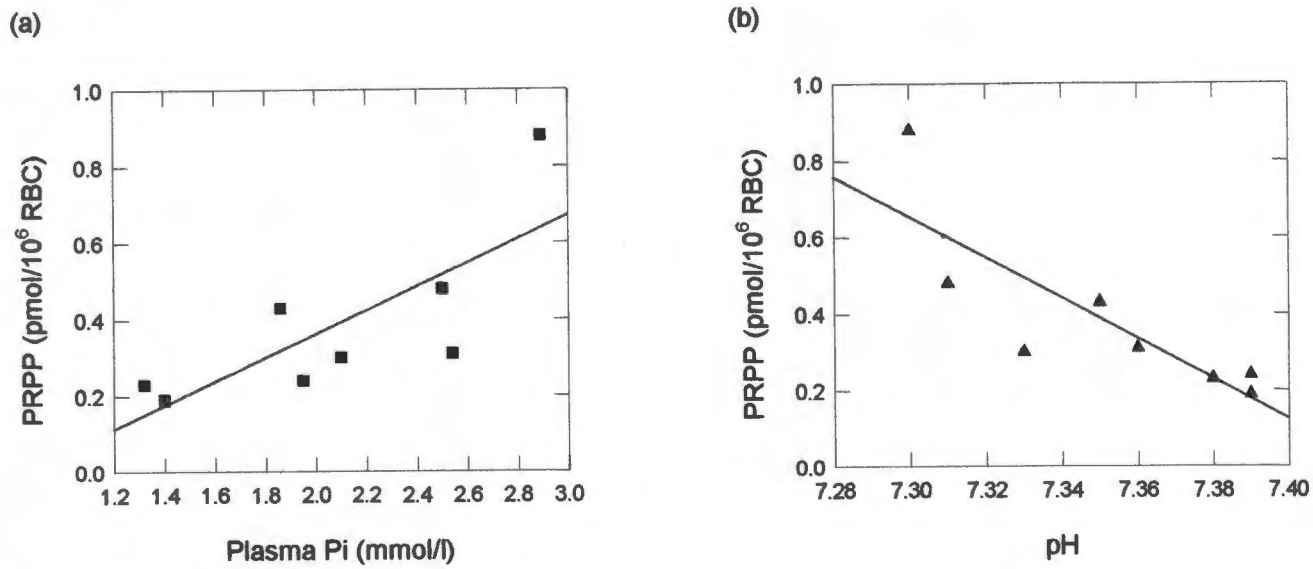

Figure 6.3: Correlation of initial erythrocyte PRPP levels with plasma Pi or whole blood pH in eight patients with chronic renal failure. (a) Initial levels of erythrocyte PRPP were positively correlated with plasma inorganic phosphate. (b) Erythrocyte PRPP levels were negatively correlated with whole blood pH.

6.3.3. PRPP Accumulation in Erythrocytes of Patients with Gout.

The mean plasma urate concentration and the FE_{ur} of the control and gouty underexcretor groups are shown in Table 6.1. The concentration of PRPP in erythrocytes at time zero and the rate of accumulation of PRPP for each group are shown in the lower part of Table 6.1. The rate of PRPP accumulation of patients in each group are shown graphically in Figure 6.4.

Table 6.1: A comparison between plasma urate (P-urate), fractional urate excretion (FE_{ur}), initial erythrocyte PRPP concentration and the rate of erythrocyte PRPP accumulation of controls and patients with gout due to urate underexcretion. Values are the mean+/-1SD, with the range shown in parenthesis. Patients on treatment for gout were excluded from the mean and range.

	Normal controls	Underexcretors
P-Urate (mmol/l)	0.28+/-0.02 (0.19-0.36) n=22	*0.45+/-0.10 (0.32-0.62) n=13
FE_{ur} (%)	8.33+/-3.35 (4.20 to 13.50) n=10	**4.06+/-1.46 (2.00 to 5.60) n=8
Initial PRPP (pmol/10^6 RBC)	0.58+/-0.50 (0.05-1.65) n=22	0.63+/-0.43 (0.05-1.30) n=13
PRPP Rate (pmol/hr/10^6 RBC)	5.48+/-1.15 (3.40 to 8.30) n=22	***4.34+/-1.71 (2.00 to 7.67) n=13

n: number of individuals.

* Serum urate values of the urate underexcretion group was significantly different (higher) than the control group (two sided t-test, $p<0.001$).

** FE_{ur} of underexcretors was significantly different (lower) than the normal control group (two sided t-test, $p<0.01$).

*** The rate of PRPP accumulation in the urate underexcretion group was significantly different (lower) than the control group (two sided t-test, $p<0.05$).

There was no significant difference in the mean of the initial PRPP level in erythrocytes of the control and underexcretor groups. There was however, a significant difference in the rate of PRPP accumulation between the two groups, with the underexcretor group being significantly lower than the control group ($p<0.05$, two sided t-test).

The slopes of linear regression lines fitted to the patient data for FE_{ur} versus initial concentration of PRPP in erythrocytes, were not significantly different from zero for either the control or underexcretor group. This suggests that there is no correlation between the

fractional excretion of urate and erythrocyte PRPP levels in either group. Similar results were obtained when FE_{ur} was plotted against the erythrocyte PRPP accumulation rate, with no correlation found between measures of urate excretion and the rate of PRPP accumulation in either of the two groups.

Four patients were provisionally identified as gouty overproducers and are listed in Table 6.2. One patient, KAT, was identified in the present study, while three other patients were originally identified in the pilot study (Cole, 1988) and were recalled for the present study.

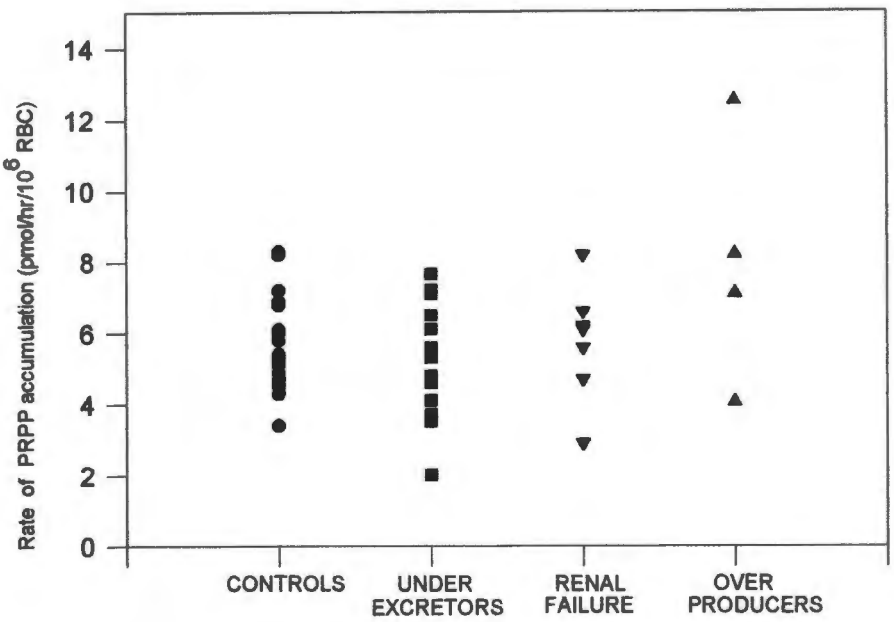

Figure 6.4: The rate of erythrocyte PRPP accumulation in controls, urate underexcretors, urate overproducers and patients with chronic renal failure.

Table 6.2: Patients identified as possible urate overproducers. The values determined in the pilot study are shown in parentheses.

Patient	P-urate (mmol/l)	U-urate (mmol/l)	P-creat. (μmol/l)	U-creat. (mmol/l)	FE_{ur} %
KAT	0.53	3.7	127	11.6	7.64
JT*	0.37 (0.41)	2.7 (3.7)	110 (106)	11.6 (11.4)	6.91 (8.39)
NL*	0.30 (0.43)	2.3 (10.0)	108 (106)	12.9 (16.2)	6.63 (15.2)
EL*	0.29 (0.44)	2.6 (0.6)	130 (132)	9.7 (3.6)	12.02 (5.00)

Abbreviations: plasma urate (P-urate), urinary urate (U-urate), plasma creatinine (P-creat.) urinary creatinine (U-creat.), fractional urate excretion (FE_{ur}).

* patients identified as urate overproducers with increased rates of erythrocyte PRPP accumulation in the pilot study.

NL was on allopurinol during current study.

El was on oestrogen therapy for cancer of the prostrate, no specific treatment for gout.

Patient NL was on allopurinol treatment during the present study, but was not on treatment during the pilot study. On the basis of a FE_{ur} of 15.2% determined in the pilot study, this patient was classified as a urate overproducer. Patient JT is unlikely to be an underexcretor with a FE_{ur} of 6.91% determined in this study and 8.39% determined in the pilot study. The patient is not on treatment and is well controlled, with no attacks of gout in the last 6 years. Patient EL is an elderly male with cancer of the prostrate for which he is on oestrogen therapy. Gout in this patient is of three years duration and could be secondary to his cancer. The FE_{ur} of 5.00% determined in the pilot study has more than doubled in the present study (12.02%).

The initial erythrocyte PRPP concentration and the rate of PRPP accumulation for the four possible gouty overproducers KAT, JT, NL and EL are shown in Table 6.3 and in Figure 6.4.

Table 6.3: The initial erythrocyte PRPP concentration and rate of erythrocyte PRPP accumulation in patients with possible overproducing gout.
The rate of erythrocyte PRPP accumulation determined in the pilot study is shown in parentheses.

Patient	Initial PRPP (pmol/10^6 RBC)	PRPP Rate (pmol/hr/10^6 RBC)
KAT	0.71	4.06
JT	0.33	8.21 (12.59)
NL	0.33	7.10 (10.33)
EL	0.51	12.52 (15.10)

The rate of PRPP accumulation (4.06 pmol/hr/10^6 RBC) measured in erythrocytes of KAT fell below the mean of the control range. The rate of PRPP accumulation determined in the pilot study for JT, NL and EL, are all increased by a similar margin compared to the rate of PRPP accumulation determined in this study. This is probably due to differences in the methodology between the two studies, notably the higher [^{14}C] hypoxanthine concentration used in this study (100 μM compared to 60 μM used in the pilot study). Nevertheless, the rate of PRPP accumulation of 8.21 and 7.10 pmol/hr/10^6 RBC determined for JT and NL respectively in this study, are at the upper end of the control range and are greater than 1 SD from the control mean. The rate of erythrocyte PRPP accumulation of 12.52 pmol/hr/10^6 RBC determined in EL is double the control mean and above the upper limit of the control range.

6.4 Discussion.

Erythrocytes lack the capacity to synthesize purines *de novo* and represent a simple system for the study of components of the purine metabolic pathways. A generalised defect in purine metabolism which is reflected in erythrocytes may be easier to recognise because of the absence of complicating components of a metabolic pathway. The absence of a *de novo* purine synthetic pathway however, potentially limits the usefulness of erythrocytes as a model system. Any defect in purine *de novo* synthesis which leads to purine overproduction, with the exception of defects in PRPP synthetase, cannot be studied. PRPP synthetase is active in the mature erythrocyte and the erythrocyte represents a convenient, easily manipulated model for the study of this highly regulated enzyme. Erythrocytes also represent a significant pool of purines within the body and it is possible that an intrinsic defect in erythrocyte purine metabolism may well play a role in the pathogenesis of overproducing gout.

The increased levels of IMP together with normal levels of PRPP reported by Mansell et al (1981) in patients with chronic renal failure, are of particular interest in view of the results of the present study. In the present study, erythrocyte PRPP levels in patients with chronic renal failure were also found to be within the control range. However, PRPP levels appeared to be inversely correlated with blood pH and positively correlated to plasma phosphate levels. No increase in the rate of erythrocyte PRPP accumulation could be detected. These findings are consistent with those of Mansell et al (1988) who reported normal activity of PRPP synthetase and normal levels of PRPP in the erythrocytes of patients with chronic renal failure.

Berman et al (1988) in their description of the erythrocyte oxypurine cycle, speculated that the reason for the increased levels of erythrocyte purine nucleotides reported in patients with chronic renal failure lies in the interplay between intracellular pH, phosphate and 2,3-DPG. Under the conditions of low blood pH and high Pi characteristic of patients in chronic renal failure, the entry of Pi into the cell is enhanced. At low pH, the

concentration of free 2,3-DPG is reduced and Pi derived from the degradation of 2,3-DPG adds to the increased levels of Pi in the erythrocyte. The net conversion of 2,3-DPG to lactate results in the conversion of 2 ADP molecules to 2 ATP molecules. While the production of ATP from 2,3-DPG may contribute to the increase in ATP levels noted in the erythrocytes of chronic renal failure patients, this will not lead to an increase in total adenine nucleotide levels. The inhibitory effect of high intracellular levels of free phosphate and the decreased stimulatory effect of a reduced 2,3-DPG level on 5'-nucleotidase activity (Bontemps, 1988) are likely to contribute to the maintenance of the increased intracellular nucleotide pool. Partial inhibition of 5'-nucleotidases may result in a decreased flux through the first step of the purine nucleotide degradation pathways and despite the increased activities of PNP and adenosine deaminase reported by Mansell et al (1981), the rate of endogenous hypoxanthine production may be reduced. Erythrocyte HPRT activity in chronic renal failure is increased (Mansell et al, 1981) and combined with a possibly decreased flux of purine nucleotides to hypoxanthine, may result in enhanced salvage of hypoxanthine leading to the notable increase in IMP in these patients. IMP is trapped in the "Berman cycle" and should not contribute to an increase in adenine nucleotide levels.

The normal erythrocyte PRPP levels noted in this study and by Mansell et al (1981) are an anomaly. Under conditions of low pH and high phosphate, PRPP levels are expected to increase (Berman et al, 1988). However, the modulation of intracellular erythrocyte Pi and hydrogen ion concentration *in vivo* is dependent on a myriad of factors and may not exactly parallel the *in vitro* model. *In vivo*, the salvage of endogenous hypoxanthine and other phosphoribosyltransferase substrates are continuously depleting PRPP. In addition, inhibition of 5'-nucleotidase may not be complete in the range of plasma Pi concentrations present in chronic renal failure. It is likely that there is some cycling between hypoxanthine and IMP within the erythrocyte. This cycling would consume PRPP in the salvage reaction and could account for the normal levels of PRPP described in the erythrocyte of renal failure patients.

In summary, although erythrocyte levels of PRPP in patients with chronic renal failure are within the control range, there does appear to be a correlation between blood pH or Pi concentration and erythrocyte PRPP levels *in vivo*.

There was no significant difference in the time zero erythrocyte PRPP levels between controls and gouty underexcretors. An unexpected finding was a significant difference in the rate of PRPP accumulation between the control group and the gouty underexcretor group. The reason why erythrocytes of underexcretors should show a lower rate of PRPP accumulation than controls, is difficult to explain. It is possible that the difference between the two groups is a consequence of the small underexcretor sample size. If a significant difference between the two groups still persists with an increased underexcretor sample size, this may be evidence of a generalised defect of anion transport across membranes and the rate and regulation of Pi transport into the erythrocyte would warrant further investigation.

The identification of patients with purine overproduction was problematical. All of the patients entered into the study had not been previously evaluated by the attending clinicians as to whether they were overproducers or underexcretors. This strategy is based on the belief, supported in the literature (Peters and Ball, 1992), that in the majority of adult patients with gout, such a classification would not influence the treatment decisions. Emmerson (1991) recommended the following protocol in order to distinguish underexcretors from overproducers. Urinary urate is determined on two consecutive 24-hour urine collections with the patient on a normal diet. The patient is then placed on a seven day purine restricted diet and a further two 24-hour urine specimens are collected on days 5 and 6. On a purine restricted diet, underexcretors excrete less than 2 mmol of uric acid in 24 hours, while overproducers excrete more than 4.5 mmol/24 hours. In patients with hyperuricemia due to excessive purine consumption, dietary purine restrictions should lead to a fall in serum urate of at least 0,06 mmol/l and a fall of at least 1.2 mmol in 24 hour urinary urate excretion. We believed that the restrictions of this protocol would discourage patients from entering the study and in addition, patient

adherence to the protocol would be difficult to control outside of the hospital environment.

Our strategy was therefore to base initial classification of hyperuricemic patients on estimates of urate clearance relative to creatinine clearance determined from untimed urine specimen (Calabrese et al, 1990).

Four patients were classified as gouty overproducers on this basis and were shown to have a FE_{ur} within the control range. The patients were not on a purine restricted diet and the estimations of urate excretion should be interpreted with this fact in mind. The initial PRPP erythrocyte concentrations in all four patients were within the normal range. The rate of PRPP accumulation in one patient fell within 1SD of the control mean, while two patients fell within the upper limits of the control range. The highest rate of PRPP accumulation, above the control range, was found in EL. This 88 year old patient has had gout for three years and is on oestrogen treatment for cancer of the prostrate. There is no evidence of widespread malignancy in the patient and cancer as a cause of gout in EL is possible, but seems unlikely.

Although the presentation of gout in EL is not typical of primary gout, the increased rate of PRPP accumulation observed in this patient is a phenomenon which warrants further attention. The effect of oestrogen therapy on PRPP metabolism is not known. However, it is known that females have a higher FE_{ur} (until the menopause) than males. The increase in the FE_{ur} of EL in the current study may be due to the effects of oestrogen therapy on urate excretion.

More urate overproducing patients will need to be identified to determine whether there is a statistical difference in the rate of PRPP accumulation between controls and urate overproducers.

The PRPP accumulation assay relies on endogenous erythrocyte HPRT activity to convert [^{14}C] hypoxanthine to [^{14}C] IMP. Unfortunately, no patients with partial HPRT deficiency were available to test the effect of HPRT deficiency on the erythrocyte PRPP accumulation assay. A deficiency of HPRT could result in a lower rate of PRPP consumption in the salvage reaction and would appear in our assay, to represent a marked decrease in the rate of PRPP accumulation. Conversely, PRPP synthetase overactivity should lead to increased rates of PRPP synthesis *in vivo*, which would be reflected as an increased PRPP level at time zero and an increased rate of PRPP accumulation *in vitro*.

The metabolic basis of the erythrocyte PRPP assay suggests that the assay has validity as a screening method for defects in both HPRT and PRPP synthetase. The assay may also prove useful in screening primary urate overproducers for these two specific enzyme defects.

Although only four candidate patients with overproducing gout have so far been identified, a phenomenon of an increased rate of PRPP accumulation in the erythrocytes of three of these patients has been demonstrated. In the group of urate underexcretors, an unexpected, statistically significant decrease in the mean rate of erythrocyte PRPP accumulation was found. The results of the study are sufficiently provocative to warrant continuation and expansion of the study. Studies on phosphate and acid/base transport across the erythrocyte and other cell membranes, could probe for logical mechanisms which might explain the basis of both urate overproducing and underexcreting gout.

7. REFERENCES.

Adams A and Harkness RA. (1976) Development changes in purine phosphoribosyltransferases in human and rat tissue. Biochem. J. 160: 565-576.

Aebi M and Weissmann C. (1987) Precision and orderliness in splicing. TIG 3: 102-107.

Allen TE, Hwang H-Y and Ullman B. (1993) Cloning and overexpression of the hypoxanthine-guanine phosphoribosylation gene from Leishmania donovani. Unpublished, Genbank accession number L25412.

Andreadis A, Broderick JA and Kosik KS. (1995) Relative exon affinities and suboptimal splice site signals lead to non-equivalence of two cassette exons. Nucl. Acids Res. 23: 3585-3593.

Aral B, de Saint Basile G, Al-Garawi S, Kamoun P and Ceballos-Picot I. (1996) Novel nonsense mutation in the hypoxanthine-guanine phosphoribosyltransferase gene and nonrandom X-inactivation causing the Lesch-Nyhan syndrome in a female patient. Human Mutation 7: 52-58.

Argos P, Hanei M, Wilson JM and Kelley WN. (1983) A possible nucleotide binding domain in the tertiary fold of phosphoribosyltransferases. J. Biol. Chem. 258: 6450-6457.

Ashton RW, Straus RS, Chung SH and Sloan DL. (1989) Orotate phosphoribosyltransferase from yeast: studies of the structure of the pyrimidine binding site. Arch. Biochem. Biophys. 272: 421-432.

Ausubel FA, Brent R, Kingston RE, Moore DD, Seidman JG, Smith JA and Struhl K (eds). (1988, 1990, 1991, 1992, 1993 and 1994) Current protocols in molecular biology. Greene Publishing and Wiley Interscience, New York.

Bachman B, Lübe W and Hunsman G. (1990) Improvement of PCR amplified DNA sequencing with the aid of detergents. Nucl. Acids Res. 18: 1309.

Baumgarten I and Harley EH. (1995) Uptake of purine substrates show major physiological variations in mammalian skin fibroblasts. Comp. Biochem. Physiol. 110B: 37-46.

Becker MA, Meyer LJ and Seegmiller JE. (1973) Gout with purine overproduction due to increased phosphoribosylpyrophosphate synthetase activity. Am. J. Med 55: 232-242.

Becker MA. (1976) Patterns of phosphoribosylpyrophospate and ribose-5-phosphate concentration and generation in fibroblasts from patients with gout and purine overproduction. J. Clin. Invest. 57: 308-318.

Becker MA, Losman MJ and Kim M. (1987) Mechanisms of accelerated purine nucleotide synthesis in human fibroblasts with superactive phosphoribosylpyrophosphate synthetase. J Biol. Chem. 262: 5596-5602.

Becker MA, Kim M and Husain K. (1989) PRPP and purine nucleotide metabolism in human lymphoblasts with both PRPP synthetase superactivity and HGPRT deficiency. Adv. Exp. Med. Biol. 253B: 13-20.

Beighton P, Solomon L, Soskoline CL and Sweet MBE. (1977) Rheumatic diseases in the South African Negro Part VI. Gout and hyperuricaemia. S. Afr. Med. J. 51: 969-972.

Benkovic SJ. (1984) The transformylase enzymes in *de novo* purine biosynthesis. TIBS 9: 320-322.

Berman PA, Black DA, Human L and Harley EH. (1988) Oxypurine cycle in human erythrocytes regulated by pH, inorganic phosphate and oxygen. J. Clin. Invest. 82: 980-986.

Blaber M, Zhang X-J, Lindstrom JD, Pepiot SD, Baase WA and Matthews BW. (1994) Determination of the α-helix propensity within the context of a folded protein: Sites 44 and 131 in bacteriophage T4 lysozyme. J. Mol. Biol. 235: 600-624.

Black D. (1992) Activation of c-src neurone-specific splicing by an unusual RNA element *in vivo* and *in vitro*. Cell 69: 795-807.

Bontemps F, Van Den Berghe G and Hers HG. (1988) Identification of a purine 5'-nucleotidase stimulated by ATP and glycerate 2,3-bisphosphate. Biochem. J. 250: 687-696.

Bouwens-Rombouts AGM, van den Boogaard M-JH, Puig JG, Mateos FA, Hennekam RCM and Tilanus MCJ. (1993) Identification of two new nucleotide mutations ($HPRT_{Utrecht}$ and $HPRT_{Madrid}$) in exon three of the human hypoxanthine-guanine phosphoribosyltransferase (HPRT) gene. Hum. Genet. 91: 451-454.

Bradford MM. (1976) A rapid and sensitive method for the quantitation of microgram quantities of protein using the principle of protein-dye binding. Anal. Bioch. 72: 248-254.

Brosh S, Sperling O, Bromberg Y and Sidi Y. (1990) Developmental changes in the activity of enzymes of purine metabolism in rat neuronal cells in culture and in whole brain. J. Neurochem. 54: 1776-1781.

Burgemeister R, Rotzer E, Gutensohn W, Gehrke M and Schiel W. (1995) Identification of a new missense mutation in exon 2 of the human hypoxanthine phosphoribosyltransferase gene ($HPRT_{Isar}$): a further example of clinical heterogeneity in HPRT deficiencies. Human Mutation 5: 341-344.

Busetta B. (1988) The use of folding patterns in the search of protein structural similarities: a three-dimensional model of phosphoribosyl transferases. Bioch. Biophys. Acta 957: 21-33.

Calabrese G, Simmonds HA, Cameron JS and Davies PM. (1990) Precocious familial gout with reduced fractional urate clearance and normal purine enzymes. Q. J. Med. 277: 441-450.

Cameron JS, Moro F and Simmonds HA. (1993) Gout, uric acid and purine metabolism in paediatric nephrology. Pediatr. Nephrol. 7: 105-118.

Cariello NF and Skopek TR. (1993) Analysis of mutations occurring at the human HPRT locus. J. Mol. Biol. 231: 41-57.

Cariello NF and Skopek TR. (1993b) *In vivo* mutation at the human HPRT locus. TIG 9: 322-326.

Casanova JL, Pannetier C, Jaulin C and Kourilsky P. (1990) Optimal conditions for directly sequencing double-stranded PCR products with sequenase. Nucl. Acids Res. 18: 4028.

Champion-Arnaud P, Gozani O, Palandjian L and Reed R. (1994) Accumulation of a novel spliceosomal complex on pre-mRNAs containing branch site mutations. Mol. Cell. Biol. 15: 5750-5756.

Chen JR. (1977) *In situ* detection of mycoplasma contamination in cell culture by fluorescent Hoechst 33258 stain. Exp. Cell Res. 104: 255-256.

Chiara MD and Reed R. (1995) A two-step mechanism for 5' and 3' splice-site pairing. Nature 375: 510-513.

Chiaverotti TA, Battula N. and Monnat RJ Jr. (1991) Rat hypoxanthine phosphoribosyltransferase cDNA cloning and sequence analysis. Genomics 11: 1158-1160.

Choi Y, Koo JW, Ha IS, Yamada Y, Goto H and Ogasawara N. (1993) Partial hypoxanthine-guanine phosphoribosyl transferase deficiency in two Korean siblings - a new mutation. Pediatr. Nephrol. 7: 739-740.

Chomzynski P and Sacchi N. (1987) Single step method of RNA isolation by acid gaunidinium thiocyanate-phenol-chloroform extraction. Anal. Biochem. 162: 156-159.

Chou PY and Fasman GD. (1978) Empirical predictions of protein conformation. Annu. Rev. Biochem. 47: 251-276.

Clark JM. (1988) Novel non-template nucleotide addition reactions catalyzed by procaryotic and eucaryotic DNA polymerases. Nucl. Acids Res. 16: 9677-9686.

Cole P. (1988) Novel studies of erythrocyte purine metabolism in primary gout. M.Med (Path), University of Cape Town, Cape Town, South Africa.

Cotton GH, Rodrigues NR, and Campbell RD. (1988) Reactivity of cytosine and thymine in single-base mismatches with hydroxylamine and osmium tetroxide and its application to the study of mutations. Proc. Natl. Acad. Sci. USA 85: 4397-4401.

Craig SP III, McKerrow JH, Newport GR and Wang CC. (1988) Analysis of cDNA encoding the hypoxanthine-guanine phosphoribosyltransferase (HGPRTase) of *Schistosoma mansoni*; a putative target for chemotherapy. Nucleic Acids Res. 16: 7087-7101.

Davidson BL, Palella TD and Kelley WN. (1988a) Human hypoxanthine guanine phosphoribosyltransferase: a single nucleotide substitution in cDNA clones isolated from a patient with Lesch-Nyhan syndrome ($HPRT_{Midland}$). Gene 68: 85-91.

Davidson B, Pashmforoush M, Kelley W and Palella T. (1988b) Genetic basis of hypoxanthine-guanine phosphoribosyltransferase deficiency in a patient with the Lesch-Nyhan syndrome ($HPRT_{Flint}$). Gene 63: 331-336.

Davidson B, Chin SJ, Wilson J, Kelley W and Palella T. (1988c) Hypoxanthine-guanine phosphoribosyltransferase - genetic evidence for two identical mutations in two partially deficient subjects. J. Clin. Invest. 82: 2164-2167.

Davidson BL, Tarle SA, Palella TD and Kelley WN. (1989a) Molecular basis of hypoxanthine-guanine phosphoribosyltransferase deficiency in ten subjects determined by direct sequencing of amplified transcripts. J. Clin. Invest. 84: 342-346.

Davidson BL, Pashmforoush M, Kelley WN and Palella TD. (1989b) Human hypoxanthine-guanine phosphoribosyltransferase deficiency. The molecular defect in a patient with gout ($HPRT_{Ashville}$). J. Biol. Chem. 264: 520-525.

Davidson BL, Tarle SA, Van Antwerp M, Gibbs DA, Watts RWE, Kelley WN and Palella TD. (1991) Identification of seventeen independent mutations responsible for human hypoxanthine-guanine phosphoribosyltransferase (HPRT) deficiency. Am. J. Hum. Genet. 48: 951-958.

Davidson BL, Golovoy N and Roessler BJ. (1994) A 13 base pair deletion in exon 1 of $HPRT_{Illinois}$ forms a functional GUG initiation codon. Hum. Genet. 93: 300-304.

de Boer JG and Glickman BW. (1991) Mutational analysis of the structure and function of the adenine phosphoribosyltransferase enzyme of Chinese hamster. J. Mol. Biol. 221: 163-174.

Dirksen WP, Sun Q and Rottman FM. (1995) Multiple splicing signals control alternative intron retention of bovine growth hormone pre-mRNA. J. Biol. Chem. 270: 5346-5352.

Eads JC, Scapin G, Xu Y, Grubmeyer C and Sacchettini JC. (1994) The crystal structure of hypoxanthine-guanine phosphoribosyltransferase with bound GMP. Cell 78: 325-334.

Eckert KA and Kunkel TA. (1991) The fidelity of DNA polymerases used in the polymerase chain reaction. In: PCR a practical approach. (McPherson MJ, Quirke P and Taylor GR, editors.) Oxford University Press, Oxford.

Edwards A, Voss H, Rice P, Civitella A, Stagemann J, Schwager C, et al. (1990) Automated DNA sequencing of the human HPRT locus. Genomics 6: 593-608.

Ehrlich M, Zhang X and Inamdar N. (1990) Spontaneous deamination of cytosine and 5-methylcytosine residues in DNA and replacement of 5-methycytosine residues with cytosine residues. Mutation Res. 238: 277-286.

Emmerson BT. (1991) Identification of the causes of persistent hyperuricaemia. Lancet 337: 1461-1463.

Ernst M, Zametkin AJ, Matochik JA, Pascualvaca D, Jons PH, Hardy K, et al. (1996) Presynaptic dopaminergic deficits in Lesch-Nyhan disease. N. Engl. J. Med. 334: 1568-72.

Fairbanks LD, Simmonds HA, and Webster DR. (1987) Use of intact erythrocytes in the diagnosis of inherited purine and pyrimidine disorders. J. Inher. Metab. Dis. 10: 174-186.

Finger S, Heavens RP, Sirinathsinghji DJS, Kuehn MR and Dunnett SB. (1988) Behavioral and neurochemical evaluation of a transgenic mouse model of Lesch-Nyhan syndrome. J. Neurol. Sci. 86: 203-213.

Fox IH and Kelley WN. (1971) Phosphoribosylpyrophosphate in man: biochemical and clinical significance. Ann. Intern. Med. 74: 424-433.

Fujimori S, Hidaka Y, Davidson BL, Palella TD and Kelley WN. (1988) Identification of a single nucleotide change in a mutant gene for hypoxanthine guanine phosphoribosyltransferase ($HPRT_{Ann\ Arbor}$). Hum. Genet. 79: 39-43.

Fujimori S, Davidson BL, Kelley WN and Palella TD. (1989) Identification of a single nucleotide change in the hypoxanthine-guanine phosphoribosyltransferase gene ($HPRT_{Yale}$) responsible for Lesch-Nyhan syndrome. J. Clin. Invest. 83: 11-13.

Fujimori S, Kamatani N, Nishida Y, Ogasawara N and Akaoka I. (1990) Hypoxanthine guanine phosphoribosyltransferase deficiency: nucleotide substitution causing Lesch-Nyhan syndrome identified for the first time among Japanese. Hum. Genet. 84: 483-486.

Fujimori S, Tagaya T, Yamaoka N, Kamatani N and Akaoka I. (1991) A germ line mutation within the coding sequence for the putative 5-phosphoribosyl-1-pyrophosphate binding site of hypoxanthine-guanine phosphoribosyltransferase (HPRT) in a Lesch-Nyhan patient: missense mutations within a functionally important region probably cause disease. Hum Genet. 90: 385-388.

Fujimori S, Tagaya T, Kamatani N and Akaoka I. (1992) A germ line mutation within the coding sequence for the putative 5-phosphoribosyl-1-pyrophosphate binding site of hypoxanthine-guanine phosphoribosyltransferase (HPRT) in a Lesch-Nyhan patient: missense mutations within a functionally important region probably cause disease. Hum. Genet. 90: 385-388.

Fujimoto WY and Seegmiller JE. (1970) Hypoxanthine-guanine phosphoribosyltransferase deficiency: activity in normal, mutant, and heterozygote-cultured human skin fibroblasts. Proc. Natl. Acad. Sci. USA 65: 577-584.

Fuscoe JC and Nelsen AJ. (1994) Molecular description of a hypoxanthine phosphoribosyltransferase gene deletion in Lesch-Nyhan syndrome. Hum. Mol. Genet. 3: 199-200.

Galloon T and Harley EH. (1988) Biochemical genetics of $HPRT_{Cape\ Town}$: is the defect in the HPRT gene. J. Inher. Metab. Dis. 11: 114-122.

Garnier J, Osguthorpe DJ and Robson B. (1978) Analysis of the accuracy and implication of simple methods for predicting the secondary structure of globular proteins. J. Mol. Biol. 120: 97-120.

German DC and Holmes EW. (1986) Hyperuricemia and Gout. Medical Clinics of North America 70: 419-437.

Giacomello A and Salerno C. (1978) Human hypoxanthine-guanine phosphoribosyltransferase steady state kinetics of the forward and reverse directions. J. Biol. Chem. 253: 6038-6044.

Gibbs DA, Headhouse-Benson CM and Watts RWE. (1986) Family studies of the Lesch-Nyhan syndrome: the use of a restriction length polymorphism (RFLP) closely linked to the disease gene for carrier state and prenatal diagnosis. J. Inher Metab. Dis. 9: 45-58.

Gibbs RA, Nguyen PN, McBride LJ, Koepf SM and Caskey CT. (1989) Identification of mutations leading to the Lesch-Nyhan syndrome by automated direct DNA sequencing of in vitro amplified cDNA. Proc. Natl. Acad. Sci. USA 86: 1919-1923.

Gibbs RA, Nguyen P, Edwards AL, Civitello AB and Caskey CT. (1990) Multiplex DNA deletion detection and exon sequencing of the hypoxanthine phosphoribosyltransferase gene in Lesch-Nyhan families. Genomics 7: 235-244.

Goldberg AL and St. John AC. (1976) Intracellular protein degradation in mammalian and bacterial cells. II. Annu. Rev. Biochem. 45: 747-802.

Gordon RB, Keough DT and Emmerson BT. (1987) HPRT-deficiency associated with normal PRPP concentration and APRT activity. J. Inher. Metab. Dis. 10: 82-88.

Gordon RB, Stout JT, Emmerson BT and Caskey CT. (1987b) Molecular studies of hypoxanthine-guanine phosphoribosyltransferase deficiency. Aust. NZ J. Med. 17: 424-429.

Gordon RB, Sculley DG, Dawson PA, Beacham IR and Emmerson BT. (1990) Identification of a single nucleotide substitution in the coding sequence of in vitro amplified cDNA from a patient with partial HPRT deficiency ($HPRT_{Brisbane}$). J. Inher. Metab. Dis. 13: 692-700.

Gordon RB, Dawson PA, Sculley DG, Emmerson BT, Caskey CT and Gibbs RA. (1991) The molecular characterisation of $HPRT_{Chermside}$ and $HPRT_{Coorparoo}$: two Lesch-Nyhan patients with reduced amounts of mRNA. Gene 108: 299-304

Gribskov M, Burgess RR and Devereux J. (1986) PEPPLOT, a protein secondary structure analysis program for the UWGCG sequence analysis software package. Nucl. Acids Res. 14: 327-334).

Grubmeyer C and Penefsky HS. (1981) The presence of two hydrolytic sites on beef heart mitochondrial adenosine triphosphatase. J. Biol. Chem. 256: 3718-3727.

Haldane JBS. (1935) The rate of spontaneous mutation in a human gene. J. Genet. 31: 317-326.

Harkness RA, McCreanor GM and Watts RWE. (1988) Lesch-Nyhan syndrome and its pathogenesis: purine concentrations in plasma and urine with metabolic profiles in CSF. J. Inher.. Metab. Dis 11: 239-252.

Harkness RA and McCreanor GM. (1991) Erythrocyte nucleotide variations in hypoxanthine phosphoribosyltransferase deficiency. J. Inherit. Metab. Dis 14: 848-849.

Harley EH, Rees KR and Cohen A. (1970) The effect of mycoplasma contamination. Biochim. Biophys. Acta 213: 171-182.

Harley EH. (1994) DAPSA: a program for DNA and protein sequence analysis, Version 2.9. Copyright, EH Harley, Department of Chemical Pathology, University of Cape Town.

Henderson JF, Brox LW, Kelley WN, Rosenbloom FN and Seegmiller JE. (1968) Kinetic studies of hypoxanthine-guanine phosphoribosyltransferase. J. Biol. Chem. 243: 2514-2522.

Henderson JF. (1993) The biochemical basis of hyperuricemia and gout. In: Gresse U (ed). Molecular genetics, biochemistry and clinical aspects of inherited disorders of purine and pyrimidine metabolism. Springer-Verlag, Berlin, Heidelberg, New York. p69-72.

Hershey HV and Taylor MW. (1986) Nucleotide sequence and deduced amino acid sequence of Esherichia coli adenine phosphoribosyltransferase and comparison with other analogous enzymes. Gene 43: 287-293.

Hershko A, Razin A, Soshani T and Mager J. (1967) Turnover of purine nucleotides in rabbit erythrocytes II. Studies *in vitro*. Biochim. Biophys. Acta. 149: 59-72.

Hershko A, Razin A and Mager J. (1969) Regulation of the synthesis of 5-phosphoribosyl-1-pyrophosphate in intact red blood cells and in cell free preparations. Biochim. Biophys, Acta. 184: 64-76.

Holden JA and Kelley WN. (1978) Human hypoxanthine-guanine phosphoribosyltransferase, evidence for tetrameric structure. J. Biol. Chem. 253: 4459-4463.

Holmes EW. Regulation of purine biosynthesis de novo. In: "Uric Acid" Kelley and Weiner eds) Vol 51 in the series Handbook of Experimental Pharmacology. pp21-41. Springer Verlag 1978.

Hornstra IK and Yang TP. (1994) High resolution methylation analysis of the human hypoxanthine phosphoribosyltransferase gene 5' on the active and inactive X chromosomes: correlation with binding sites for transcription factors. Mol. Cell. Biol. 14: 1419-1430.

Horovitz A, Mathews JM and Fersht AR. (1992) α-Helix stability in proteins II. Factors that influence stability at the internal position. J. Mol. Biol. 227: 560-568.

Horowitz DS and Krainer AR. (1994) Mechanisms of selecting 5' splice sites in mammalian pre-mRNA splicing. TIG 10: 100-106.

Horowitz H, Christie GE and Platt T. (1982) Nucleotide sequence of the *trpD* gene encoding anthranilate synthetase component II of *Escherichia coli*. J. Mol. Biol. 156: 245-246.

Hove-Jensen B, Harlow KW, King CJ and Switser RL. (1986) Phosphoribosylpyrophosphate synthetase of *Eschericia coli*: properties of the purified enzyme and primary structure of the *prs* gene. J. Biol. Chem. 261: 6765-6771.

Igarashi T, Minami M and Nishida Y. (1989) Molecular analysis of hypoxanthine-guanine phosphoribosyltransferase mutations in five unrelated Japanese patients. Acta Paediatr Jpn 31: 303-313.

Iizasa T, Taira M, Shimada H, Ishijima S and Tatibana M. (1989) Molecular cloning and sequencing of human cDNA for phosphoribosyl pyrophosphate synthetase subunit II. FEBS Letters 244: 47-50.

Jackson IJ. (1991) A reappraisal of non-consensus mRNA splice sites. Nucl. Acids Res. 19: 3795-3798.

Jinnah HA, Langlais PJ, and Friedmann P. (1992) Functional analysis of brain dopamine systems in a genetic mouse model of Lesch-Nyhan syndrome. J. Pharmacol. Exp. Ther. 263: 596-607.

Jinnah HA, Page T and Friedmann P. (1993) Brain purines in a genetic mouse model of Lesch-Nyhan disease. J Neurochem. 60: 2036-2045.

Johnson GG, Eisenberg LR and Migeon BR. (1979) Human and mouse hypoxanthine-guanine phosphoribosyltransferase: dimers and tetramers. Science 203: 174-176.

Johnson GG, Ramage AL, Littlefield JW and Kazazian HH. (1982) Hypoxanthine-guanine phosphoribosyltransferase in human erythroid cells: posttranslational modification. Biochemistry 21: 960-966.

Jolly DJ, Okayama H, Berg P, Esty AC, Filpula D, Bohlen P, et al. (1983) Isolation and characterisation of a full-length expressible cDNA for human hypoxanthine phosphoribosyltransferase. Proc Natl. Acad. Sci. USA 80: 477-481.

Kelley WN, Greene ML, Rosenbloom FM, Henderson JF and Seegmiller JE. (1967) A specific defect in gout associated with overproduction of uric acid. Proc Natl. Acad. Sci. 57: 1735-1739.

Kelley WN, Greene ML, Rosenbloom FM, Henderson JF and Seegmiller JE. (1969) Hypoxanthine-guanine phosphoribosyltransferase deficiency in gout. Ann. Intern. Med. 70: 155-206.

Kelley WN, (1971) Studies on the adenine phosphoribosyltransferase enzyme in human fibroblasts lacking hypoxanthine-guanine phosphoribosyltransferase. J. Lab. Clin. Med. 77: 33-38.

Keough DT, Gordon RB, de Jersey J and Emmerson BT. (1988) Biochemical basis of hypoxanthine-guanine phosphoribosyltransferase deficiency in nine families. J. Inher. Metab. Dis. 11: 229-238.

Kessler O, Jiang Y and Chasin L. (1993) Order of intron removal during splicing of endogenous adenine phosphoribosyltransferase and dihydrofolate reductase pre-mRNA. Mol. Cell. Biol. 13: 6211-6222.

Konecki DS, Brennand J, Fuscoe JC, Caskey CT and Chinault AC. (1982) Hypoxanthine-guanine phosphoribosyltransferase genes of mouse and Chinese hamster: Construction and sequence analysis of cDNA recombinants. Nucl. Acids Res. 10: 6763-6775.

Kraft R, Tardiff J, Krauter KS, and Leinwand LA. (1988) Using mini-prep plasmid DNA for sequencing double stranded templates with Sequenase. BioTechniques 6: 544-547.

Kraus JP, Le K, Swaroop M, Ohura T, Tahara T, Rosenberg LE, Roper RD and Kozich V. (1993) Human cystathionine β-synthase cDNA: sequence, alternative splicing and expression in cultured cells. Hum. Mol. Genet. 2: 1633-1638.

Krenitsky TA and Papaioannou R. (1969) Human hypoxanthine phosphoribosyltransferase. II. Kinetics and chemical modification. J. Biol. Chem. 244: 1271-1277

Krenitsky TA, Papaioannou R and Elion GB. (1969) Human hypoxanthine phosphoribosyltransferase. 1. Purification, properties and specificity. J. Biol. Chem. 244: 1263-1270.

Kühl PW. (1994) Excess-substrate inhibition in enzymology and high-dose inhibition in pharmacology: a re-interpretation. Biochem. J. 298: 171-180.

Lear AL, Eperon LP, Wheatley LM and Eperon LC. (1990) Hierarchy for 5' splice site preference determined *in vivo*. J. Mol. Biol. 211: 103-115.

Lehninger A. (1978) Biochemistry, 24 ed, New York, Worth. p742.

Lesch M. and Nyhan WL. (1964) A familial disorder of uric acid metabolism and central nervous system function. Am. J. Med. 36: 561-570.

Lightfoot T, Joshi R, Nuki G and Snyder FF. (1992) The point mutation of hypoxanthine-guanine phosphoribosyltransferase ($HPRT_{Edinburgh}$) and detection by allele-specific polymerase chain reaction. Hum. Genet. 88: 695-696.

Lightfoot T, Lewkonia RM and Snyder FF. (1994) Sequence, expression and characterisation of $HPRT_{Moose\ Jaw}$: a point mutation resulting in cooperativity and decreased substrate affinities. Hum. Mol. Genet 3: 1377-1381.

Liu ZG and Schwarz LM. (1992) An efficient method for blunt end ligation of PCR products. BioTechniques 12: 28-30.

Lloyd KG, Hornykiewicz O, Davidson L, Shannak K, Farley I, Goldstein M et al. (1981) Biochemical evidence of dysfunction of brain neurotransmitters in the Lesch-Nyhan syndrome. N. Engl. J. Med. 305: 1106-1111.

Lyu PC, Liff MI, Marky LA and Kallenbach NR. (1990) Side chain contribution to the stability of alpha-helical structure in peptides. Science 250: 669-673.

Mansell MA, Allsop J, North ME, Simmonds RJ, Harkness RA and Watts RWE. (1981) Effect of renal failure on erythrocyte purine nucleotide, nucleoside and base concentrations and some related enzyme activities. Clinical Science 61: 757-764.

Marcus S, Steen AM. Andersson B, Lambert B, Kristoffersson U and Franke U. (1992) Mutation analysis and prenatal diagnosis in a Lesch-Nyhan family showing non-random X-inactivation interfering with carrier detection tests. Hum. Genet. 89: 395-400.

Marcus S, Hellgren D, Lambert B, Fallstrom SP and Wahlstrom J. (1993) Duplication in the hypoxanthine phosphoribosyl-transferase gene caused by Alu-Alu recombination in a patient with Lesch Nyhan syndrome. Hum. Genet. 90: 477-482.

Mateos FA and Puig JG. (1994) Purine metabolism in Lesch-Nyhan syndrome versus Kelly-Seegmiller syndrome. J. Inherit. Metab. Dis. 17: 138-142.

McKeran RO, Andrews TM, Howell A, Gibbs DA, Chinn S and Watts RWE. (1975) The diagnosis of the carrier state for the Lesch-Nyhan syndrome. Q. J. Med. 44: 189-205.

Minor DL and Kim PS. (1994) Measurement of the ß-sheet-forming propensities of amino acids. Nature 367: 660-663.

Mita S, Rizzuto R, Moraes CT, Shanske S, Arnaudo E, Fabrizi GM, et al. (1990) Recombination via flanking direct repeats is a major cause of large-scale deletions of human mitochondrial DNA. Nucl. Acids. Res. 18: 561-567.

Mount S. (1982) A catalogue of splice junction sequences. Nucl. Acids. Res. 10: 459-472.

Muhlrad D and Parker R. (1994) Premature translation termination triggers mRNA decapping. Nature 370: 578-581.

Mullis KB and Faloona FA. (1987) Specific synthesis of DNA in vitro via a polymerase-catalyzed chain reaction. Methods in Enzymology 155: 335-350.

Nalbantoglu J Hartley D, Phear G, Tear G and Meuth M. (1986) Spontaneous deletion formation at the APRT locus of hamster cells: the presence of short sequence homologies and dyad symmetries at deletion termini. EMBOJ 5: 1199-1204.

Nishikawa K and Noguchi T. (1991) Predicting protein secondary structure based on amino acid sequences. Methods in Enzymology 202: 31-44.

Norton PA. (1994) Alternative pr-mRNA splicing: factors involved in splice site selection. J. Cell Science 107: 1-7.

Ogasawara N, Stout JT, Goto H, Sonta S, Matsumoto A and Caskey CT. (1989) Molecular analysis of a female Lesch-Nyhan patient. J. Clin. Invest. 84: 1024-1027

Orita M, Suzuki Y, Sekiya T, and Hayashi K. (1989) Rapid and sensitive detection of point mutations and DNA polymorphisms using the polymerase chain reaction. Genomics 5: 874-877.

Page T, Bakay B, Nisinen E, and Nyhan WL. (1981) Hypoxanthine-guanine phosphoribosyltransferase variants: correlation of clinical phenotype with enzyme activity. J. Inher. Metab. Dis. 4: 203-206.

Pai GS, Sprenkle JA, Do TT, Mareni CE and Migeon BK. (1980) Localisation of loci for HPRT and glucose-6-phosphate dehydrogenase and biochemical evidence for non-random X-chromosome expression from studies of a human X-autosome translocation. Proc. Natl. Acad. Sci. USA 77: 2810-2813.

Palella TD and Fox IH. (1989) Hyperuricemia and gout. In: Scriver CR, Beaudet AL, Sly WS, Vally D (eds). The metabolic basis of inherited disease, 6th edn. Mcgraw-Hill, New York. p965-1006.

Patel PI, Nussbaum RL, Framson PE, Ledbetter D, Caskey CT and Chinault AC. (1984) Organisation of the HPRT gene and related sequences in the human genome. Somat. Cell Mol. Genet. 10: 483-493.

Patel PI, Framson PE, Caskey CT and Chinault AC. (1986) Fine structure of the human hypoxanthine phosphoribosyltransferase gene. Mol. Cell. Biol. 6: 393-403.

Peters TD and Ball GV. (1992) Gout and hyperuricemia. Current Opinion in Rheumatology 4: 566- 573.

Piszkiewicz D, Tilley BE, Rand-Meir T and Parsons SM. (1979) Amino acid sequence of ATP phosphoribosyltransferase of *Salmonella typhimurium*. Proc. Natl. Acad. Sci. USA 76: 1589-1592.

Poulsen P, Jensen KF, Valetin-Hansen P, Carlsson P and Lundberg LJ. (1983) Nucleotide sequence of the *Escherichia coli pyr*E gene and of the DNA in front of the protein-coding region. Eur. J. Biochem. 135: 223-229.

Puig JG and Mateos FA. (1993) The biochemical basis of HGPRT deficiency. In: Gresse U (ed). Molecular genetics, biochemistry and clinical aspects of inherited disorders of purine and pyrimidine metabolism. Springer-Verlag, Berlin, Heidelberg, New York. p12-26.

Rassin Dk, Lloyd KG, Kelley WN and Fox I. (1982) Decreased amino acids in various brain areas with Lesch-Nyhan syndrome. Neuropediatrics 13: 130-134.

Ravio K and Seegmiller JE. (1973) Adenine, hypoxanthine and guanine metabolism in fibroblasts from normal individuals and from patients with hypoxanthine phosphoribosyltransferase deficiency. Biochim. Biophys. Acta 299: 273-282.

Reid LH, Gregg RG, Smithies O and Koller BH. (1990) Regulatory elements in the introns of the human HPRT gene are necessary for its expression in embryonic stem cells. Proc. Natl. Acad. Sci. USA 87: 4299-4303.

Richardson KK, Fostel J and Skopek T. (1983) Nucleotide sequence of the xanthine guanine phosphoribosyltransferase gene of *E. coli*. Nucl. Acids Res. 11: 8809-8815.

Rideout W, Coetzee G, Olumi A and Jones P. (1990) 5-Methylcytosine as an endogenous mutagen in the human LDL receptor and p53 genes. Science 249: 1288-1290.

Rincon-limas DE, Krueger DA and Patel PI. (1991) Functional characterization of the human hypoxanthine phosphoribosyltransferase gene promoter: evidence for a negative regulatory element. Mol. Cell. Biol. 11: 4157-4164.

Roberson BL, Cote GJ and Berget SM. (1990) Exon definition may facilitate splice site selection in RNAs with multiple exons. Mol. Cell Biol. 10: 84-94.

Rosenbloom FM, Kelley WN, Miller J, Henderson JF and Seegmiller JE. (1967) Inherited disorders of purine metabolism: correlation between central nervous system dysfunction and biochemical defects. JAMA 202: 175-177.

Rosenbloom FM, Henderson JF, Caldwell IC, Kelley WN and Seegmiller JE. (1968) Biochemical basis of accelerated purine biosynthesis *de novo* in human fibroblasts lacking hypoxanthine-guanine phosphoribosyltransferase. J. Biol. Chem. 243: 1166-1173.

Roubenoff R. (1990) Gout and Hyperuricemia. Rheumatic Disease Clinics of North America 16: 539-550.

Rozen R, Buhl S, Mohynnidin F, Caillibot V and Schriver C. (1977) Evaluation of metabolic pathway activity in cultured skin fibroblasts and blood leucocytes. Clin. Chim. Acta 77: 379-386

Saiki RK, Gelfand DH, Stoffel S, Scharf SJ, Higuchi R, Horn GT et al. (1988) Primer-directed enzymatic amplification of DNA with a thermostable DNA polymerase. Science 239: 487-491.

Sanger F, Niklen S and Coulsen AR. (1977) DNA sequencing with chain-terminating inhibitors. Proc. Nat. Acad. Sci. USA 80: 3963-3965.

Sarkar G, Kapelner S and Sommer SS. (1990) Formamide can dramatically improve the specificity of PCR. Nucl. Acids Res. 18: 7465.

Scapin G, Grubmeyer C and Sacchettini JC. (1994) Crystal structure of orotate phosphoribosyltransferase. Biochemistry 33: 1287-1294.

Sculley DG, Dawson PA, Beacham IR, Emmerson BT and Gordon RB. (1991) Hypoxanthine-guanine phosphoribosyltransferase deficiency: analysis of HPRT mutations by direct sequencing and allele-specific amplification. Hum. Genet. 87: 688-692.

Sculley DG, Dawson PA, Emmerson BT and Gordon RB. (1992) A review of the molecular basis of hypoxanthine-guanine phosphoribosyltransferase (HPRT) deficiency. Hum. Genet. 90: 195-207.

Seegmiller JE, Rosenbloom FE and Kelley WN. (1967) An enzyme defect associated with a sex-linked human neurological disorder and excessive purine synthesis. Science 155: 1682-1684.

Sege-Peterson K, Chambers J, Page T, Jones OW and Nyhan WL. (1992) Characterisation of mutations in phenotypic variants of hypoxanthine phosphoribosyltransferase deficiency. Hum. Mol. Genet. 1: 427-432.

Shin-Buehring YS, Osang M, Hass WB, Rahm P and Schaub J. (1980) Prenatal diagnosis of Lesch-Nyhan syndrome and some characteristics of hypoxanthine-guanine phosphoribosyltransferase and adenine phosphoribosyltransferase in human tissues and cultivated cells. Pediatr. Res. 14: 825-829.

Shnier MH, Sims F and Zail S. (1972) The Lesch-Nyhan syndrome first case description in a South African family. S. Afr. J. 46: 947-949.

Sidi Y and Mitchell BS. (1985) Z-nucleotide accumulation in erythrocytes from Lesch-Nyhan patients. J. Clin Invest. 76: 2416-2419.

Simmonds HA, Fairbanks LD, Morris GS, Webster DR and Harley EH. (1988) Altered erythrocyte nucleotide patterns are characteristic of inherited disorders of purine and pyrimidine metabolism. Clin. Chim. Acta 171: 197-210.

Simmonds HA. (1994) When and how does one search for inborn errors of purine and pyrimidine metabolism? Pharm. World Sci 16: 139-148.

Sirand-Pugnet P, Durosay P, Brody E and Marie J. (1995) An intronic (A/U)GGG repeat enhances the splicing of an alternative intron of the chicken beta-tropomyosin pre-mRNA. Nucl. Acids Res. 23: 3501-3507.

Skandalis A, Ford BN and Glickman BW. (1994) Strand bias in mutation involving 5-methycytosine deamination in the human HPRT gene. Mutation Res. 314: 21-26.

Skopek TR, Recio L, Simpson D, Dallaire L, Melancon SB, Ogier H, et al. (1990) Molecular analysis of a Lesch-Nyhan syndrome mutation ($HPRT_{Montreal}$) by use of T-lymphocyte cultures. Hum. Genet. 85: 111-116.

Smith CWJ, Patton JG and Nadal-Ginard B. (1989) Alternative splicing in the control of gene expression. Annu. Rev. Genet. 23: 527-577.

Smithers GW and O'Sullivan WJ. (1984) Hypoxanthine-guanine phosphoribosyltransferase from human brain: purification and partial characterisation. Biochem. Med. 32: 106-121.

Snedecor GW and Cochran WG. (1980) Statistical methods, 7th ed. The Iowa State University Press, Ames, Iowa, USA. p248-250.

Snyder FF, Chudley AE, MacLeod PM, Carter RJ, Fung E and Lowe JK. (1984) Partial deficiency of hypoxanthine-guanine phosphoribosyltransferase with reduced affinity for PP-ribose-P in four related males with gout. Hum. Genet. 67: 18-22.

Snyder FF, Joyce JE, Carter-Edwards T, Joshi R, Rylance HL, Wallace RC and Nuki G. (1989) Hypoxanthine-guanine phosphoribosyltransferase deficiency in three brother with gout: characterization of a variant $HPRT_{Edinburgh}$ having altered isoelectric point, increased thermal lability and normal levels of messenger RNA. J. Inher. Metab. Dis. 12: 390-402.

Sorens JB. (1991) Rapid and reliable cloning of PCR products. PCR methods and applications 1: 140-141.

Steen AM, Sahlen S and Lambert B. (1991) Expression of the hypoxanthine phosphoribosyltransferase gene in resting and growth-stimulated human lymphocytes. Biochim. Biophys. Acta 1088: 77-85.

Steingrimsdottir H, Rowley G, Dorado G, Cole J and Lehman AR. (1992) Mutations which alter splicing in the human hypoxanthine-guanine phosphoribosyltransferase gene. Nucleic Acids Res. 20: 1201-1208.

Stephens RM and Schneider TD. (1992) Features of spliceosome evolution and function inferred from an analysis of the information at human splice sites. J. Mol. Biol. 228: 1124-1136.

Steyn LM. (1983) Kinetic and metabolic studies in HPRT deficiency. Phd thesis. University of Cape Town, South Africa

Steyn LM and Harley EH. (1984) Substrate inhibition in a human variant of hypoxanthine-guanine phosphoribosyltransferase. J. Biol. Chem. 259: 338-342.

Stout JT and Caskey CT. (1985) First trimester diagnosis of the Lesch-Nyhan syndrome: applications to other disorders of purine metabolism. Prenatal Diagnosis 5: 183-189.

Stout JT and Caskey CT. (1989) Hypoxanthine phosphoribosyltransferase: the Lesch-Nyhan syndrome and gouty arthritis. In: Scriver CR, Beaudet AL, Sly WS, Vally D (eds). The metabolic basis of inherited disease, 6th edn. Mcgraw-Hill, New York. p1007-1028.

Streisinger G and Owen J. (1985) Mechanisms of spontaneous and induced frameshift mutation in bacteriophage T4. Genetics 109: 633-659.

Stryer L. (1988) Biochemistry. W. H. Freeman and Company, New York. p601-607.

Takeshima Y, Nishio H, Sakamoto H, Nakamura H and Matsuo M. (1995) Modulation of *in vitro* splicing of the upstream intron by modifying an intra-exon sequence which is deleted from the dystrophin gene in dystrophin Kobe. J. Clin. Invest. 95: 515-520.

Tarle SA, Davidson BL, Wu VC, Zidar FJ, Seegmiller JE, Kelley WN and Palella TD. (1991) Short communication. Determination of the mutations responsible for the Lesch-Nyhan syndrome in 17 subjects. Genomics 10: 499-501.

Tarn W-Y and Steitz JA. (1995) Modulation of 5'splice site choice in pre-messenger RNA by two distinct steps. Proc. Natl. Acad. Sci. USA 92: 2504-2508.

Tohyama J, Nanba E and Ohno K. (1994) Hypoxanthine-guanine phosphoribosyltransferase (HPRT) deficiency: identification of point mutations in Japanese patients with Lesch-Nyhan syndrome and hereditary gout and their permanent expression in an HPRT-deficient mouse cell line. Hum. Genet. 93: 175-181.

Tso JY, Zalkin H, Van Cleemput M, Yanofsky C and Smith JM. (1982) Nucleotide sequence of Escherichia coli purF and deduced amino acid sequence of glutamine phosphoribosyl pyrophosphateamidotransferase. J. Biol. Chem. 257: 3525-3531.

Ungerstedt U. (1971) Postsynaptic supersensitivity after 6-hydroxydopamine induced degeneration of the nigrostriatal dopamine system. Acta Physiol. Scand. Suppl. 361: 69-91.

United States Biochemical Corporation. (1987). Step by step protocols for DNA sequencing with Sequenase™ version 2.0 T7 DNA polymerase. 7th Edition.

Vasanthakumar G, Davis RL Jr, Sullivan MA and Donahue JP. (1989) ,Nucleotide sequence of cDNA clone for hypoxanthine-guanine phosphoribosyltransferase from *Plasmodium falciparum*. Nucleic Acids Res. 17: 8382.

Vreede HW. (1994) The validity of whole cell labelling assays in HPRT deficiency. M.Med (Path), University of Cape Town, Cape Town, South Africa.

Watts RWE, Spellacy E, Gibbs DA, Allsop J, McKeran RO and Slavin GE. (1982) Clinical, postmortem, biochemical and therapeutic observation on the Lesch-Nyhan syndrome with particular reference to the neurological manifestations. Q. J. Med. 51: 43-78.

Watts RWE. (1985) Defects of tetrahydrobiopterin synthesis and their possible relationship to a disorder of purine metabolism (the Lesch-Nyhan syndrome). Advances in Enzyme Regulation 23: 25-58.

Willers I, Singh S and Goedde HW. (1984) Studies in the fibroblasts of patients with the Lesch-Nyhan syndrome and HPRT variants. Enzyme 32: 241-247.

Wilson JM, Landa LE, Kobayashi R and Kelley WN. (1982a) Human hypoxanthine-guanine phosphoribosyltransferase: tryptic peptides and post translational modification of the erythrocyte enzyme. J. Biol. Chem. 257: 14830-14834.

Wilson JM, Tarr GE, Mahoney WC and Kelley WN. (1982b) Human hypoxanthine-guanine phosphoribosyltransferase: complete amino acid sequence of the erythrocyte enzyme. J. Biol Chem. 257: 10878-10985.

Wilson JM, Baugher BW, Mattes PM, Daddona PE and Kelley WN. (1982c) Human hypoxanthine-guanine phosphoribosyltransferase: demonstration of structural variants in lymphoblastoid cells derived from patients with a deficiency of the enzyme. J. Clin. Invest. 69: 706-715.

Wilson J, Tarr G and Kelley W. (1983a) Human hypoxanthine-guanine phosphoribosyltransferase: an amino acid substitution in a mutant form of the enzyme isolated from a patient with gout ($HPRT_{London}$). Proc Natl. Acad. Sci. USA 80: 870-873.

Wilson J, Frossard P, Nussbaum R, Caskey T and Kelley W. (1983b) Human hypoxanthine-guanine phosphoribosyltransferase - Detection of a mutant allele by restriction endonuclease analysis ($HPRT_{Toronto}$). J. Clin. Invest. 72: 767-772.

Wilson J, Kobayashi R, Fox I and Kelley W. (1983c) Human hypoxanthine-guanine phosphoribosyltransferase - molecular abnormality in a mutant form of the enzyme ($HPRT_{Toronto}$). J. Biol. Chem. 258: 6458-6460.

Wilson JM, Young AB and Kelley WN. (1983d) Hypoxanthine-guanine phosphoribosyltransferase deficiency. The molecular basis of the clinical syndrome. N. Engl. J. Med. 309: 900-910.

Wilson JM and Kelley WN. (1984) Human hypoxanthine-guanine phosphoribosyltransferase. Structural alteration in a dysfunctional enzyme variant ($HPRT_{Munich}$) isolated from a patient with gout. J. Biol. Chem. 259: 27-30.

Wilson JM, Stout JT, Palella TD, Davidson BL, Kelley WN and Caskey CT. (1986a) A molecular survey of hypoxanthine-guanine phosphoribosyltransferase deficiency in man. J. Clin. Invest. 77: 188-195.

Wilson JM, O'Toole TE, Argos P, Shewach DS, Daddona PE and Kelley WN. (1986b) Human adenine phosphoribosyltransferase. Complete amino acid sequence of the erythrocyte enzyme. J. Biol. Chem. 261: 13677-13683.

Wolf H, Modrow S, Motz M, Jameson BA and Hermann G. (1988) An integrated family of amino acid sequence analysis programs. CABIOS 4: 189-191.

Wolf SF and Migeon BR. (1985) Clusters of CpG dinucleotides implicated by nuclease hypersensitivity as control elements of housekeeping genes. Nature 314: 467-469.

Wohlhueter RM. (1975) Hypoxanthine phosphoribosyltransferase activity in normal, developing and neoplastic tissue of the rat. Europ. J. Cancer 11: 463-472.

Wu CL and Melton DW. (1993) Production of a model for Lesch-Nyhan syndrome in hypoxanthine phosphoribosyltranferase deficient mice. Nature Genetics 3: 235-240.

Yamada Y, Goto H, Suzumori K, Adachi R and Ogasawara. (1992) Molecular analysis of five independent Japanese mutant genes for hypoxanthine guanine phosphoribosyltransferase (HPRT) deficiency. Hum. Genet. 90: 379-384.

Yang TP, Stout JT, Konecki DS, Patel PI, Alford RL and Caskey CT. (1988) Spontaneous reversion of novel Lesch-Nyhan mutation by HPRT gene rearrangement. Somat. Cell Mol. Genet. 14: 293-303.

Yu TF, Balis ME, Krenitsky TA, Dancis J, Silvers DN, Elion GB and Gutman AB. (1972) Rarity of X-linked partial hypoxanthine-guanine phosphoribosyltransferase deficiency in a large gouty population. Ann. Int. Med. 76: 255-264.

Yuan L, Craig SP, McKerrow JH and Wang CC. (1992) Steady-state kinetics of the schistosomal hypoxanthine-guanine phosphoribosyltransferase. Biochemistry 31: 806-810.

Zoref E, Sivan O, Sperling O. (1978) Synthesis and metabolic fate of purine nucleotides in cultured fibroblasts from normal subjects and from purine overproducing mutants. Biochim. Biophys. Acta 521: 452-458.

Zoref-Shani E, Bromberg Y, Brosh S, Sidi Y and Sperling O. (1993) Characterization of the alterations in purine nucleotide metabolism in hypoxanthine-guanine phosphoribosyltransferase-deficient rat neuroma cell line. J. Neurochem. 61: 457-463.